AD NUMBER

ADB038409

NEW LIMITATION CHANGE

TO

Approved for public release, distribution unlimited

FROM

Distribution authorized to U.S. Gov't. agencies only; Test and Evaluation; MAY 1978. Other requests shall be referred to Manufacturing Technology Div., Air Force Materials Lab., Wright-Patterson AFB, OH 45433.

AUTHORITY

AFWAL ltr, 19 Jan 1988

AFML-TR-78-138

LEVEL II

AD B038409

ACOUSTO-ELASTIC FASTENER PRELOAD INDICATOR

The acousto-elastic effect is used to directly measure stress in fasteners.

J. C. Couchman

GENERAL DYNAMICS
Fort Worth Division
P.O. Box 748, Fort Worth, Texas 76101

October 1978

Final Report July 1976 - July 1978

Prepared for

United States Air Force
Air Force Systems Command
Aeronautical Systems Division
Wright-Patterson Air Force Base, Ohio 45433

NOTICE

When Government drawings, specifications, or other data are used for any purpose other than in connection with a definitely related Government procurement operation, the United States Government thereby incurs no responsibility nor any obligation whatsoever; and the fact that the Government may have formulated, furnished, or in any way supplied the said drawings, specifications, or other data, is not to be regarded by implication or otherwise as in any manner licensing the holder or any other person or corporation, or conveying any rights or permission to manufacture, use, or sell any patented invention that may in any way be related thereto.

This technical report has been reviewed and is approved for publications.

Edward Wheeler
Project Engineer

For The Director

H. A. Johnson
Chief, Metals Branch
Manufacturing Technology Division

"If your address has changed, if you wish to be removed from our mailing list, or if the addressee is no longer employed by your organization please notify AFML/LTM, W-P AFB, OH 45433 to help us maintain a current mailing list".

Copies of this report should not be returned unless return is required by security considerations, contractual obligations, or notice on a specific document.

AIR FORCE/56780/6 June 1979 -- 200

SECURITY CLASSIFICATION OF THIS PAGE (When Data Entered)

(19) REPORT DOCUMENTATION PAGE

READ INSTRUCTIONS BEFORE COMPLETING FORM

1. REPORT NUMBER (18) AFML-TR-78-138	2. GOVT ACCESSION NO.
3. RECIPIENT'S CATALOG NUMBER	
4. TITLE (and Subtitle) (6) Acousto-Elastic Fastener Preload Indicator	5. TYPE OF REPORT & PERIOD COVERED (9) Final Report, July 1976 - July 1978
6. PERFORMING ORG. REPORT NUMBER	
7. AUTHOR(s) (10) J. C. Couchman	8. CONTRACT OR GRANT NUMBER(s) (15) F33615-76-C-5251
9. PERFORMING ORGANIZATION NAME AND ADDRESS General Dynamics Fort Worth Division P.O. Box 748, Fort Worth, Texas 76101	10. PROGRAM ELEMENT, PROJECT, TASK AREA & WORK UNIT NUMBERS
11. CONTROLLING OFFICE NAME AND ADDRESS United States Air Force, Air Force Systems Command, Aeronautical Systems Division Wright-Patterson Air Force Base, OH 45433	12. REPORT DATE (11) October 1978 13. NUMBER OF PAGES 89
14. MONITORING AGENCY NAME & ADDRESS (if different from Controlling Office) (12) 99 p.	15. SECURITY CLASS. (of this report) Unclassified 15a. DECLASSIFICATION/DOWNGRADING SCHEDULE N/A

16. DISTRIBUTION STATEMENT (of this Report)

Distribution limited to U.S. Government agencies only; test and evaluation; May 1978. Other requests for this document must be referred to the Manufacturing Technology Division (AFML/LT), Air Force Materials Laboratory, Wright-Patterson Air Force Base, Ohio 45433.

17. DISTRIBUTION STATEMENT (of the abstract entered in Block 20, if different from Report)

18. SUPPLEMENTARY NOTES

None

19. KEY WORDS (Continue on reverse side if necessary and identify by block number)

Acousto-Elastic Effect
Material Constants
Elastic constants
Torque Wrench
Fasteners
Fastener Preload

20. ABSTRACT (Continue on reverse side if necessary and identify by block number)

This report describes the assembly, calibration, and testing of an acousto-elastic fastener preload indicator that has been demonstrated to preload fasteners with better than 5% accuracy within the elastic range. The system is computer automated and includes a calibration procedure for checking cutoff accuracy. The new capability afforded by this computer-controlled acousto-elastic torque wrench improves state-of-the-art (continued)

DD FORM 1 JAN 73 1473 EDITION OF 1 NOV 65 IS OBSOLETE

Unclassified

SECURITY CLASSIFICATION OF THIS PAGE (When Data Entered)

402 709

20. (Continued)

capabilities by nearly an order of magnitude in accuracy for setting preloads and can be used on flaw-free fasteners of the flat-head type.

FOREWORD

This two-year program to establish a fastener preload indicator is being performed under Air Force Systems Command sponsorship by the Aeronautical Systems Division at Wright-Patterson Air Force Base, Ohio 45433. Mr. E. Wheeler (LTM) is the Air Force Project Engineer on this program.

The program was performed under the direction of the Materials Research Laboratory of the Materials Technology Section of the Structures and Design Department, General Dynamics' Fort Worth Division. Key Fort Worth personnel associated with this program and their areas of responsibility during this reporting period are:

J. C. Couchman, Program Manager
A. H. Gardner, Prototype Fabrication
J. R. Williamson, Prototype Calibration, Systems Integration
J. H. Baucum, Dynamic Coupling, Calibration Standard Fabrication
P. J. Noronha, Specimen Selection
A. R. Robinson, Torque Wrench Integration, Calibration Standard Design
W. A. Rogers, Finite Elements Calculations
R. A. Carmin, Non Uniform Tension Studies
J. M. Norton, Multiple Regression Analysis
G. D. Hager, Control Program Preparation
G. Arnett, Control Program Preparation
S. P. Henslee, Mechanical Design

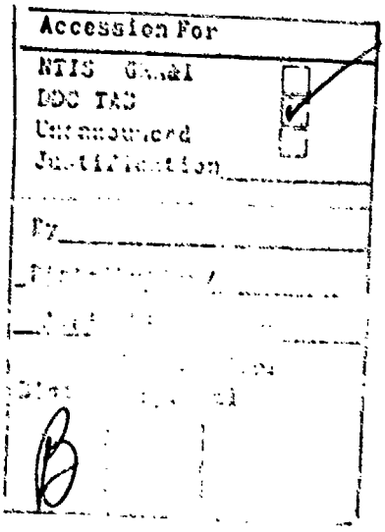

TABLE OF CONTENTS

TABLE OF CONTENTS (CONT.)

LIST OF ILLUSTRATIONS

LIST OF ILLUSTRATIONS (CONT.)

LIST OF ILLUSTRATIONS (CONT.)

LIST OF TABLES

SUMMARY

Direct measurements of the ultrasound travel time has been chosen as a means for using the acousto-elastic effect in measuring tensions in fasteners. It has been demonstrated under laboratory conditions that it is possible to torque fasteners to within five percent of preload specifications. It has further been shown that accuracy potentials approaching 2 or 3 percent are possible if the effects of such observables as relaxation phenomena, non-uniform stress distributions, and thermal related variations are fully understood. Geometry related factors such as surface roughness and curved or non-parallel fastener ends are assumed to be factors that can be accounted for by tightening procurement specifications on critical fasteners.

The computer controlled prototype system described in this report and in an accompanying process specification includes a PDP 11/03 digital computer, a software control algorithm, and input/output interfaces needed to control a Thor air impact wrench. The ultrasonics system uses a Metrotec P203 pulser module with a remote FET preamplifier for low noise signal conditioning. Signal processing and timing is accomplished with a specially designed electronics system, which generates a start timing pulse upon detection of a first ultrasonic back surface echo and a stop timing pulse upon detection of the second back surface echo. Time interval counting is performed in a HP 5345A time interval counter which transfers the measured time over a GPIB interface to the microcomputer.

The results from special supporting tasks involving (1) prototype calibration, (2) non uniform tension in fasteners, (3) fastener properties, (4) temperature effects, and (5) pulse shape effects are presented in included appendexes.

SECTION I

INTRODUCTION

Structural mechanical fasteners must be installed with a designated tensile preload in order to function in a predictable manner over the anticipated design lifetime. Current manufacturing procedures for airframe structure calls for the torque controlled installation of fasteners in virtually all areas where preload is important. Whether the fastener is wrenched manually to a specific torque value or a torque-sensitive collar fails in shear to halt the advance of a powered wrench, the frictional components of the torque value vary considerably and can lead to preload variations of ±20% (some authors report ±200% variations Ref. 1). The objective of this project was to establish a prototype automatic fastener installation system which will permit control of clamp up within ±5% of any specified preload value in bolts tensioned in the elastic region. Accomplishment of this objective will permit the achievement of consistent and accurate uniform preload in mechanical fastened joints, thus permitting designers to take full advantage of material strength in specifying fastener size, type, and spacing.

The failure of improperly torqued fasteners is the principle failure mode in critical aircraft structures. This fact is adequately demonstrated by failure mechanism data on a wing carry through box that was fatigue tested through four simulated service lives. A graphical representation of these data (Figure 1) shows that 82.5 percent of the failures detected were fastener related perhaps due to improper fastener preloading.

This is the final report on the results of a two-year program that was sponsored by the United States Air Force to assemble, calibrate and test the requisite automatic fastener installation system. During this program, a computer controlled torque wrench was operated by utilizing the acousto-elastic change in ultrasound travel time through a fastener in directly measuring the clamping force. The change in sound travel time proved to be linearly proportional to the clamping force within one percent over the elastic region for steel, titanium, and aluminum fasteners. Clamp up accuracies better than ±5% were observed during the calibration program. It is likely that 2 or 3 percent accuracies will eventually be achievable through future improvements in this system.

63 Failure Mechanisms from Test Program - 4 Service Lives

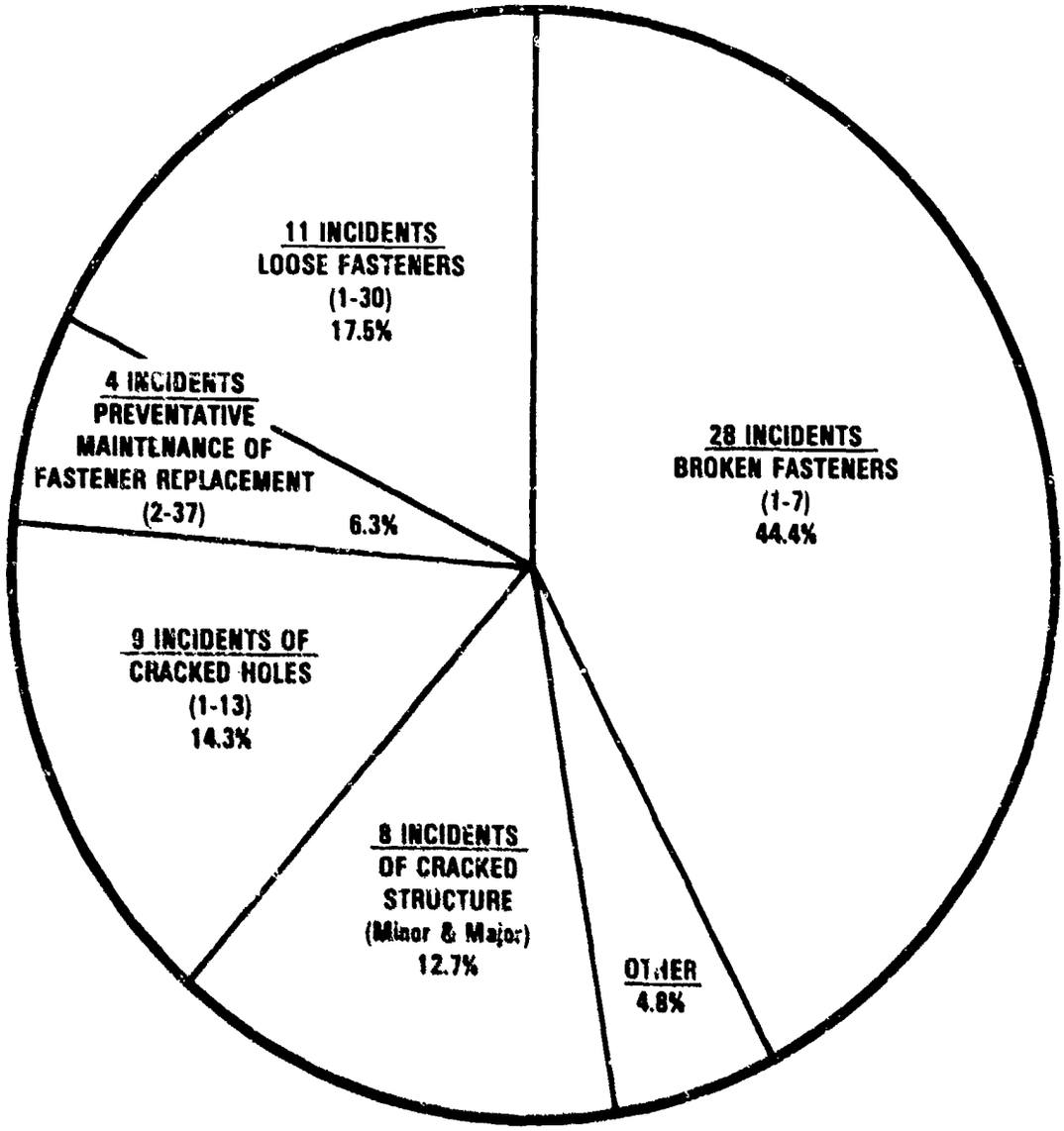

WING-CARRY-THRU-BOX

Figure 1. Failure Mechanisms Observed During Fatigue Testing of an Aircraft Wing-Carry-Thru-Box

The acousto-elastic fastener preload indicator (shown in Figure 2) has a computer control system to monitor the travel time of 20 megahertz ultrasound through a fastener in real time as the fastener is being torqued. When the change in travel time reaches a magnitude which corresponds to the desired fastener tension, the computer inactivates the torque wrench then displays the torque and tension achieved. Prior to reactivating the torque wrench the system checks for good acoustic coupling, checks for faulty fasteners, and verifies that the correct fastener length and bolt material are being used. The overall system is capable of expansion to multiple wrench station operation and is designed around a PDP 11/03 digital computer interfaced to control a Thor torque wrench that has an ultrasonic transducer built into its drive spindle. An electronic system designed and built by General Dynamics performs timing, signal amplification, gain stabilization, and pulse shaping required to start and stop a Hewlett Packard time interval counter which delivers ultrasound travel times to the PDP 11/03 computer. Computer software for the control system is written in DEC basic with linkable assembly language subroutines for input/output control. The system is designed so that the decision to issue each torque wrench impact is made by the computer control algorithm as a special precaution against over-loading fasteners.

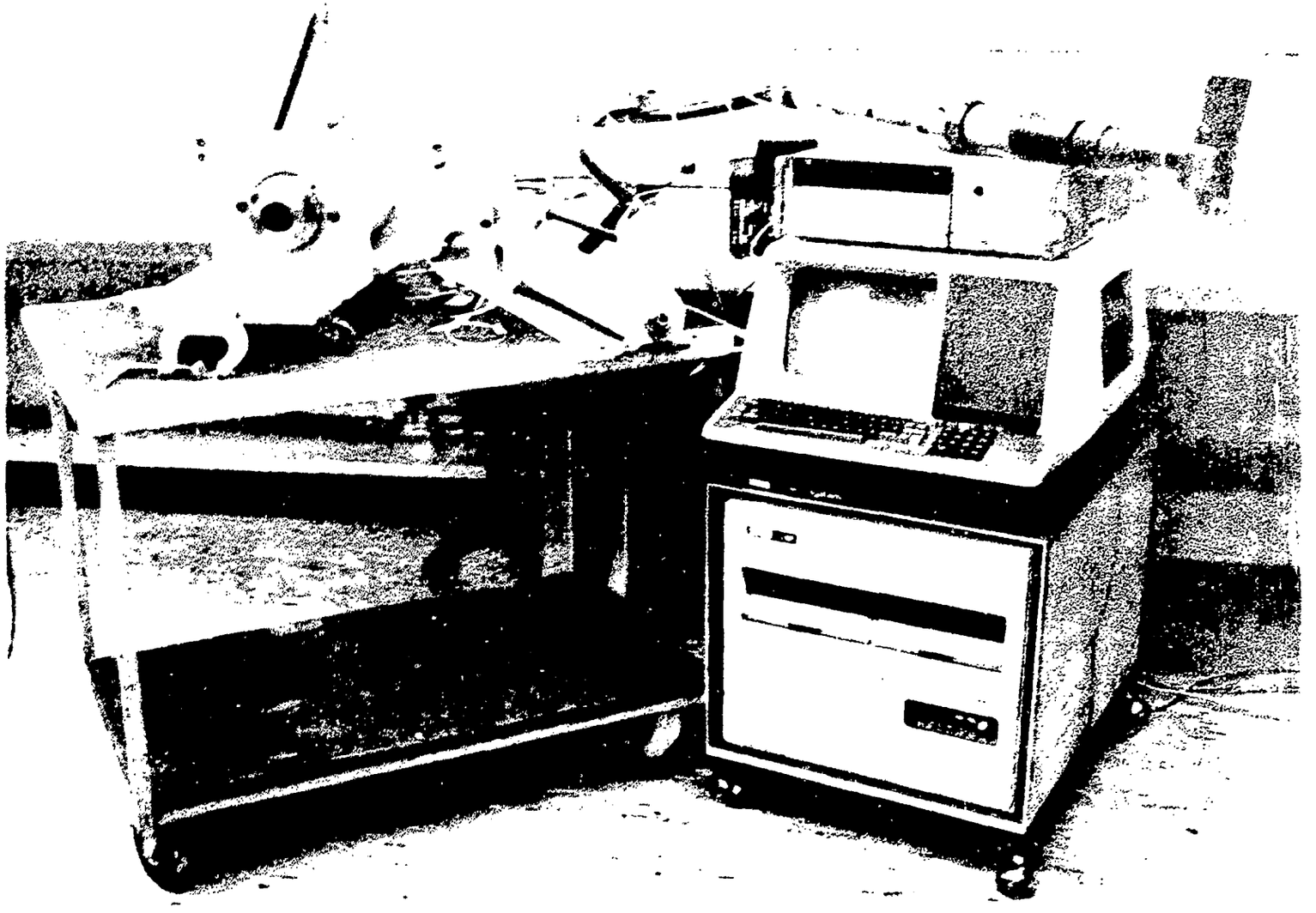

Figure 2. Acousto-Elastic Fastener Preload Indicator System

SECTION II

CONCEPT REALIZATION

The higher order Lame' and Murnaghan elastic constants produce the so called acousto-elastic effect. The acousto-elastic effect is a phenomena through which the velocity of sound in a material increases when the material is placed under compression and slows down when the material is placed under tension. Analytically, the velocity of sound in the direction of the applied stress is given by

$$v = v_o \sqrt{1 - \frac{S}{3K\,(2\mu+\lambda)}\left[\frac{\mu+\lambda}{\mu}\,(10\mu+4\lambda+4m)+\lambda+21\right]} \qquad (1)$$

where v_o = velocity of sound with no stress (cm/sec)
S = stress (dynes/cm^2)
K = compressibility (dynes/cm^2)
μ,λ = Lame' constants
l,m = Murnaghan constants

It can be shown that if a rod of length L is placed under uniform tension S and the acoustical travel time of an ultrasonic beam traveling a distance 2L is measured, then the travel time is reduced by an amount

$$\Delta T = \frac{L}{M}\,S \qquad (2)$$

where $M = \frac{v_o}{2}\left[\frac{(\mu+\lambda)\,(10\mu+4\lambda+4m)}{6\mu K\,(2\mu+\lambda)} + \frac{(\lambda+21)}{6K\,(2\mu+\lambda)} + \frac{1}{Y}\right]$

v_o = velocity of sound without a load applied

Y = Young's Modulus

It has been verified through a comprehensive calibration program that ΔT is linearly proportional to tension S to within one percent and that the material constant is determined only by the elastic constants and is not dependent upon the tension applied to a rod nor to the fastener geometry.

The calibration study (Appendix A) provided the values for M in steel and titanium fasteners that are given in Table 1 and which were determined to a standard deviation of about 5 percent. It has been shown empirically that one can replace L with $\delta + .6D$ (where δ is the clamping grip length of a fastener and D is the fastener diameter) and obtain an equation

$$\Delta T = \frac{\delta + .6D}{M} S \qquad (3)$$

which relates ΔT to the average tension S along the centerline of a fastener with an accuracy of 5 percent or better.

The fastener preload indicator described in this report consists of a digital computer utilizing the relationship in equation 3 to cut off a Thor torque wrench when the desired ΔT has been achieved during the torquing of a fastener.

TABLE 1

VALUES FOR THE MATERIAL CONSTANTS OBTAINED DURING THE CALIBRATION PHASE OF THE DEVELOPMENT OF THE FASTENER PRELOAD INDICATOR.

Material	Value for M (Cgs Units)
Steel 160 ksi	$-1.71 \pm .05 \times 10^{17}$
Steel 220 ksi	$-1.70 \pm .06 \times 10^{17}$
Steel 260 ksi	$-1.66 \pm .07 \times 10^{17}$
Steel Mixed	$-1.71 \pm .06 \times 10^{17}$
Titanium	$-1.41 \pm .09 \times 10^{17}$

The details of the calibration program which produced the material constants listed in Table 1 are given in Appendix A. The empirical parameter (.6D in equation 3) was derived as a result of a finite elements study of non uniform tensions in loaded fasteners. The justification for the empirical parameter is given in Appendix B.

SECTION III

PROTOTYPE ACOUSTO-ELASTIC WRENCH SYSTEM

A block diagram of the fastener preload indicator system (Figure 3) shows a PDP 11/03 computer controlling a Thor torque wrench in use; the computer monitor asks the operator what bolt material, length, diameter, grip length, and load level are required. This is input on the console keyboard and displayed on a graphics terminal monitor for verification. The torque wrench is applied to the fastener and the computer tests for adequate acoustical coupling then verifies that the material and fastener length are correct. It then computes the ΔT in ultrasonic travel time required to achieve the desired tension. If the acoustical coupling remains good, the torque wrench operates in a nut runner mode until a change in ultrasonic travel time is detected. At that time, the system goes into a pulsed driven mode where the travel time is checked for the desired tension before the computer issues the next impulse command. As soon as the desired ΔT has been achieved, the computer ceases to issue impulse commands then computes and displays the tension level achieved.

The system is equipped with a safety override which monitors the torque and ultrasonic travel time in order to terminate torquing when the elastic limit is reached. An alternate torque-cut-off mode of operation is provided for situations where the computer senses problems with the ultrasonic system yet where it is still necessary to tension the fastener by the best alternate method.

The computer is interfaced with a calibrated pressure washer (described later) which makes it possible to verify the accuracy of the system. The computer can also measure the material constant m during another calibration mode and verify that it is statistically comparable to the average value accumulated in mass memory. The material constant M is used to determine what value of ΔT is required to achieve a design fastener preload tension from equation 3 above.

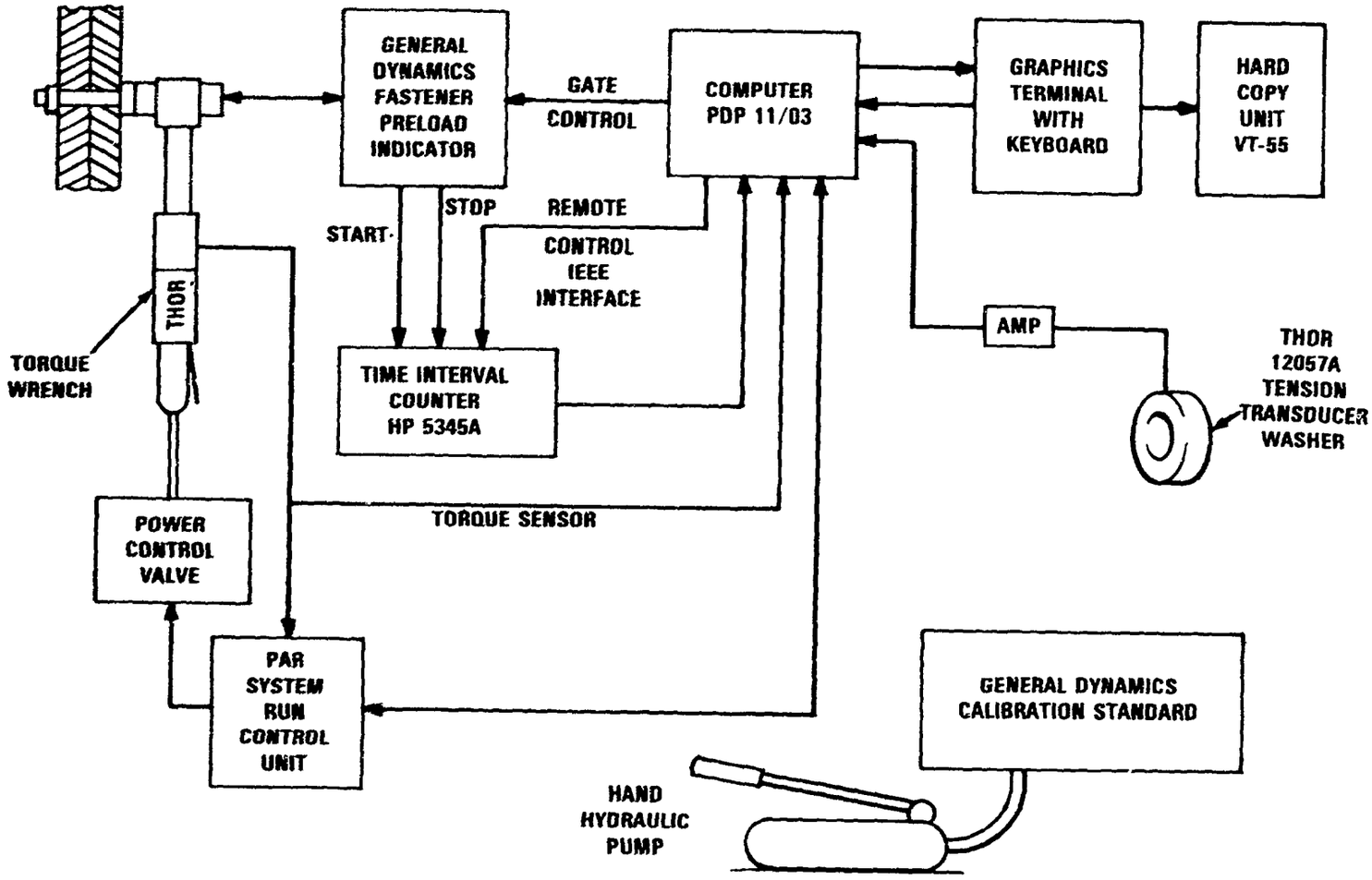

Figure 3. Block Diagram of the Fastener Preload Indicator System

SECTION IV

MODES OF OPERATION

Four operating modes are being provided by operator choice. They are (1) a calibration mode whereby wrench cut-off can be tested against a calibration standard, (2) the acousto-elastic ultrasonic mode in which torquing is cut-off by the fastener preload indicator unit, and (3) a computer adaptation of the conventional Thor control unit whereby torquing can be stopped by a torque or elastic limit sensor. The wrench system therefore provides a special backup capability so the torque wrench can be operated in the manual mode as needed. Modes of operation are as follows:

4.1 Calibration Modes

Properly operating, this system does not require calibration. Equation 3 (above) has to be satisfied. It is necessary, however, to provide a means for testing that the ultrasonic and timing circuitry is properly operating. Further, a means must be provided for measuring new material constants or non-uniform tension factors α. The latter measurements would most properly be performed under laboratory conditions.

4.1.1 Cut-off Checks

A calibration check can be made in either an ultrasonic or torque mode of operation and will provide the operator with a readout of the peak tension applied to a calibrated pressure washer. This can be compared to the acousto-elastically measured tension or with the cut-off torque. In either case, a few repeated cut-off checks can be used to measure the stability of the cut-off threshold and assure proper operation of the system.

4.1.2 Measuring New Material Constants

Often it will be necessary to tighten a fastener made from a different alloy or to tighten a fastener under some temperature extreme. In either case it will be necessary to measure the material constant.

The computer logic for measuring and computing a new material constant is shown in Figure 4. The calibration curve showing ΔT plotted against P_N is shown on the graphics display. Under normal conditions the data collected will be linear with less than one percent deviation from linearity. Nonlinearity indicates inelastic strain in a fastener. After 50 data points are collected, the computer proceeds with the computation of the material constant. Data output include fastener length "L", fastener diameter "D", Grip Length, "δ", initial load travel time "To" and material constants M, and M*. These output data are added to other calibration data in mass memory storage.

4.2 Acousto-Elastic Ultrasonic Mode

The operator selects the ultrasonic mode from two other alternatives calibration or torque modes. The following questions appear on the graphics terminal:

Bolt material? - the operator chooses from steel, aluminum or titanium

Bolt length? - the operator enters the bolt length L

Bolt diameter? - the operator enters the bolt diameter D

Grip length? - the operator enters the grip length δ

Tension desired- the operator enters the desired tension S.

The computer graphics respond with "READY". The operator then places the torque wrench on the fastener and a ready light comes on showing that a satisfactory ultrasonic signal is detected. The computer computes the ΔT required to obtain the desired stress level from equation 3. The computer determines the no tension ultrasonic travel time and verifies that the fastener is of proper length and material. An error message may signify that something is wrong, otherwise the operator can pull the trigger and the computer issues an impact impulse to the torque wrench. After, the impulse ΔT is measured and compared to the ΔT computed from equation 3. The sequence of impulsing, measuring ΔT and comparing to the desired ΔT continues until the desired ΔT has been achieved or slightly exceeded. The computer then keeps the air

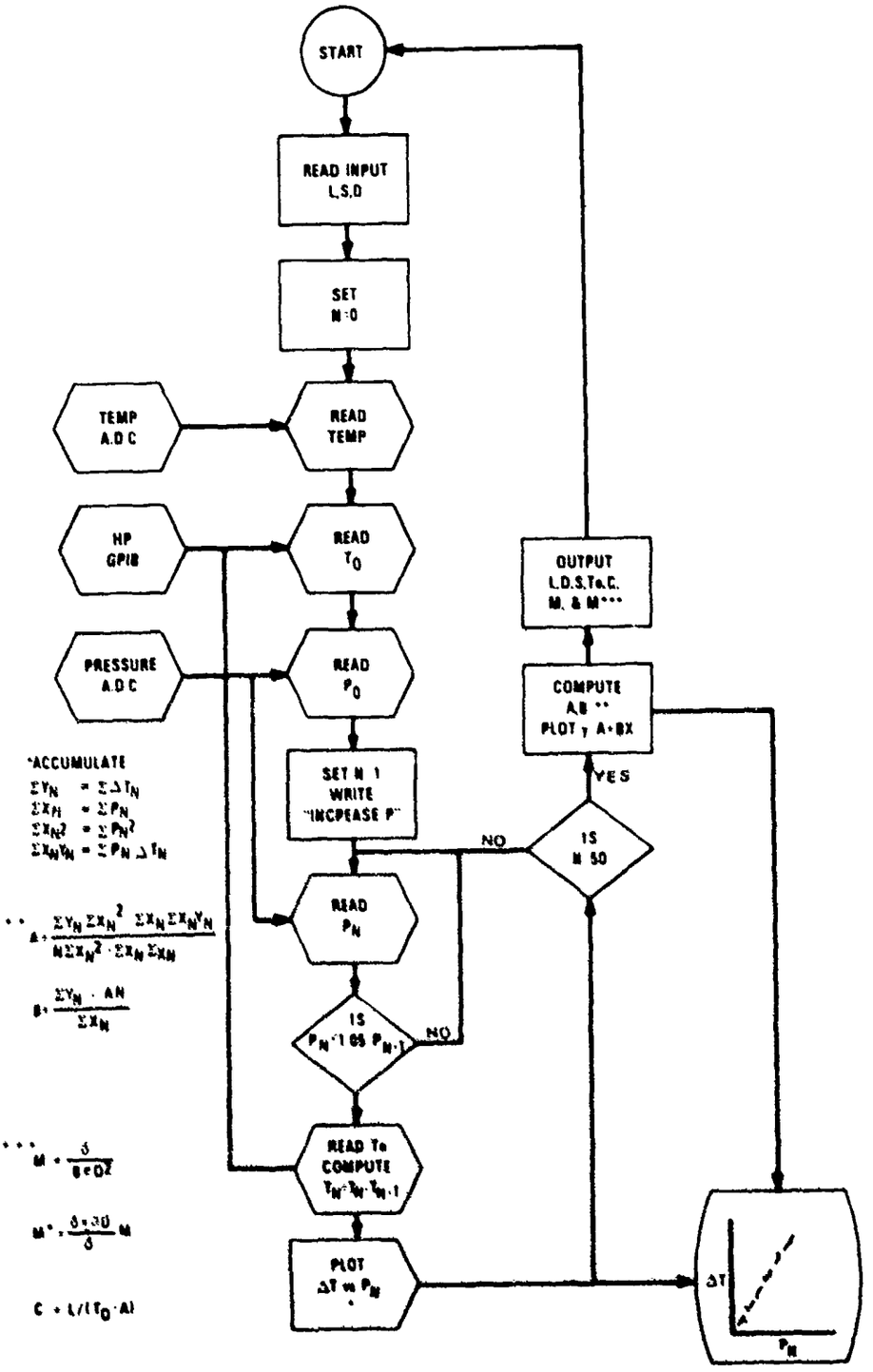

Figure 4. Logic Diagram for Measurement of Material Constant

flow solenoid closed, displays the tension achieved, and allows the operator to either torque another identical parameter, change bolt geometry, or select another mode of operation.

4.3 Conventional Torque Modes

When the torque mode is selected, the computer requires that the operator enter either the cut-off torque required or that the elastic limit cut-off be used. After each impulse, the computer reads the torque from the Thor torque transducer and sequentially issues succeeding impulses until the desired torque has been equaled or exceeded. The torque achieved at cut-off is displayed to the operator. If the elastic limit cut-off is used, the torque wrench is stopped whenever the increase in torque per impulse begins declining. This non-linear behavior is an indication of inelastic strain.

SECTION V

DISCUSSION

Seventy-four steel fasteners, 22 titanium fasteners, and over 100 threaded-rod stock specimens were tested (Appendix C) in a calibration program (Appendix A) to measure the material constant and observe its dependence upon stress, fastener geometry, and temperature. It was shown, as documented in Appendix A, that the material constants of all specimens tested were independent of the stress applied. It was further shown, as expected, that material constants for different materials (e.g., titanium, steel, aluminum, copper, and molybdenum) were significatnly different but that the material constants for different heat treatment conditions in steel were the same within the accuracy of the measurements made.

It was found that non-uniform stresses within fasteners that tend to concentrate near the fastener head cause an apparent variation of the material constant with the grip-length to fastener-diameter, δ/D, ratio. This variation was eliminated, as shown in Appendix B, through a comprehensive finite-element study. It was found that the variation could be removed by introduction of an empirical parameter α, shown in equation 3 as .6. A 5% variation in material constants persisted and was concluded to be caused by temperature-dependence effects, which need to be calibrated for. Such a calibration to show the dependence of the material constants upon temperature should be performed in order to achieve a potential accuracy of 1% or 2% in preloading fasteners by the acousto-elastic effect.

Fasteners having safety wire holes, internal flaws, or any surface feature that diffuses a beam of ultrasound cannot be preloaded ultrasonically to within 5% of the desired preload. This new level of quality in critical tension fasteners is consistent with their role of holding critical aircraft structures together. Out of the 200 or 300 critical-load-bearing fasteners that will be used on the wing root section, fuselage mating joints, landing gear mounting, vertical-tail mounting, or engine mounting of the F-16, it is estimated that about 50% are flat-head fasteners, which could be acousto-elastically preloaded. Most of the remaining fasteners could be replaced by flat-head types. A torque sensor backup mode of operation is available for emergency use or the broader range of fastener geometries, which have safety wire holes or geometrical features which diffuse ultrasound.

An error analysis study was performed to identify the cause of the five percent variation in material constants. The specific gravities and acoustic velocities were measured and found to vary less than one percent (See Appendix C). It was only when the temperature dependence of sound velocity was studied that an effect was observed that could explain the five percent variations in M (See appendix D).

SECTION VI

CONCLUSIONS

This Air Force-sponsored program has prepared the way for utilizing the acousto-elastic effect for setting preloads in fasteners. Determination of the important variables involved and the development of a functioning prototype of a computer-automated acousto-elastic fastener-preload indicator, documerted in this report, will be useful to the design of production systems.

Several important conclusions are derived from this program:

(1) One- or two-percent accuracy in setting fastener preload is feasible with a properly designed and operating acousto-elastic system.

(2) A simple analytic relationship

$$\Delta T = \frac{\delta + \alpha D}{M} S$$

linearly relates the acousto-elastic change in sound travel time to the average stress within a fastener.

(3) The material constant M may depend upon temperature but is independent of stress applied.

(4) The effects of non-uniform stress (fastener geometry) can be corrected for by selecting a value of that minimizes the variation of

$$M = \frac{\delta + \alpha D}{\Delta T} S$$

Alpha was experimentally determined to be approximately .6 for steel and titanium fasteners (Appendix B).

(5) Fasteners that are to be acousto-elastically preloaded must be free of internal flaws and of the flat-head type. This dictates a level of quality control that is consistent with the fasteners' use in critical aircraft structures.

APPENDIX A

CALIBRATION OF FASTENER PRELOAD INDICATOR

A.1 Conventional Torquing

The specifications for torquing bolts at General Dynamics are very specific. The F-111 standard for torque values and sealant applications in threaded fasteners is an example. The referenced standard gives minimum and maximum torques that bolts of different thread sizes can be pre-stressed to and defines drawing callouts for indicating torquing specifications. Instructions tell (1) how to clean surfaces, (2) how to apply thread compound, (3) what to do if maximum torques are exceeded, (4) how to line up cotter pin holes, (5) how to lubricate washers, (6) how to apply sealants, (7) how to retorque, (8) what to do when torque values are not specified, etc.

The use of a torque wrench for tightening fasteners to a specific design preload is not straightforward. Many variables enter into the calibration of a torque wrench. Even when the torque wrench accurately shuts off at the selected torque, several variables can still produce 20-30 percent errors in pretensioning the bolt to the desired preload.

A simple experiment shows that bolt preload (measured with a calibrated strain gage) is not a linear function of the moment applied by a torque wrench. A .75" diameter steel bolt was used in an experiment in which shear and tensile loads were monitored in the shank of the bolt while it was being manually torqued. Three separate tests were performed to determine (1) a dry clean nut-bolt baseline, (2) the effects of a washer under the nut, and (3) the effects of a lubricant applied to the bolt threads. The results in Figure A.0 show that none of the curves relating preload to the applied moment was linear. If these data were used for calibration, an error as large as 30% might be expected in trying to produce a 7.5 ksi preload at a 600 in-lb torque. These data are consistent with reported difficulties (Ref. 1, 2) in using torque wrench or other torque measuring devices for measuring stresses in bolts.

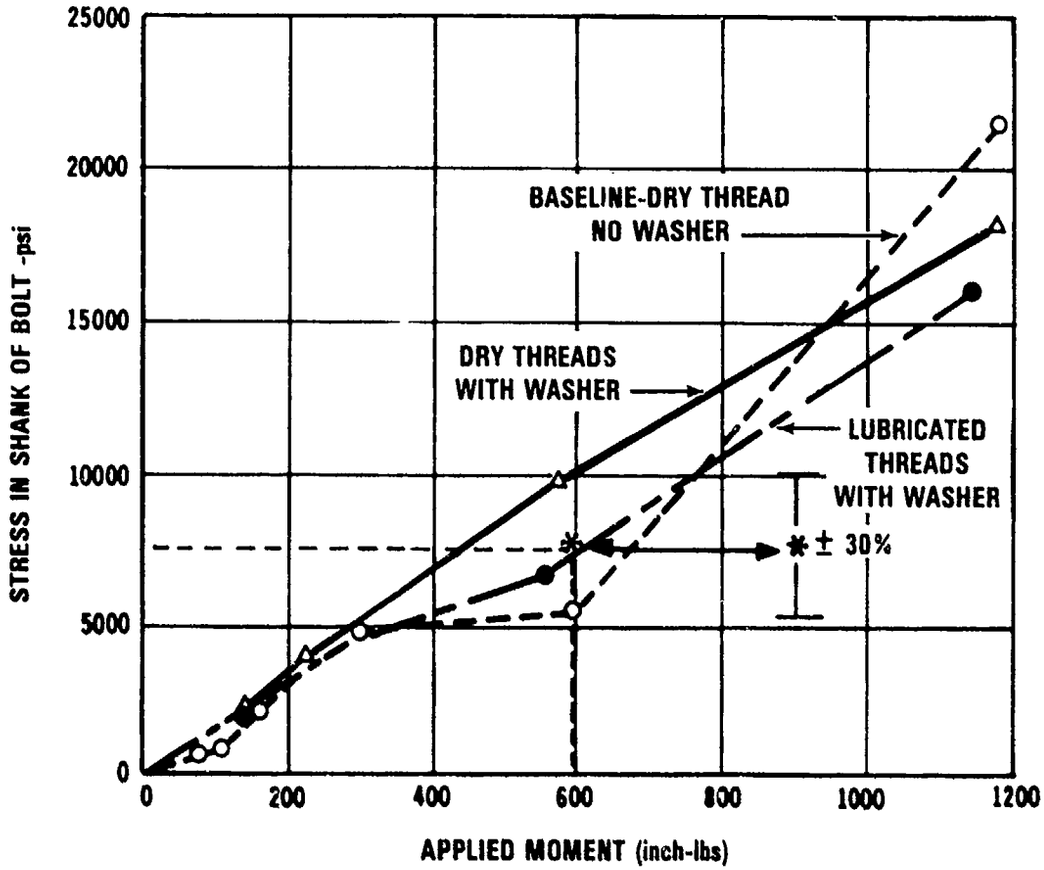

Figure A.0 Typical Calibration Curves for a Conventional Manual Torque Wrench

Notice that the baseline curve in Figure A.0 has an increasing prestress until a 300 in-lb moment was reached, then it was necessary to nearly double the moment before the bolt threads slipped and produced an over-preload-level of 21.3 ksi at a torque of 1160 in-lb. The washer and the lubrication improved the linearity of the prestress-moment graph. If this experiment were repeated, the exact results would be different but the same conclusion would be drawn about non-linearities and errors in torquing to a specific preload.

Figure A-1 shows how the shear stresses in the bolt shank varied as the nut was torqued on the steel bolt. Insufficient data were generated in this experiment to establish a specific trend, but the results do show that the ratio of shear-to-tensile loads in the shank of a bolt are quite variable. Notice the exaggerated shear at the 600 in-lb moment where the nut was slipping on the plate but the threads were seizing.

NASA (Ref. 3) describes the uses of macrosonics (high intensity ultrasonics) to achieve shear strain relief. An impact torque wrench may also achieve some shear stress relief. Sonabond (Ref. 4) manufactures an ultrasonic wrench that uses macrosonics to relieve torsional stresses in a torqued bolt.

If preload stress is to be measured directly, it is necessary to make the measurement in such a way that the stored shear energy does not effect the measurement. The data in Figure A.1 show that the shear stress in steel is sometimes as high as 10 percent of the axial stress in a bolt but on the average it ranges between 5 and 6 percent. Referring back to the baseline data presented in Figure A.0, one is faced with a dilemma. What should be measured when an increased torque fails to linearly increase prestress because of stored shear energy? If, as in the example, the bolt is torqued until a preload of 5.3 ksi is indicated by an axial strain gauge and the torque wrench is then stopped, the potential energy stored in the twisted bolt can be relieved by (1) the nut slipping on the flange or (2) by the nut turning tighter on the threads. In the first case, the prestress might be relieved and in the latter case it might be increased by a few percent.

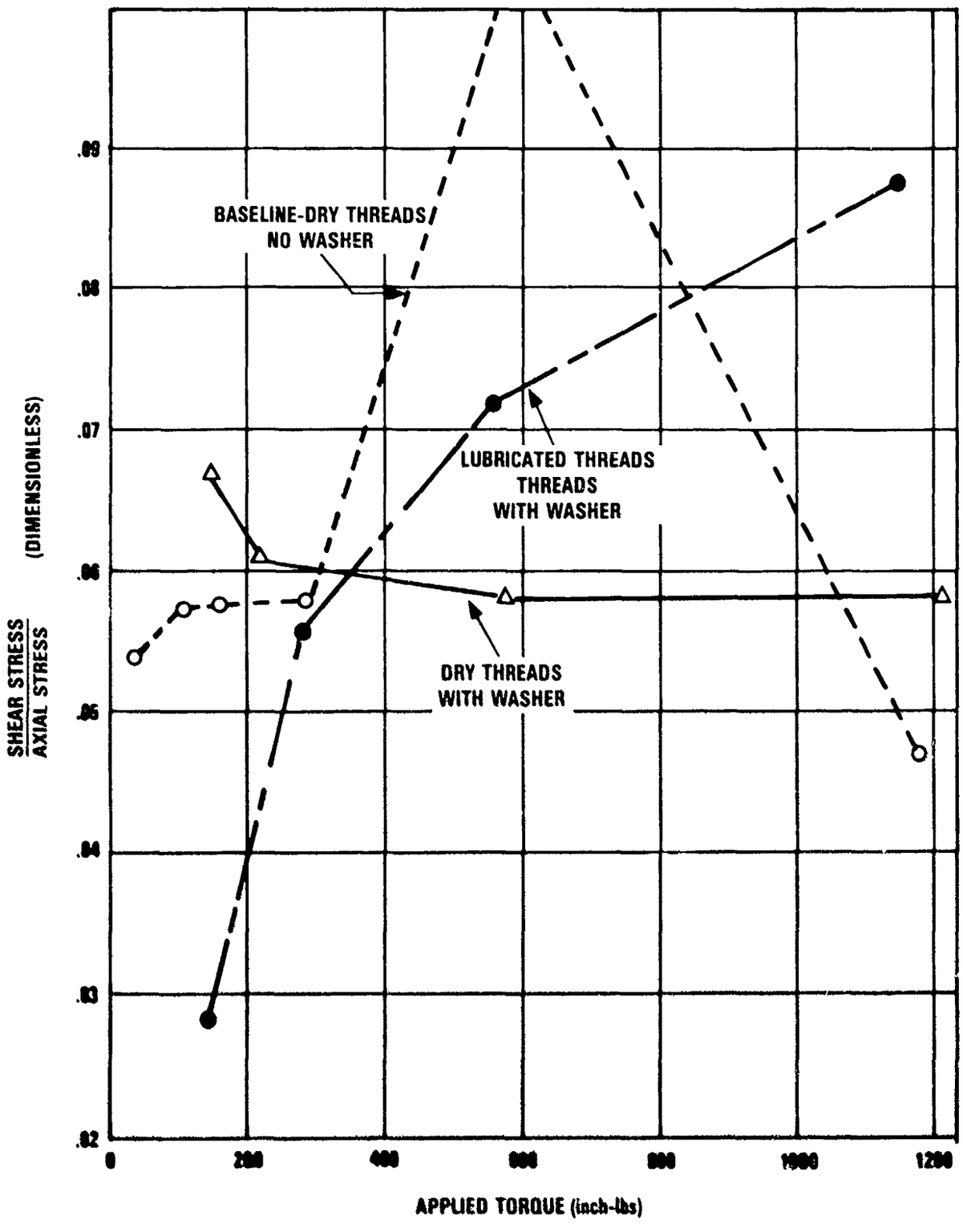

Figure A.1 Lab Experiment to Compare Shear and Tensile Loads in Torqued Bolt (.75" Diameter Steel)

An experiment was performed to determine if shear stresses might cause the acousto-elastic change in ultrasonic travel time through a fastener to be different for a torqued fastener than for a tension loaded fastener. The results plotted in Figure A.2 showed that for both cases the change in travel time was a linear function of axial stress load and that the effects of shear stresses could not be detected. The absence of non-linearities for the torqued fasteners showed that shear stress relaxations did not detectably change the calibration curve. It was concluded that the fasteners preload indicator could be calibrated on a 120 Kip Baldwin tensile testing machine.

A top-of-the-line pneumatic torque wrench was demonstrated by vendors and cut-off data taken during the expert demonstration are plotted in Figure A.3. Data were based on an electronically controlled cut-off that shut off the air supply when elastic limit loading was sensed. The tension was measured by torque gage and calibrated pressure washer reading taken at cut-off. The arrows indicate manufacturer's specifications as to expected cut-off accuracies. Although a linear relationship between torque and tension within the shaded area might be desired, data were scattered. This scatter is consistent with the results presented in Figure A.0.

A.2 Search for Suitable Prototype

Data files were collected on at least 16 different thickness gages (See Bibliography) and some of the most promising candidates were tested. One of the systems tested is shown in Figure A.4 (Bibliography listing #14). The calibration curve for the ultrasonic stress gauge in Figure A.5 shows that there was a tendency for linearity between ΔT and applied load but the spread in data was appreciable. The source of the trouble was concluded to be partly due to variations in travel time through the coupling between the fastener and the transducer. The fix for this problem (which was common to commercially available systems) was to measure the travel time between the first and second back surface echos because both sound beams travel through the same coupling thickness. The tacit assumption is that the coupling thickness does not vary significantly during the 50 microseconds separating the first and second back surface echos.

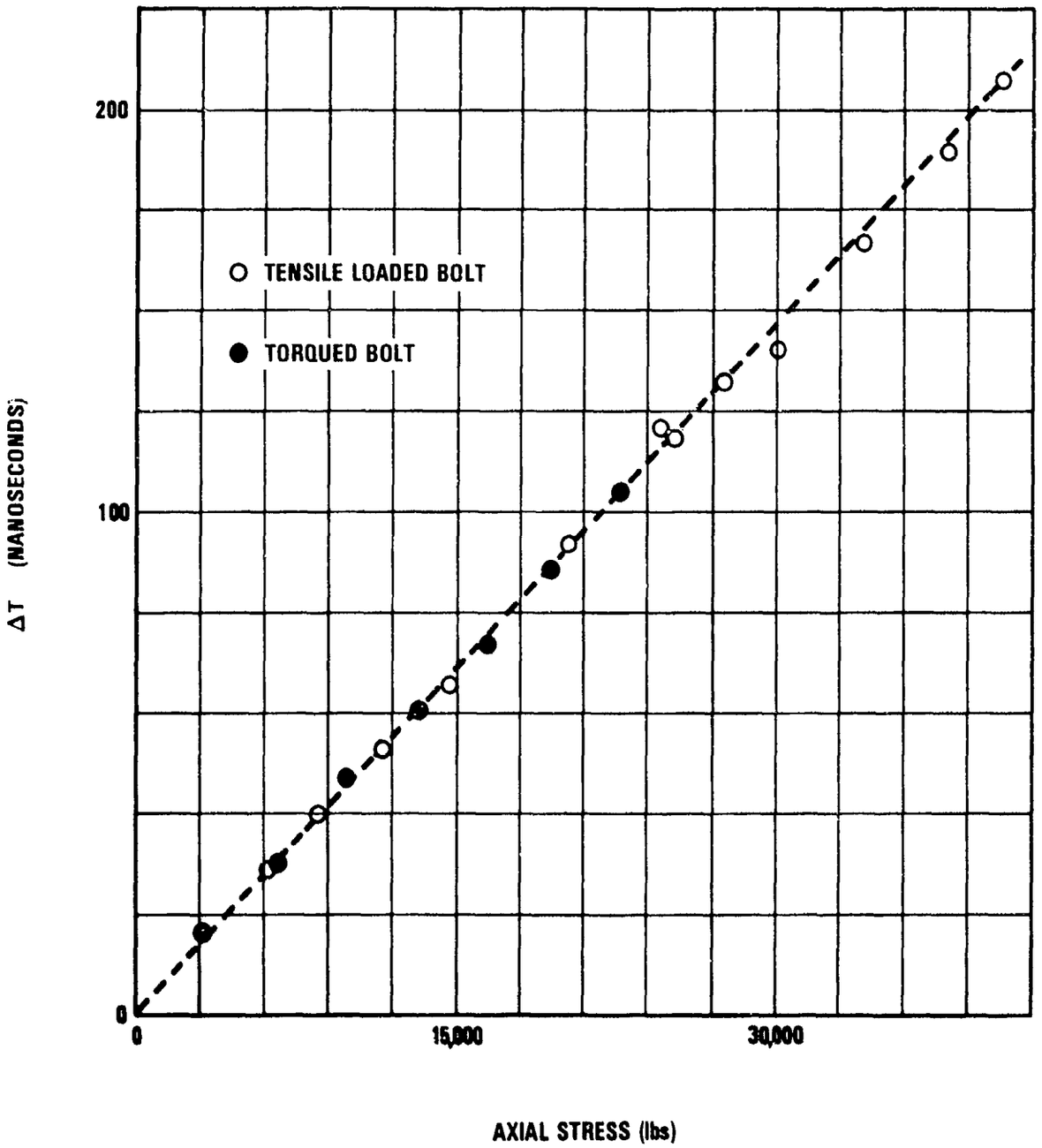

Figure A.2 A Comparison of ΔT Versus Axial Stress Applied by a Tensile Machine with the Corresponding ΔT Values Obtained When the Bolt was Torqued. The Presence of Shear Loading Did Not Effect ΔT

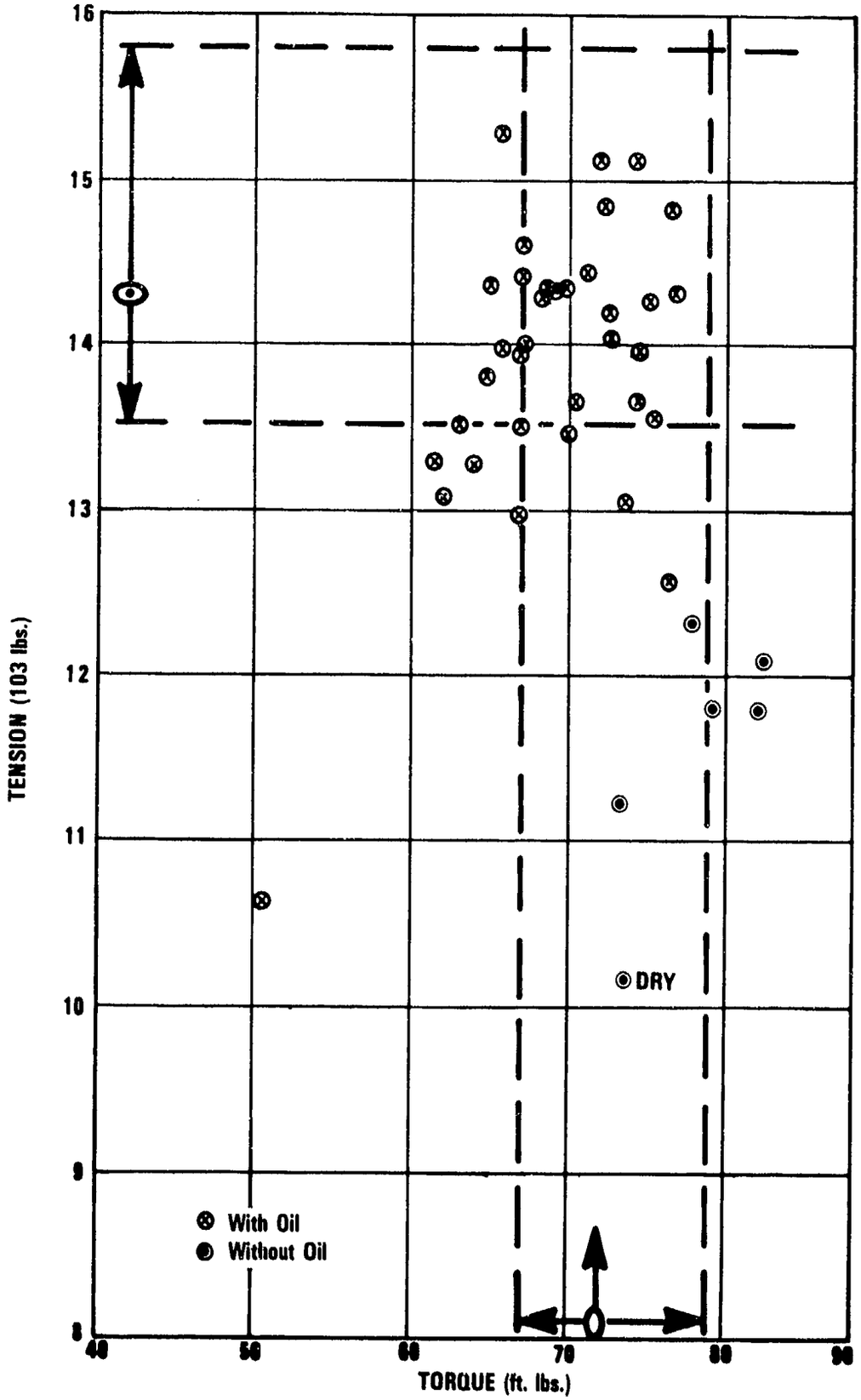

Figure A.3 Scatter in Tension Torque Data for Commercial Torque Wrench

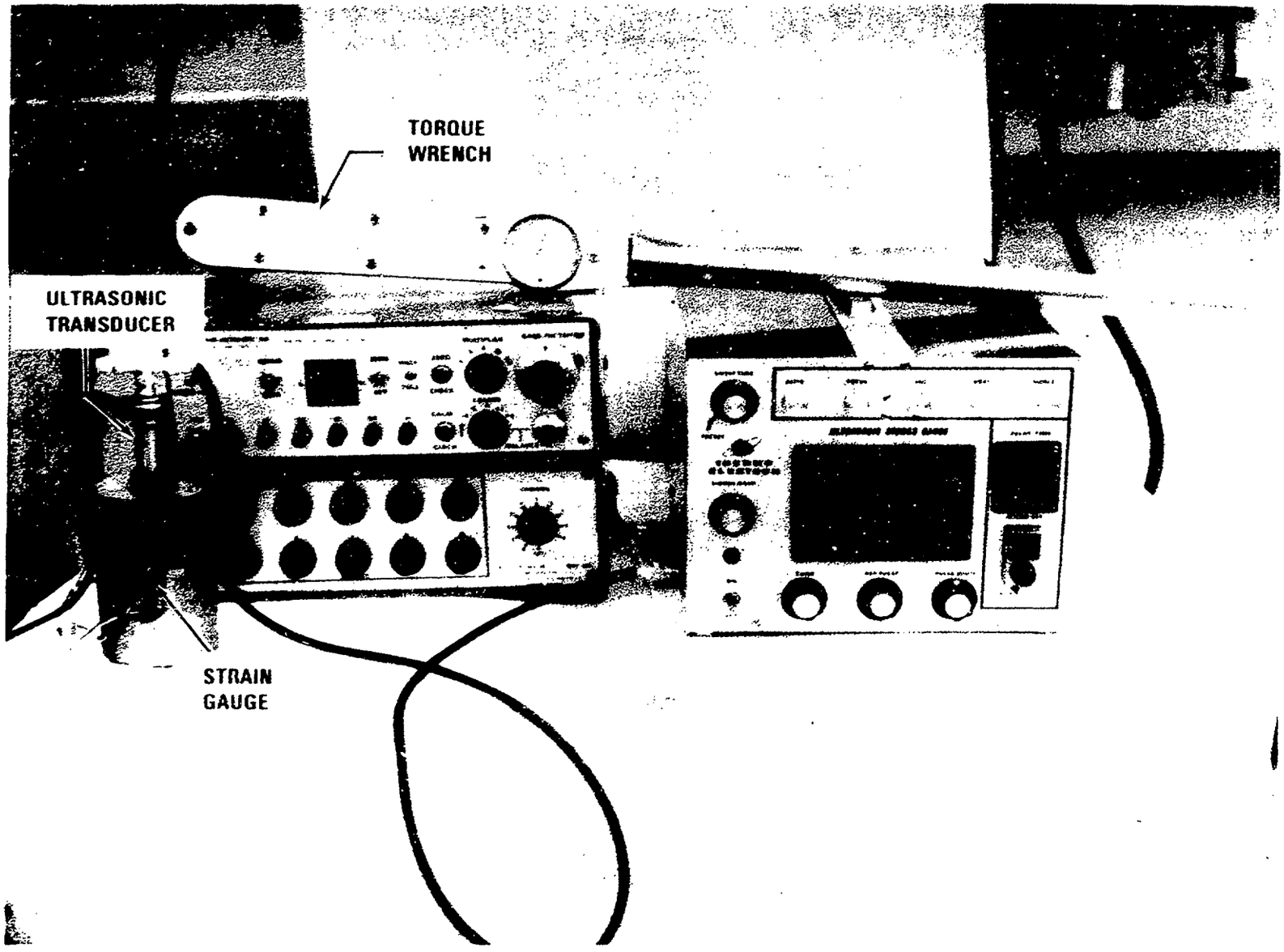

Figure A.4 Commercially Available Ultrasonic Stress Gauge

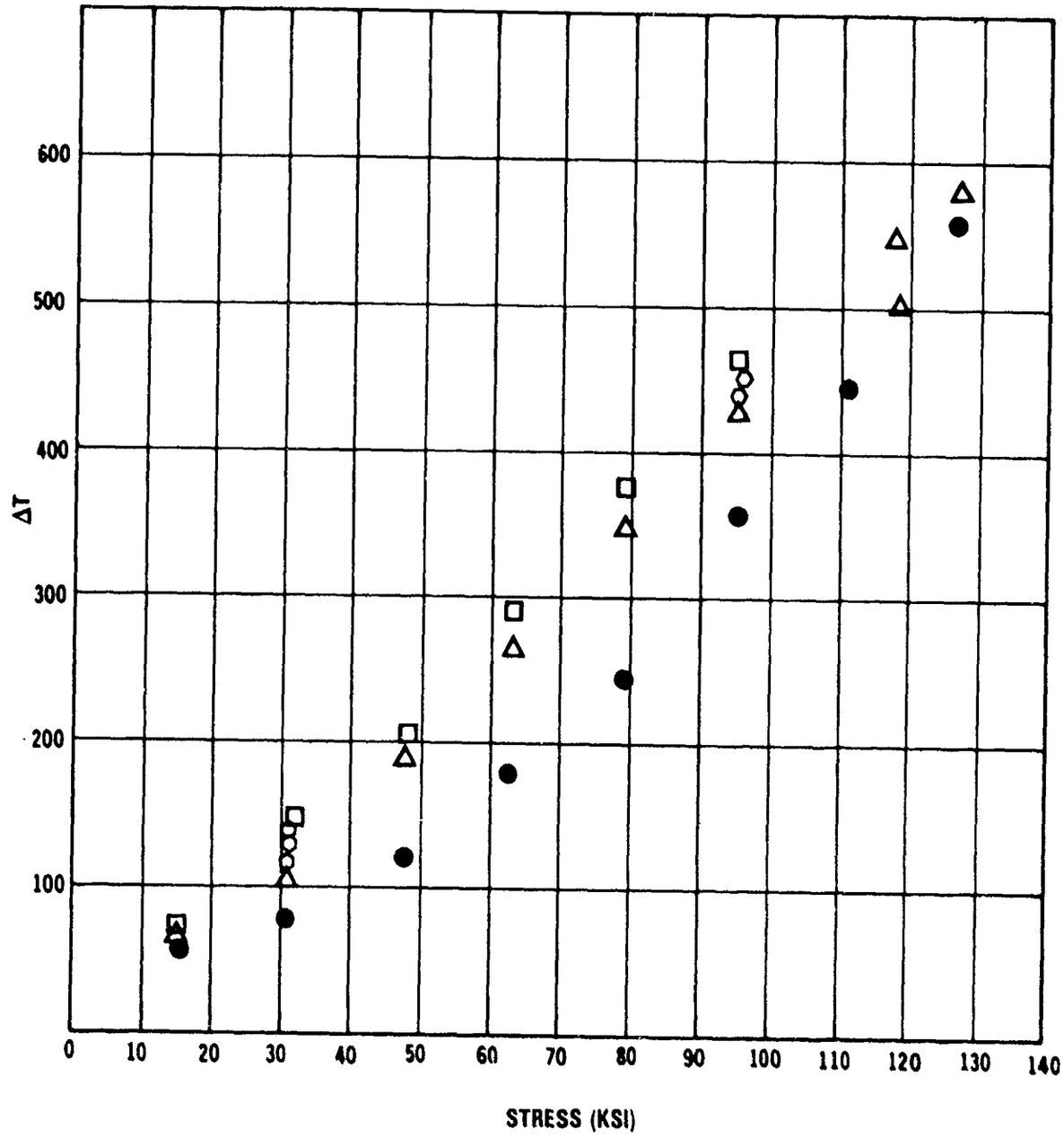

Figure A.5 Calibration Measurement Made with the Thermoelectron Strain Gauge (Phase Shift Method) ½" Steel

A.3 Calibration Procedures

A custom built electronic timing system (fully described in the process specification document ref. 5) was built for the calibration study. The system functioned without failure during the entire calibration phase of this contract.

The calibration plan was to test the relationship given in equation 3 (section II). That is to measure

$$\Delta T = \frac{\delta + \alpha D}{M} S$$

where δ = grip length
α = adjustment parameter assumed to be zero in calibration
D = fastener diameter
S = Applied stress
ΔT = acousto-elastic change in ultrasonic travel time
M = Material Constant

It was necessary to show that

(1) ΔT is linearly proportional to the average applied load (S = applied load divided by fastener area) and

(2) that the constant of proportionality "M" was not dependent upon stress nor on the fastener geometry.

Otherwise complete sets of calibration curves giving values for M as a function of all significant independent variables needed to be prepared.

A set of fastener holders similar to the one shown in Figure A.6 were built for the calibration measurements.(Figure A.7). Fasteners were loaded with a 120 Kip Baldwin testor while ΔT was measured after each increase in load.

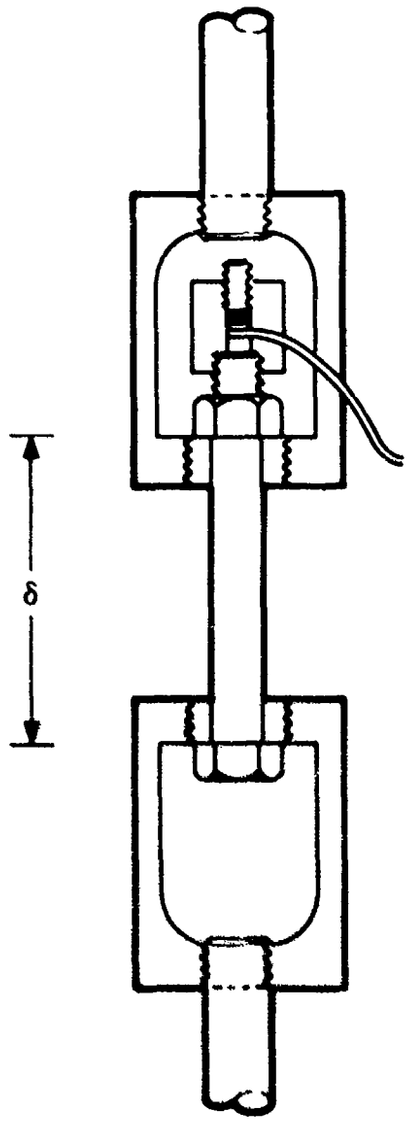

Figure A.6 Fixture Design for Use in Calibrating the Acousto-elastic Fastener Preload Indicator.

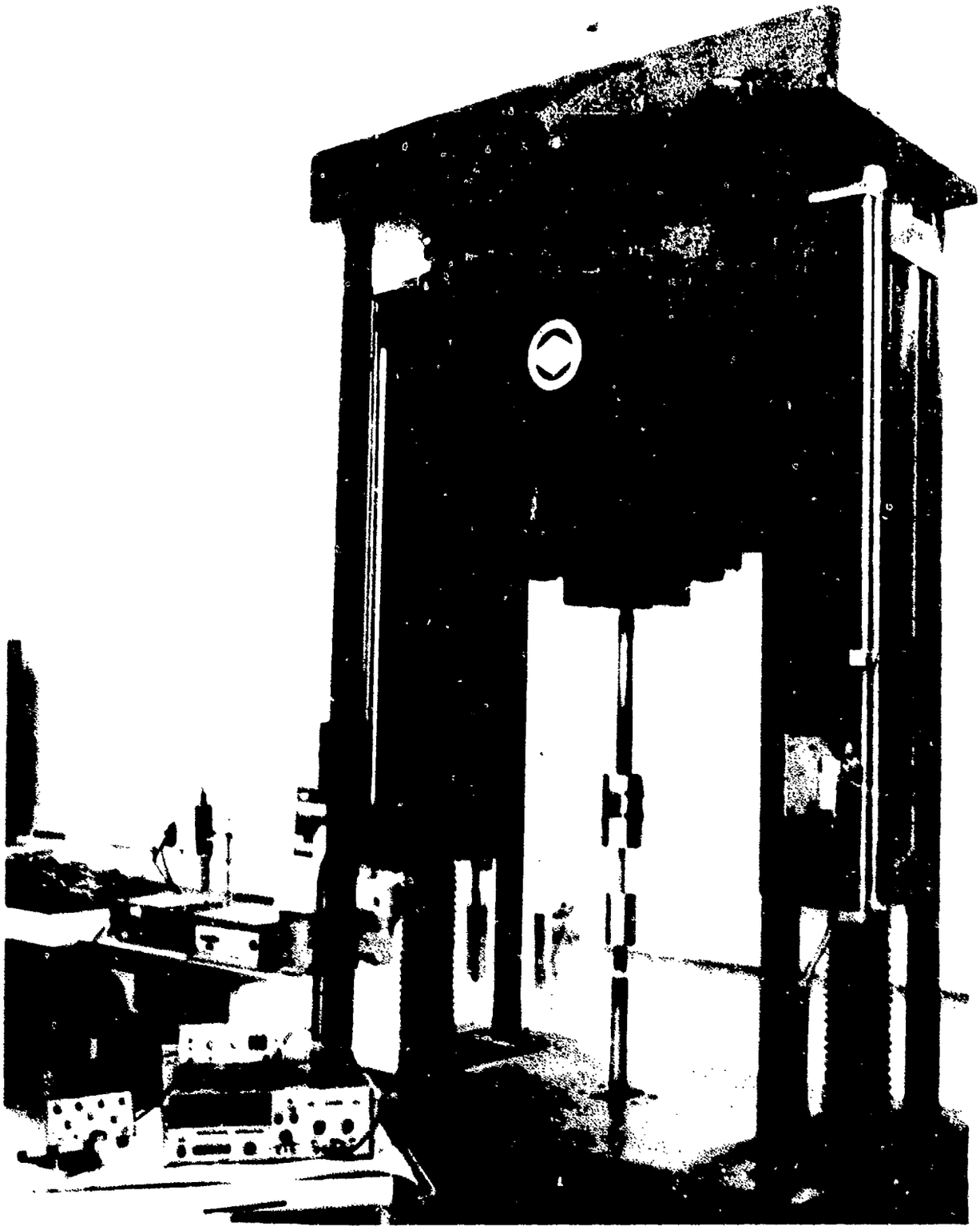

Figure A.7 120 Kip Baldwin with Fixture, 3/4" Fastener, and Early Version of Preload Indicator Prototype Set Up for Calibration Study.

A HP 9820 computing calculator program has been written (Figure A8) to perform data reduction as the data are collected during calibration measurements. This real time data reduction makes it possible to detect calibration problems when they occur or to continue with successive load - ΔT measurements until the material constant has been calculated with the desired statistical accuracy. This real time data recording and reduction requires dedicated use of a HP 9820.

The permanent calibration record for measurement number 124 is reproduced in Figure A9. Data beginning at the bottom of the first column and sequentially after that include:

Line #	Symbol	Result
1	L	Baldwin load (pounds)
2	T	Last Four digits of transit time (n.s.)
3	DTO	ΔT measured from T_o (n.s.)
4	S	Stress in fastener (ksi)
5	MO	Uncorrected material constant ($10^{-1.7}$)
6	DT	ΔT from least squares curve fit (n.s.)
7	M	Corrected material constant
8	MBAR	Average value for material constant
9	SIG	Standard deviation for the average

Notice in the code (Figure A.8) that the program computes a running least squares curve fit which should converge to the material constant but produce an upper bound to the standard deviation. The value of MBAR will be improved and the value for σ reduced if the data set $|\Delta T, S|$ are later fitted by a least squares curve fit to obtain a best fit value for T_o. Then a new set of M is computed and averaged as shown in Figure A.10.

When data in Figure A-10 are plotted, it can be seen from the graphical representation in Figure A.11 that ΔT is linearly dependent upon applied stress and from Figure A.12 that the material constant M is independent of the applied stress. These data are typical of data collected on all threaded rod stock and fasteners calibrated. Data are summarized in Tables A.1 through A.4 and the σ is indicative of how little M varied during a calibration test.

```
0:
ENT "DIAM"→R1,"F
LANGE"→R5,"TO"→R
7,"LOAD"→R2,"TIM
E"→R3⊢
1:
1.751→C;π→R11→R1
2→R13→R14→R15→R1
6→X⊢
2:
4R2/πR1R1→R6⊢
3:
R3-R7→R8→R10⊢
4:
CR5R6/R8→R9⊢
5:
R6/1000→R6⊢
6:
R9/1000→R9⊢
7:
IF X=1;R15+R9→R1
5;R16+R15→R16
⊢
8:
IF X>1;GTO 11⊢
9:
PRT "L,T,DTO,S,M
O,DT","M,MBAR,SI —
G"⊢
10:
PRT R2,R3,R8,R6,
R9,"F","F","F","
F";SPC 1;X+1→X⊢
11:
R6→A;R10→B;R11+A
→R11⊢
12:
R12+AB→R12⊢
13:
R13+AA→R13;B+A→B
⊢
14:
IF X≤1;GTO 17⊢
15:
(R11R12-R13R14)/
(R11R11-R13)→R4
;R8-R4→R 0⊢
16:
IF X>2;R9R8/R10→
R30;R15+R30→R15;
R16+R30R30→R16⊢
17:
IF X=1;ENT "LOAD
"→R2,"TIME"→R3;
GTO 2⊢
18:
IF X>2;PRT R2,R3
,R8,R6,R9,R10⊢
19:
IF X>2;PRT R9R8/
R10,R15/ X-1)⊢
20:
IF X>2;PRT SQR((R1
6-R15R15/(X-1))/
(X-2));SPC 1⊢
21:
X+1→X;ENT "LOAD"
→R2,"TIME"→R3⊢
22:
R11→R21;R12→R22;
R13→R23;R14→R24;
R15→R25;R16→R26;
X→R27⊢
23:
GTO 2⊢
24:
R21→R11;R22→R12;
R23→R13;R24→R14;
R25→R15;R26→R16;
R27-1→X⊢
25:
GTO 21⊢
26:
END ⊢
```

Figure A.8 Data Reduction Code Prepared for Real Time Processing of Calibration Results on the HP 9820 Computing Calculator

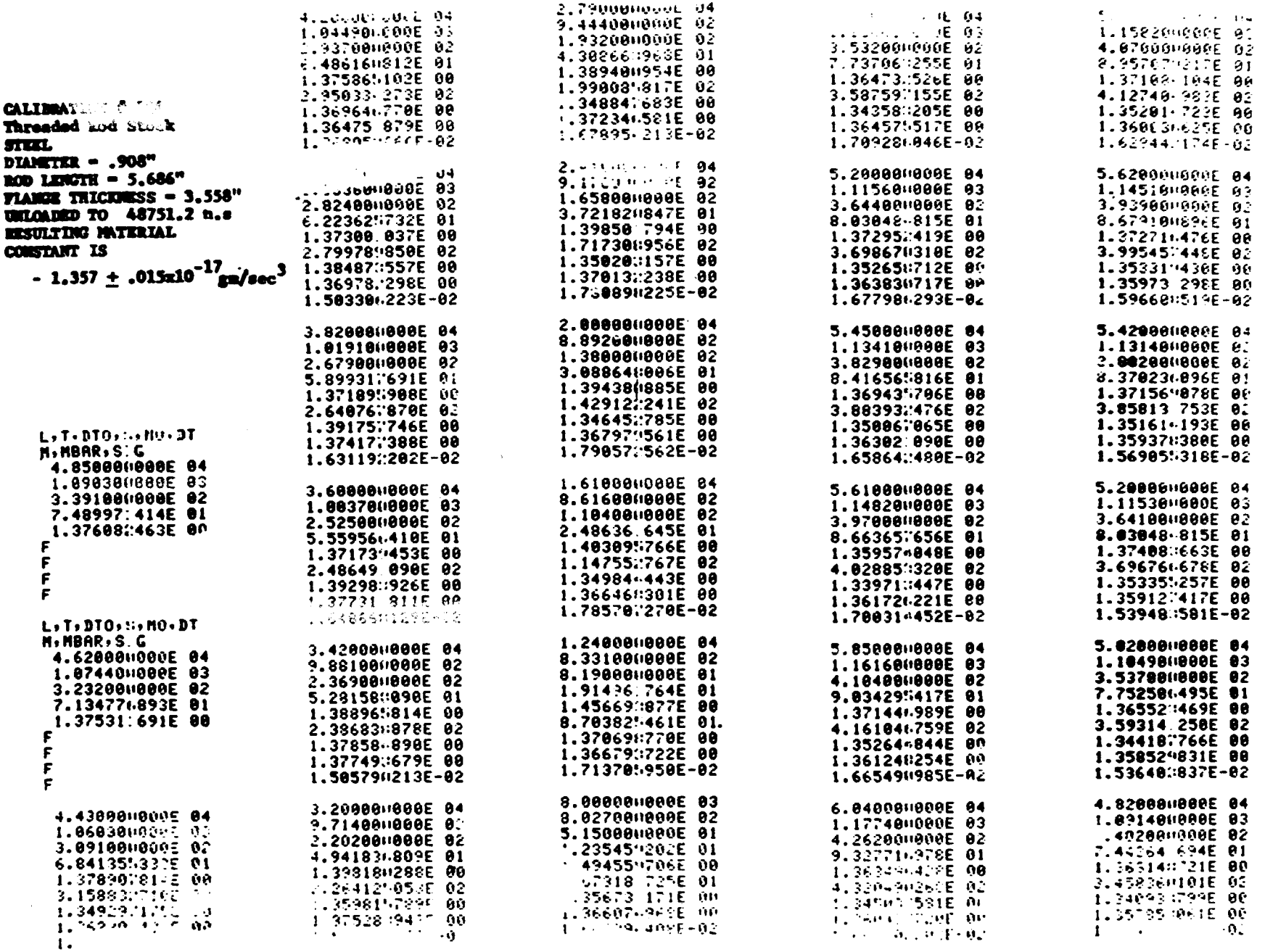

Figure A.9 Complete Listing of HP 9820 Results for the Measurement of the Material Constant for the Inch Diameter Threaded Steel Rod Stock

CALIBRATION RESULTS

Bolt Identification Threaded rod Bolt Number 124

Material Steel

TENSION Ksi	ΔT nanoseconds	M gm/sec^3
[illegible]	3.	-1.
7.1347[illegible]01	3.28836[illegible]02	-1.35173[illegible]17
6.84135[illegible]01	3.14736[illegible]02	-1.35421[illegible]17
6.48616[illegible]01	2.99336[illegible]02	1.34995[illegible]17
6.22362[illegible]01	2.88036[illegible]02	1.34613[illegible]17
5.89931[illegible]01	2.73536[illegible]02	-1.34362[illegible]17
5.55956[illegible]01	2.58136[illegible]02	-1.34178[illegible]17
5.28158[illegible]01	2.42536[illegible]02	-1.35668[illegible]17
4.94183[illegible]01	2.25836[illegible]02	-1.36328[illegible]17
4.30866[illegible]01	1.98836[illegible]02	-1.35001[illegible]17
3.72182[illegible]01	1.71436[illegible]02	-1.35252[illegible]17
3.08864[illegible]01	1.43636[illegible]02	-1.33966[illegible]17
2.48636[illegible]01	1.16036[illegible]02	-1.33494[illegible]17
1.91496[illegible]01	8.75360[illegible]01	-1.36290[illegible]17
1.23545[illegible]01	5.71360[illegible]01	-1.34713[illegible]17
7.73706[illegible]01	3.58836[illegible]02	-1.34329[illegible]17
8.03048[illegible]01	3.70036[illegible]02	-1.35204[illegible]17
8.41656[illegible]01	3.83536[illegible]02	-1.34957[illegible]17
8.66365[illegible]01	4.02636[illegible]02	-1.34054[illegible]17
9.03429[illegible]01	4.16036[illegible]02	-1.35286[illegible]17
9.32771[illegible]01	4.31836[illegible]02	-1.34570[illegible]17
8.95707[illegible]01	4.12636[illegible]02	-1.35235[illegible]17
8.67910[illegible]01	3.99536[illegible]02	-1.35335[illegible]17
8.37023[illegible]01	3.85836[illegible]02	-1.35153[illegible]17
8.03048[illegible]01	3.69736[illegible]02	-1.35313[illegible]17
7.75250[illegible]01	3.59336[illegible]02	-1.34410[illegible]17
7.44364 [illegible]01	3.45836[illegible]02	-1.34093[illegible]17
		-1.34917[illegible]17
		-6.75182[illegible]14

Bolt length (L) 5.686"
Bolt diameter (D) .908"
Grip length (S) 3.558"
Travel Time (T) 48745.6 ns
Sound Velocity (C) 5.926 x 10^5 cm/sec

δ/D 3.919

Figure A.10 Final Calibration Data for Threaded Steel Rod Stock

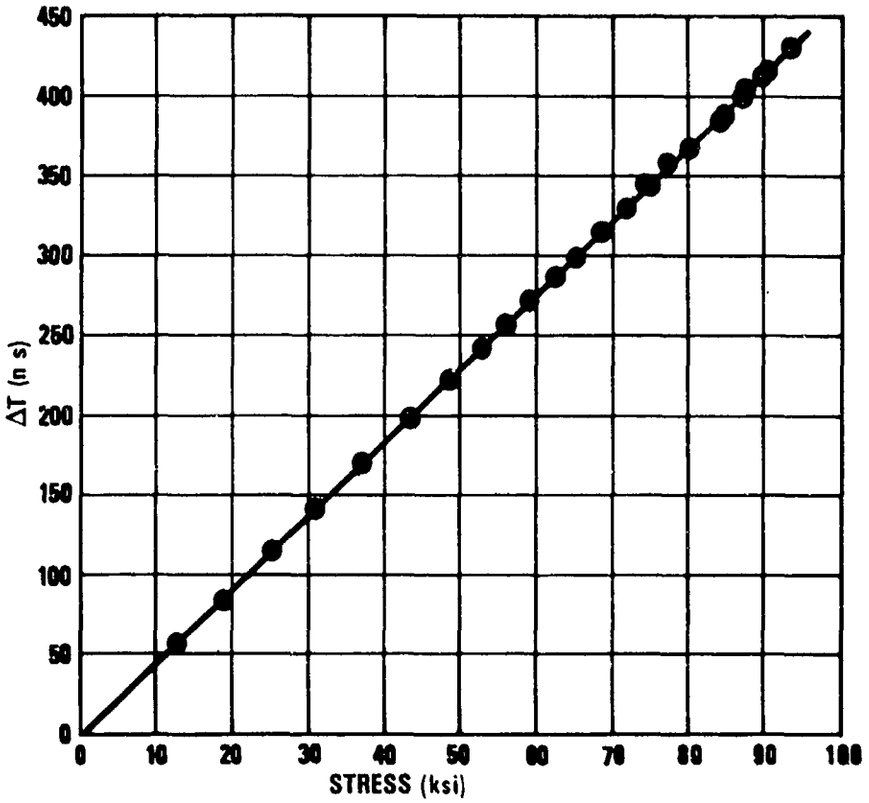

Figure A.11 Verification that the Increase in Ultrasonic Travel Time Through a Fastener is Linearly Dependent Upon Stress

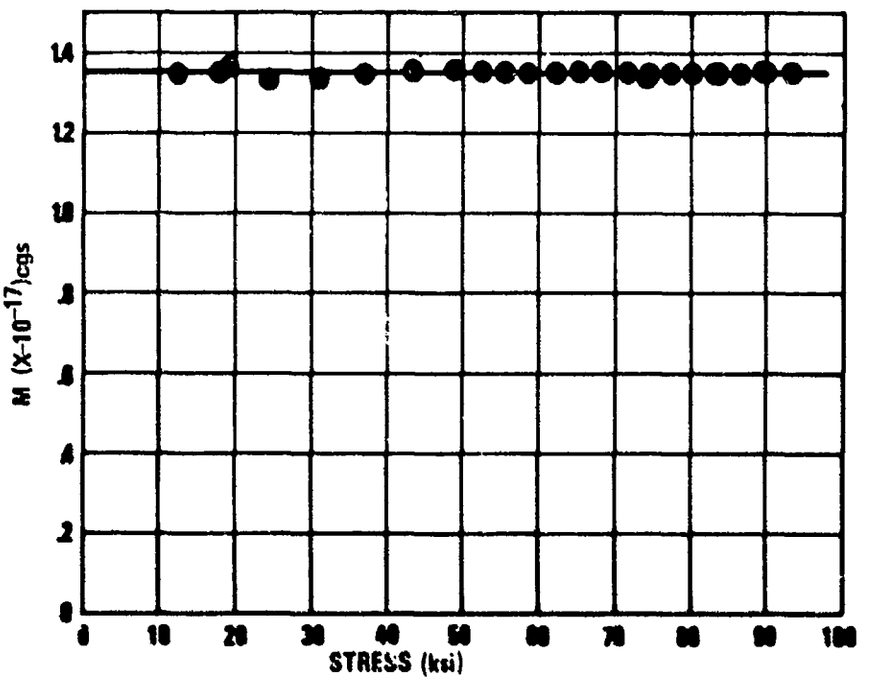

Figure A.12 Verification that a Material Constant M can be Measured that is Independent of Stress

TABLE A.1
CALIBRATION RESULTS (I)

160 KSI/Steel	L	D	δ	T	C	δ/D	M	σ	ρ
NAS 1106 16	1.502	.374	1.062	12970.2	5.883(5	2.840	1.353	.008	7.783
NAS 1112 44	3.521	.747	2.830	30315.1	5.900	3.788	1.554	.002	
NAS 1112 52	4.060	.752	3.321	34985.7	5.895	4.42	1.469	.006	
NAS 1112 96	6.768	.749	6.019	58668.1	5.860	8.04	1.606	.007	
NAS 1312 39	3.710	.747	2.362	32065.4	5.878	3.16	1.407	.010	
NAS 1310 24	2.604	.623	1.564	22443.1	5.903	2.51	1.405	.007	
NAS 1310 29	2.918	.623	1.865	25209.7	5.880	2.99	1.487	.011	7.832
NAS 1306 34	2.806	.374	2.176	24165.1	5.898	5.82	1.554	.018	7.809
NAS 1308 21	2.224	.497	1.345	19195.9	5.886	2.71	1.384	.013	7.808
NAS 1306 34	2.632	.373	2.171	22754.0	5.876	5.82	1.591	.007	7.778
NAS 1316 24	3.140	.998	1.549	27147.3	5.876	1.552	1.203	.013	
NAS 1106 34	2.631	.374	2.163	22711.1	5.885	5.783	1.504	.013	7.831
NAS 1316 32	3.660	.997	2.074	31581.1	5.887	2.08	1.342	.011	
NAS 1312 24	2.786	.747	1.573	24059.2	5.883	2.11	1.378	.004	
NAS 1316 29	3.466	.997	2.026	29920.0	5.885	2.03	1.357	.012	
NAS 1316 72	6.109	.997	4.568	53110.0	5.843	4.582	1.475	.014	
NAS 1316 32	3.633	.997	2.074	31387.5	5.880	2.08	1.300	.009	
NAS 1316 24	3.118	.997	1.532	26987.4	5.869	1.54	1.204	.011	
LSC	2.881	.997	1.039	24729.9	5.918	1.04	1.090	.013	
NAS 1309 28	2.776	.560	1.804	23939.6	5.891	3.221	1.381	.005	7.841
NAS 6206 13	1.384	.374	.844	11889.3	5.914	2.25	1.436	.009	7.801
NAS 6206 10	1.189	.374	.731	10212.9	5.914	1.95	1.315	.068	7.823

220 KSI/Steel	L	D	δ	T	C	δ/D	M	σ	ρ
C081 12A 43	3.942	.747	2.691	33503.8	5.977(5	3.60	1.468	.014	
C081 8 12	1.550	.497	.932	13141.5	4.992	1.88	1.294	.009	7.765
C7521 80 23	2.435	.497	1.685	20707.1	5.974	3.39	1.490	.014	7.749
C083 5A 72	4.516	.310	3.998	38496.0	5.959	12.90	1.566	.010	7.696
C081 6A 27	2.268	.375	1.765	19339.1	5.958	4.65	1.579	.008	7.741
C081 14A 25	3.040	.872	1.678	25721.4	6.004	1.92	1.243	.007	
C081 14A 48	4.467	.873	3.019	37961.1	5.978	3.46	1.434	.010	
C081 12A 35	3.439	.746	2.200	29203.1	5.982	2.95	1.442	.011	
C081 12A 28	3.014	.747	1.998	25546.1	5.994	2.67	1.383	.009	
C081 12A 14	2.136	.747	1.092	18138.6	5.982	1.46	1.147	.006	
C083 9A 52	4.373	.560	3.320	37105.4	5.987	5.93	1.474	.002	
C081 7A 35	2.903	.435	2.287	24652.2	5.982	5.234	1.577	.005	7.752
C081 7A 36	2.982	.435	2.386	25335.9	5.979	5.485	1.547	.010	7.751
C083 10 32	3.209	.623	2.094	27281.4	5.976	3.36	1.531	.007	
C083 12 34	3.516	.747	2.212	29818.2	5.990	2.96	1.489	.009	
C083 16 04	5.942	.497	4.093	50358.5	5.994	4.11	1.523	.010	
C081 16A 32	3.688	.998	2.026	31311.8	5.983	2.030	1.317	.008	
C083 16 32	3.736	.998	1.963	31725.2	5.982	1.97	1.242	.004	

TABLE A.2

CALIBRATION RESULTS (II)

260 KSI Steel	L	D	δ	T	C	δ/D	M	σ	ρ
MS 21296 05019	2.035	.310	1.393	17388.9	5.945	4.494	1.143	.049	
MS 21296	3.061	.558	1.868	26228.6	5.928	3.348	1.358	.008	
MS 21297 14056	5.276	.871	3.534	44851.6	5.976	4.057	1.464	.012	
MS 21297 14054	5.196	.872	3.450	44162.0	5.977	3.96	1.465	.005	
MS 21296 09 28	3.128	.562	1.851	26593.3	5.975	3.29	1.362	.005	
MS 21297 A 12044	4.415	.747	2.833	37705.7	5.948	3.79	1.474	.005	
MS 21297 12034	3.774	.747	2.206	32004.4	5.990	2.95	1.414	.008	
MS 21296 10018	2.609	.623	1.404	22207.9	5.968	2.254	1.371	.017	
MS 21296 7 17	2.173	.436	1.172	18506.2	5.965	2.688	1.341	.014	7.745
MS 21296 09026	2.947	.560	1.835	25087.0	5.968	3.277	1.416	.010	
MS 21296 09027	3.046	.560	1.715	25967.3	5.959	3.063	1.343	.006	
MS 21296 05 19	2.031	.311	1.443	17357.1	5.944	4.640	1.327	.004	7.737
MS 21296 06 16	1.959	.372	1.045	16727.9	5.949	2.809	1.292	.019	7.750
MS 21296 07048	4.059	.436	3.114	34694.5	5.940	7.142	1.48[illegible]	.009	7.743
MS 21296 06016	1.935	.374	1.027	16462.8	5.971	2.746	1.379	.020	7.719
MS 21297 06026	2.536	.373	1.653	21594.1	5.966	4.442	1.543	.026	7.724
MS 21297 08013	2.456	.497	1.339	20847.1	5.985	2.690	1.[illegible]46	.014	
MS 21297 16072	6.687	1.002	4.538	56654.7	5.996	4.53	1.500	.007	
Mixed Steel	**L**	**D**	**δ**	**T**	**C**	**δ/D**	**M**	**σ**	**ρ**
EWSB 930 5	3.924	.310	3.357	33629.3	5.928(5	10.82	1.554	.004	7.867
NAS 1005 12	1.581	.311	1.017	13999.1	5.737	3.270	1.649	.231	7.930
EWSB 930 7	3.010	.436	2.354	25775.1	5.932	5.399	1.581	.014	
	1.916	.497	.934	16507.7	5.896	1.879	1.295	.008	7.801
EWSB 930-6	1.507	.372	.930	12919.0	5.926	2.50	1.331	.011	7.904
GD Alloy		.862	3.288	46564.3		3.81	1.538	.014	
4450-8	1.968	.497	1.184	16713.6	5.982	2.38	1.347	.021	7.752
6A1-4V-Ti	**L**	**D**	**δ**	**T**	**C**	**δ/D**	**M**	**σ**	**ρ**
NAS 675 V16	1.639	.310	1.133	13720.7	6.008	3.645	.979	.010	4.418
NAS 676 V21	2.087	.374	1.422	173248	6.120	3.802	1.239	.005	4.424
NAS 675 V17	1.698	.310	1.125	14157.3	6.093	3.629	1.096	.012	4.422
NAS 674 V29	2.375	.249	1.868	19697.4	6.125	7.502	1.430	.010	4.424
NAS 674 V38	2.940	.249	2.461	24460.8	6.106	9.883	1.307	.004	4.431
NAS 674 V36	2.806	.249	2.312	23367.1	6.100	9.285	1.351	.008	4.418
NAS 677 V18	1.946	.437	1.380	16011.6	6.174	3.160	.795	.022	4.427
NAS 674 V24	2.054	.246	1.566	17110.2	6.098	6.366	1.365	.013	4.414
NAS 674 V32	THREADS STRIPPED AT 3100#								4.298
NAS 6407 21	2.002	.436	1.439	16697.4	6.091	3.300	1.238	.005	4.428
NAS 674 V28	2.307	.249	1.796	19101.6	6.135	7.213	1.302	.009	4.429
NAS 655 V20	1.784	.311	1.321	14863.7	6.097	4.248	1.066	.010	4.422
NAS 675 V23	2.069	.310	1.504	17193.0	6.113	4.852	1.261	.005	4.424
NAS 676 V20	2.028	.373	1.296	16863.4	6.109	3.475	1.215	.005	4.424
NAS 6406 L 12	1.326	.374	.805	11067.	6.371	2.152	1.407	.035	4.408
NAS 675 V 32	BOLT BROKE AT 2500#								4.424
NAS 677 V18	1.950	.435	1.19[illegible]	16111.6	6.148	2.74	1.266	.008	4.422
NAS 674 V48	2.692	.246	2.19[illegible]	22588.5	6.054	8.915	1.310	.006	4.404
B30 MR 12	3.765	.747	2.444	31241.4	6.122	3.27	1.211	.009	

TABLE A.3

CALIBRATION RESULTS (III)

THREADED ALUMINUM	L	D	δ	T	C	δ/D	M	σ
Al 116	5.993	.343	2.167	48012.4	6.341	6.32	-.400(17	-.007(17
Al 115	5.993	.343	2.637	48006.1	6.342	7.69	-.437	-.003
Al 114	5.993	.343	3.417	48004.6	6.342	9.96	-.430	-.006
Al 113	5.993	.343	3.846	47991.7	6.344	11.21	-.426	-.020
Al 112	5.993	.343	4.633	48007.9	6.342	13.51	-.437	-.008
Al 88	5.992	.461	1.480	47869.2	6.359	3.21	-.413	-.004
Al 87	5.992	.461	2.322	47861.5	6.360	5.04	-.438	-.006
Al 86	5.992	.461	3.648	47866.9	6.359	7.91	-.464	-.007
Al 85	5.992	.461	4.648	47912.5	6.353	10.08	-.496	-.008
Al 84	5.992	.461	4.648	47870.4	6.359	10.08	-.455	-.007
Al 90	5.455	.680	3.307	43593.6	6.357	4.86	-.416	-.025
Al 89	5.455	.680	3.920			5.77	-.438	-.013
Al 136	5.754	.800	2.978	45909.0	6.367	3.72	-.416	-.002
Al 135	5.754	.800	3.758	45902.0	6.37	4.69	-.431	-.002
Al 134	5.754	.800	4.092	45954.5	6.36	5.12	-.383	-.007
Al 133	5.817	.903	2.770	46378.3	6.37	3.07	-.387	-.001
Al 132	5.817	.903	3.196	46418.2	6.366	3.54	-.381	-.001
Al 131	5.817	.903	3.566			3.95	-.408	-.001
THREADED - Ti	**L**	**D**	**δ**	**T**	**C**	**δ/D**	**M**	**σ**
Ti 110	5.910	.345	1.779	49818.5	6.026	5.16	-1.09(17	-.007(17
Ti 111	5.910	.345	2.381	49821.6	6.026	5.16	-1.15	±.009
Ti 109	5.910	.345	2.870	49813.6	6.027	8.32	-1.16	-.007
Ti 108	5.910	.345	3.599	49838.9	6.024	10.43	-1.18	-.017
Ti 102	5.910	.345	4.407	49793.7	6.029	12.77	-1.12	±.028
Ti 103	5.910	.345	4.407	49841.2	6.023	12.77	-1.18	-.009
Ti 104	5.910	.345	4.407	49844.1	6.023	12.77	-1.20	-.011
Ti 105	5.910	.345	4.563	49916.6	6.014	13.23	-1.23	-.014
Ti 106	5.910	.345	4.407	49808.2	6.028	12.77	-1.16	-.011
Ti 107	5.910	.345	4.407	49796.1	6.029	12.77	-1.11	-.016
Ti 98	5.980	.461	2.634	50493.8	6.016	5.71	-1.17	-.012
Ti 96	5.980	.461	3.069	50517.5	6.013	6.66	-1.16	±.001
Ti 95	5.980	.461	4.171	50469.0	6.019	9.05	-1.18	-.004
Ti 94	5.980	.461	4.892	50516.9	6.013	10.61	-1.21	-.002
Ti 123	5.330	.797	2.822	44817.8	6.041	3.54	-1.26	.007
Ti 122	5.330	.797	3.206	44790.3	6.045	4.02	-1.32	-.006
Ti 130	5.754	.906	2.842	47569.7	6.15	3.14	-1.14	-.004
Ti 129	5.754	.906	3.297	47567.6	6.14	3.64	-1.08	-.008
Ti 128	5.754	.906	3.297	47567.9	6.14	3.64	-1.07	-.006
Ti 127	5.754	.906	4.009	47554.9	6.15	4.42	-1.25	-.007
Ti 97	5.980	.461	2.634	50511.9	6.014	5.71	-1.11	-.006
Ti 137	5.506	.686	4.326	47038.7	5.946	6.31	-1.50	-.006

TABLE A.4

CALIBRATION RESULTS (IV)

THREADED STEEL	L	D	δ	T	C	δ/D	M	σ
S-119	5.904	.337	3.303	46896.8	6.395 (5	9.80	-1.34(17	-.021(17
S-118	5.904	.337	3.749	50893.0	5.893	11.12	-1.33	-.020
S-117	5.904	.337	4.350	50975.1	5.884	12.91	-1.32	-.020
S-74	5.983	.461	1.160	51468.9	5.906	2.52	1.21	-.011
S-75	5.983	.461	1.160	51461.3	5.906	2.52	1.25	-.005
S-72	5.983	.461	2.469	51467.2	5.905	6.43	1.325	-.022
S-76	5.983	.461	2.768	51489.8	5.903	6.00	1.322	-.008
S-71	5.983	.461	2.963	5.359.4	5.918	6.43	1.394	-.013
S-59	5.983	.461	3.071	51331.4	5.921	6.66	1.378	-.014
S-60	5.983	.461	3.071	51390.7	5.914	6.66	1.319	-.009
S-70	5.983	.461	2.963	51464.1	5.906	6.43	1.418	-.017
S-69	5.983	.461	3.8135	51498.8	5.902	8.27	1.396	-.017
S-68	5.983	.461	3.8135	51452.5	5.907	8.27	1.402	-.011
S-66	5.983	.461	4.145	51446.9	5.909	8.99	1.425	-.012
S-67	5.983	.461	4.170	51449.8	5.907	9.05	1.439	-.015
S-78	5.983	.461	4.465	51193.2	5.937	9.69	1.371	-.017
S-63	5.983	.461	4.756	51452.5	5.907	10.32	1.371	-.013
S-64	5.983	.461	4.779	51421.9	5.911	10.37	1.294	-.035
S-65	5.983	.461	4.779	51411.9	5.918	10.37	1.298	-.031
S-93	5.204	.685	1.954	44612.2	5.926	2.85	-1.34	-.008
S-92	5.204	.685	2.881	44609.5	5.926	4.21	-1.40	-.015
S-91	5.204	.685	3.860	44602.5	5.927	5.64	-1.52	-.010
S-121	5.415	.797	2.948	46372.1	5.932	3.70	-1.30	-.005
S-120	5.415	.797	3.303	46379.2	5.931	4.14	-1.37	-.008
S-126	5.686	.908	2.836	48747.7	5.925	3.12	-1.25	-.006
S-125	5.686	.908	3.076	48754.7	5.925	3.39	-1.31	-.016
S-124	5.686	.908	3.558	48745.6	5.926	3.919	-1.349	-6.75
THREADED MOLY	L	D	δ	T	C	δ/D	M	σ
MO 83	5.936	.461	3.706	46719.9	6.454	8.04	-2.99(17	-.017(17
MO 82	5.936	.461	4.624	46723.7	6.454	10.03	-3.29	-.001
MO 80	5.936	.461	6.313	59106.8	5.101	13.69	-3.37	-.073
MO 81	5.936	.461	6.313	51106.1	5.900	13.69	-3.32	-.069
THREADED COPPER	L	D	δ	T	C	δ/D	M	σ
Cu 138	4.964	.875	3.254	54034.6	4.667	3.718	-.382(17	-.007
Cu 139	4.964	.875	3.254	54014.0	4.668	3.718	-.384	-.008
Cu 140	4.964	.875	3.254	54090.8	4.662	3.718	-.441	-.014
Cu 141	4.955	.875	3.312	54122.2	4.651	3.785	-.406	-.005

When data (e.g. all steel fastener data) are plotted against fastener length or grip length, data are scattered. A non-linear regression analysis had to be performed in order to identify that a significant correlation between ΔT and the ratio δ/D existed.

When steel data were plotted as a function of δ/D, the correlation shown in Figure A.13 was observed. The lines drawn show the $\pm$ five percent limits.

The apparent dependence of M upon fastener diameter which was not expected at the beginning of the calibration study was found to be caused by non uniform tension in loaded fasteners. The correction for this effect is discussed in Appendix B.

A.4 Effects of Inelastic Strain

A fully annealed threaded rod stock specimen made of titanium was installed on a 12,000 lb Baldwin and the material constant was measured. Figure A.14 shows that the bolt strained inelastically as the load was increased to 12 ksi, then the strain relieved elastically. The increase in zero load travel time for the ultrasonic beam from 561 to 627 ns was due to the inelastic strain of work hardening.

These results show that inelastic strain produces a non-linearity between ΔT and stress and then after work hardening, the relationship becomes linear. It is questionable whether the threshold for inelastic strain can be measured with much accuracy by acousto-elasticity.

The increase in travel time over the linear range in Figure A-14 was 851-627 = 224 ns. 59.2 nanoseconds can be attributed to elastic strain and the remaining 164 ns are due to the nut seating in the threads and to the effects of third order elastic constants. This finding, that .264 ΔT is due to physical changes in length and .736 ΔT is due to higher order elastic constant effects, is consistent with the theoretical prediction that the strain portion of ΔT should be:

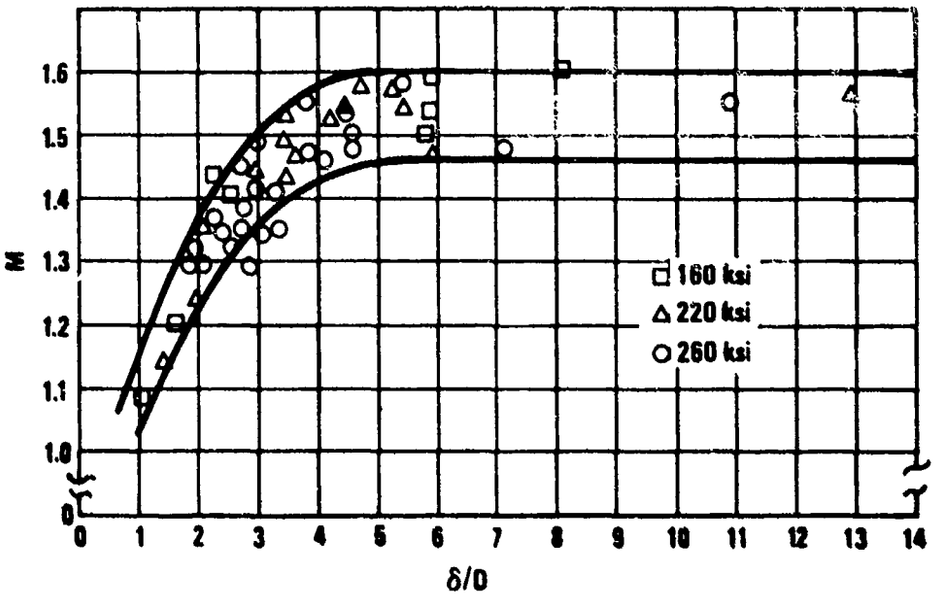

Figure A.13 Graphical Representation Showing the Dependence of the Material Constant for Steel upon the Ratio δ/D.

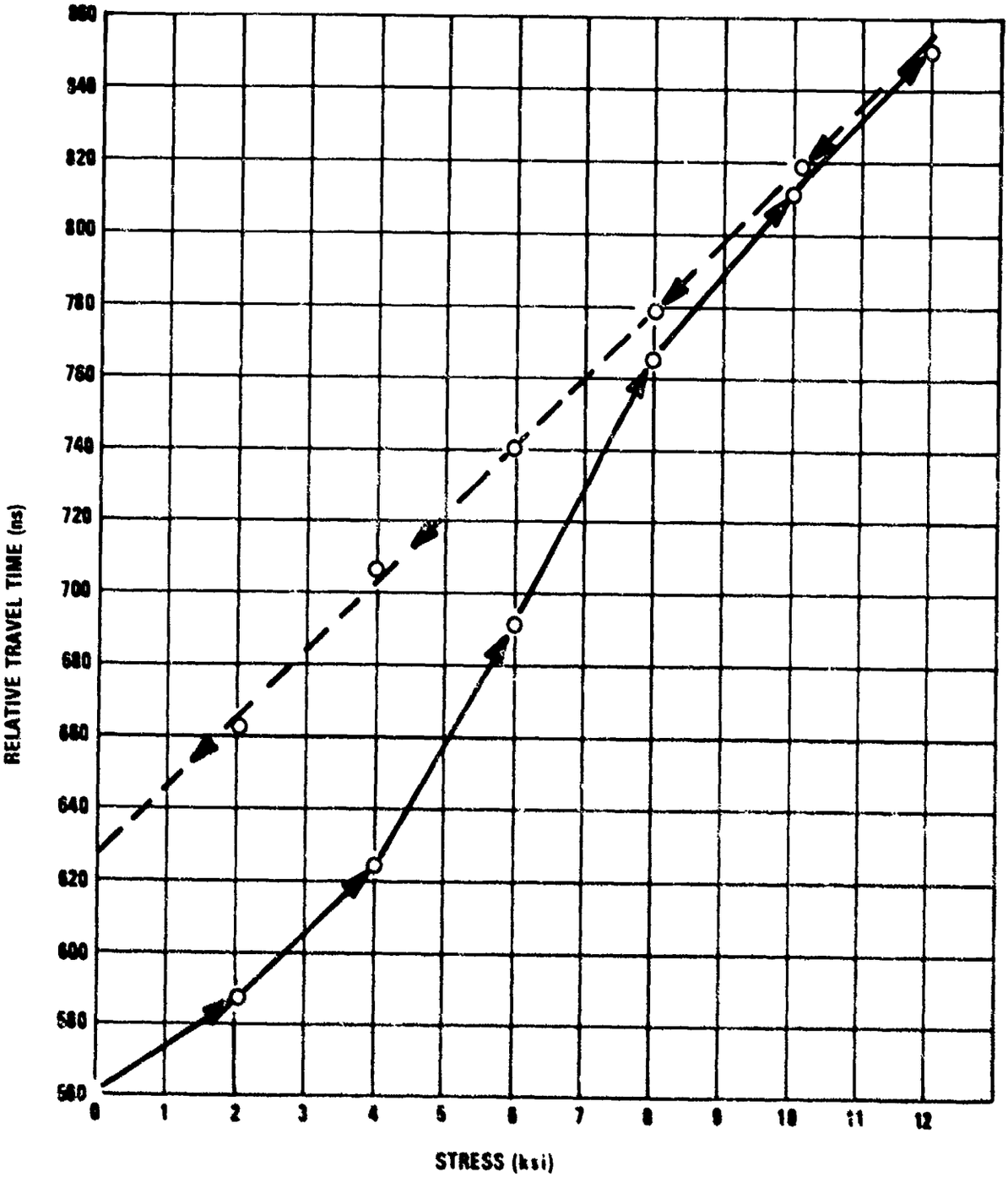

Figure A.14 The Signature of Inelastic Strain in Annealed Titanium Threaded Rod Stock Showing Work Hardening

$$\frac{\Delta T \text{ due to strain}}{\text{Total } \Delta T} = \frac{1}{2 + \frac{\mu(\lambda + 2\ell)}{(\mu+\lambda)(2\mu+\lambda)} + \frac{10\mu + 4\lambda + 4m}{2\mu + \lambda}}$$

which evaluates to be: *

STEEL	REX 535 NICKEL-Steel	.341
	Hecla 37 (0.4%c)	.256
	Hecla 17(0.6%c)	.342
	Hecla 138A	.274
	Rex 535 Ni Steel	.364
	Hecla ATV Austenitic	.119
	Rail Steel	.330

$.293 \pm .079$

Al *	2S	.105
	B53S M	.308
	P	.196
	D54S	.099
	JH77S	.105

$.243 \pm .104$

The consistency between the theoretical predictions of the strain fraction and the experimental finding is another good test of the soundness of acousto-elastic theory.

* The higher order elastic constants are given in Reference 6.

APPENDIX B

EMPIRICAL CORRECTION FOR NON UNIFORM TENSION

B.1 Evidence in the Literature of Non Uniform Tension in Fasteners

A literature search provided data reproduced in Figure B-1 which indicated by the photoelastic effect that tensions are extremely non-uniform near the head and nut ends of a fastener. Figure B-1 shows that there is some tension symmetry at the flange-head interface with a concentration of tension that may be as much as four times the average tension in the fastener. The figure also shows that the tension in a fastener becomes uniform at about one fastener diameter below the head. Fastener length to diameter ratios less than 2 could not be treated analytically without special concern for non-uniformity of stress.

The effects of stress perturbations can be observed in fastener calibration as shown in the apparent dependence of the material constant upon δ/D. This is shown in Figure B-2 where all of the material constants for steel are normalized to unity at $\delta/D = 13$ and plotted as a function of δ/D. The correlation (grip length to fastener diameter ratio) between the material constant and the ratio δ/D was revealed by a non linear regression analysis performed by the Operations Research Group at General Dynamics. As expected from the graph in Figure B-1, the tension reduction along the centerline of short fasteners was seen when the material constant was computed from the simple relationship

$$M = \frac{\delta}{\Delta T} S \qquad \text{B.1}$$

where δ = grip length
S = Average applied stress
ΔT = Acoustio-elastic change in sound travel time

Equation B.1 can be derived by assuming that the average stress occurs only through the grip length along the center line of the fastener.

Unless this apparent dependence of M upon δ/D can be resolved, one must prepare a family of calibration curves where the appropriate value of M must be selected by table look-up in order to accurately preload a fastener of diameter D on a flange of thickness δ .

B.2 Finite Elements Studies of Non Uniform Tension in Fasteners

The acousto-elastic effect is a phenomena through which the velocity of sound in a media depends upon the stress forces "S" applied to the media. Analytically, the velocity of sound in the direction of the applied stress is giver by

$$v = v_o \sqrt{1 - \frac{S}{3K\ (2\mu+\lambda)} \left[\frac{\mu+\lambda}{\mu}\ (10\mu+4\lambda+4m^*)+\lambda+21^*\right]} \qquad \text{B.1}$$

where v_o = velocity of sound with no stress (cm/sec)
S^o = stress (dynes/cm^2)
K = compressibility (dynes/cm^2)
P = specific gravity
μ, λ = Lame' constants
l^*, m^* = Murnaghan constants

The change in travel time through an elemental length dl is approximately

$$dt = \left(\frac{1}{v_o} - \frac{1}{v}\right) dl \simeq \frac{S(l)\ dl}{2m} \qquad \text{B.2}$$

where m is a constant depending only on the properties of the fastener material and given by:

$$m = \frac{3\mu K\ (2\mu+\lambda)^{3/2}}{\sqrt{\rho}\ \left|(\mu+\lambda)\ (10\mu+4\lambda+4m^*+\mu(\lambda+21^*)\right|} \qquad \text{B.3}$$

The round trip change in travel time of a pulse of ultrasound that travels down the centerline of a fastener of length L and returns to the start point is given by

$$\Delta T = 2 \int_0^L \frac{S(l)}{2m}\ dl = \frac{1}{m} \int_0^L S(l)\ dl \qquad \text{B.4}$$

Defining a stress reduction factor

$$s(1) = \frac{S(1)}{\bar{S}} = \frac{S(1)}{(4\ F)/(\pi D^2)} \qquad B.5$$

where F = Load applied to a fastener and
D = Fastener diameter

we find

$$\Delta T = \frac{\bar{S}}{m} \int_0^L s(1)\ dl \qquad B.6$$

In the first progress report (IR 818-6 (I)) we derived an expression of the form

$$\Delta T = \frac{\delta \bar{S}}{M} \qquad B.7$$

in which it was assumed that (to a first approximation) the average tension might be applied over the grip length δ. That is, we assumed that

$$\int_0^L s(1)\ dl = \left(\frac{m}{M}\right)\delta \qquad B.8$$

and that m/M was given by a non uniform tension factor

$$G = \frac{\int_o^L S(1)\ \ dl}{(4\ \delta F/\ \pi D^2} = \frac{1}{\delta} \int_0^L s(1)\ dl \qquad B.9$$

Calibration data showed (See Figure B.2) that the experimentally determined G is a function of δ/D becoming a constant of about unity as δ/D exceeded 4.

Finite elements calculations were performed and internal stress distributions were computed for 10 different typical fastener geometries. The problems solved are listed in Table B.1 and results are plotted in Figures B-3 through B-12. These solutions make it possible to observe the behavior of s(1,r) within a fastener and to compute the integral

$$G = \frac{1}{\delta} \int_0^L s(1)\ dl$$

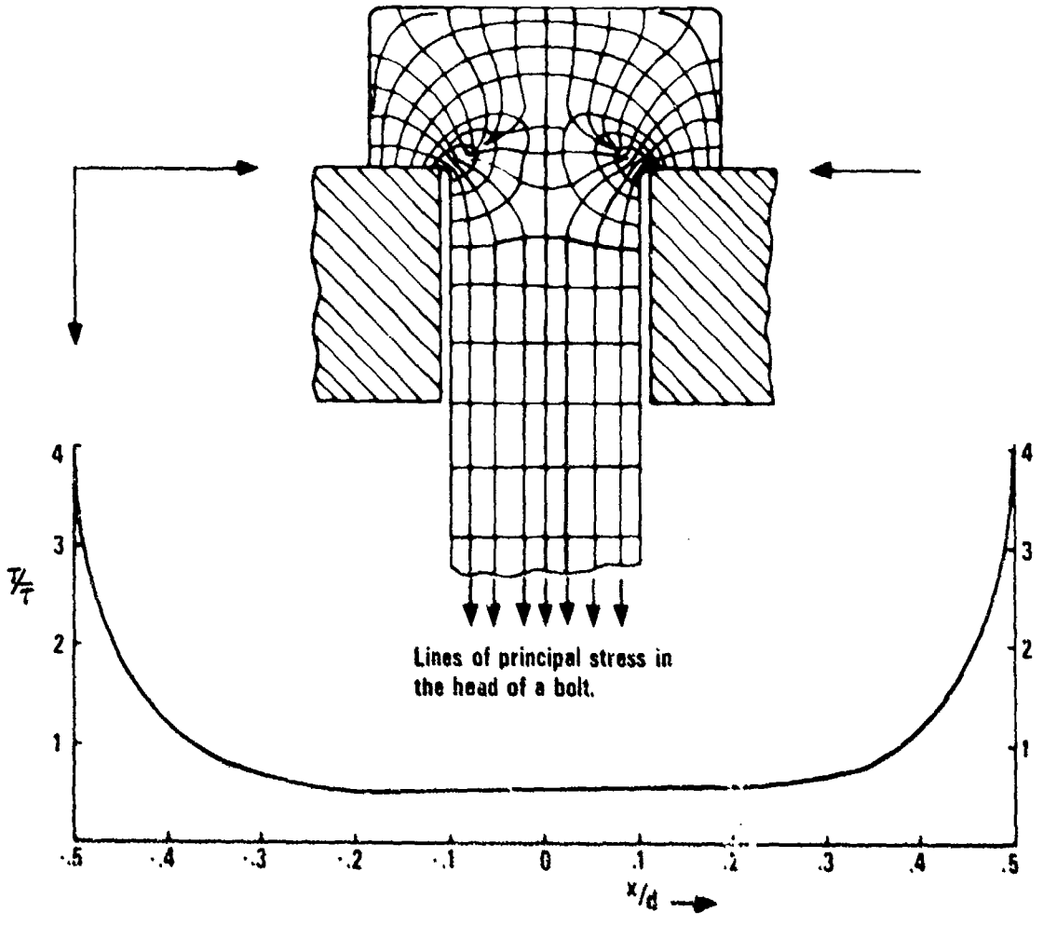

Figure B-1 The photoelastic tension distribution of a .1" thick section of a 3/4" diameter bolt.

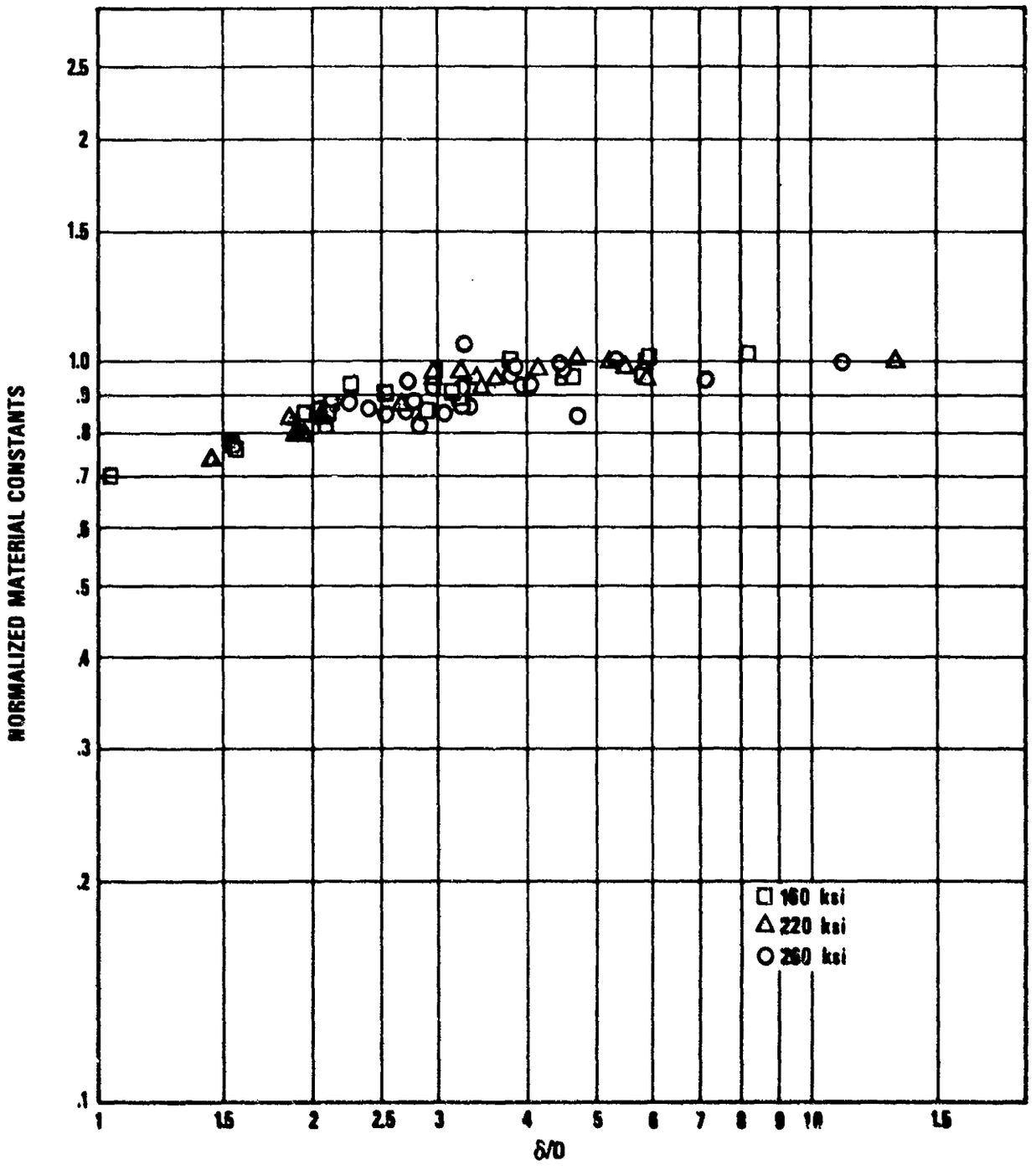

Figure B.2 Material Constants for Three Heat Treatments of Steel Normalized to Unity at δ/D=13

Table B.1 Finite Elements Problems Solved to Study Non Uniform Tension in Fasteners

Problem #	Fastener ID	Material	Fastener Length	Grip Length	Fastener Diameter	Average Stress	Code Used
1	8	Al.	4.7"	4.55 *	.3115	100,000	2D
2	8	Steel	4.7"	4.55 *	.3115	38,500	2D
3	8	Ti	4.7"	4.55 *	.3115	38,500	2D
4	33	Ti	3.85"	2.1	.750	66,667	2D
5	33	Steel	3.85"	2.85	.750	66,667	2D
6	84	Steel	2.85"	.975	1.0	50,000	2D
7	84	Steel	2.85"	.975	1.0	50,000	3D
8	84	Ti	2.85"	.975	1.0	15,916	3D
9	84	Steel	2.85"	1.35	1.0	50,000	2D
10	84	Steel	2.85"	1.725	1.0	50,000	2D
			In.	In.	In.	Psi	

* NO NUT USED

PROBLEM #1
L = 4.7″
D = .3115″
δ = 4.55″
S = 100,000 psi

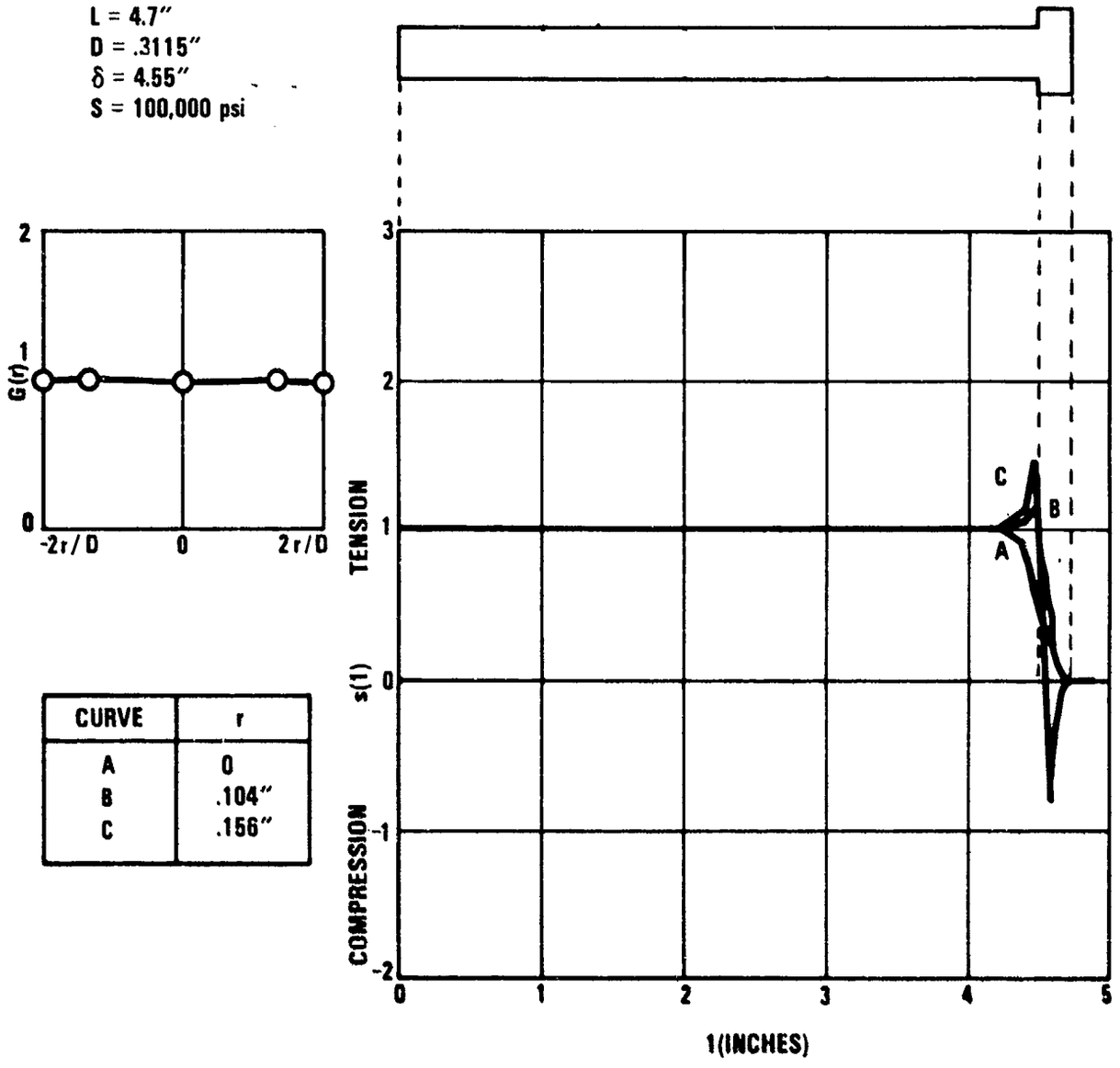

CURVE	r
A	0
B	.104″
C	.156″

Figure B.3 Coaxial Tensions in an Aluminum Fastener with an Exaggerated Tension of 100,000 psi Applied Showing Values of the Integral $G(r) = \int_0^L s(1)\ d1$

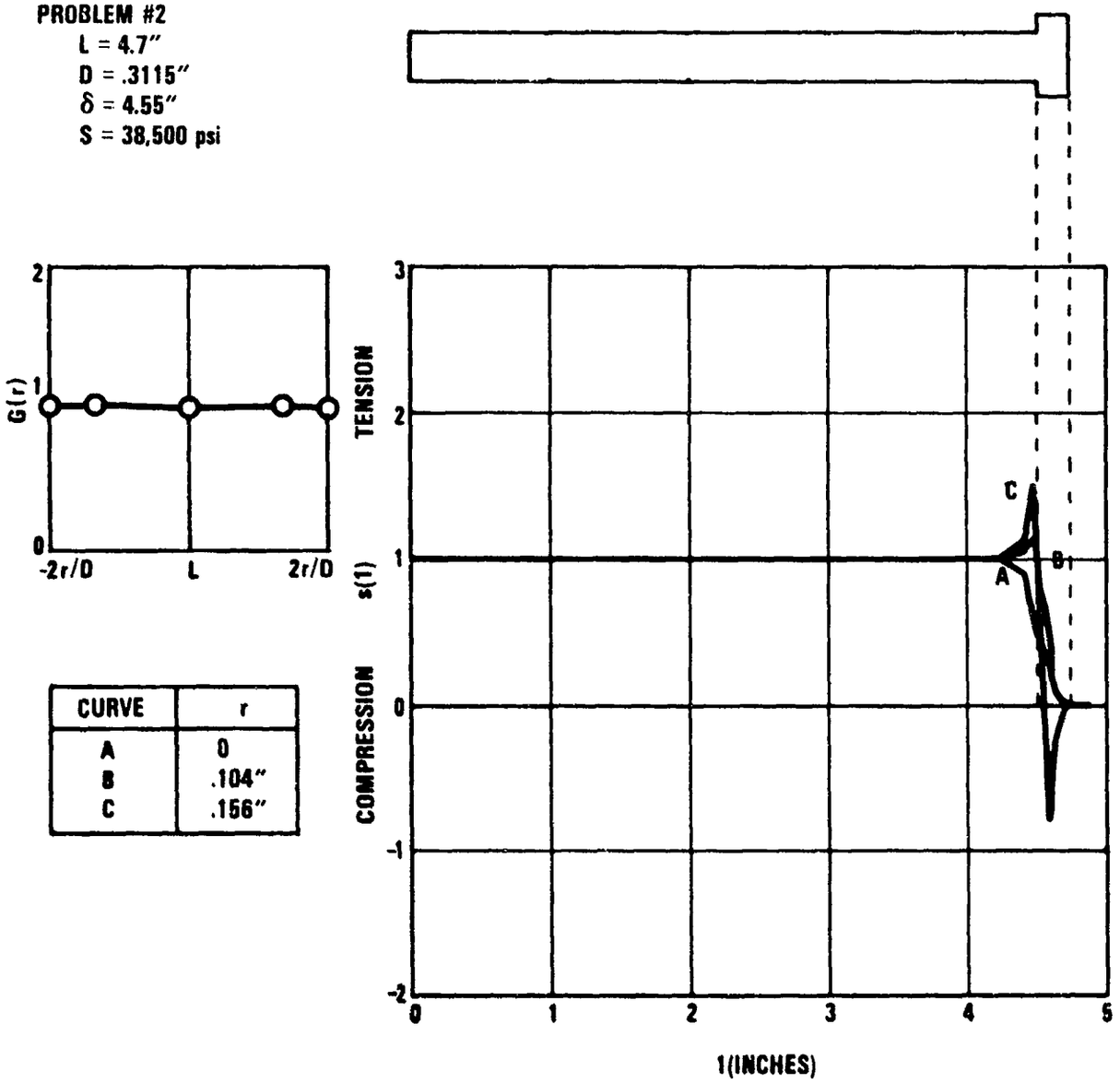

Figure B.4 Coaxial Tensions in a Steel Fastener Showing Values of the Integral G(r)

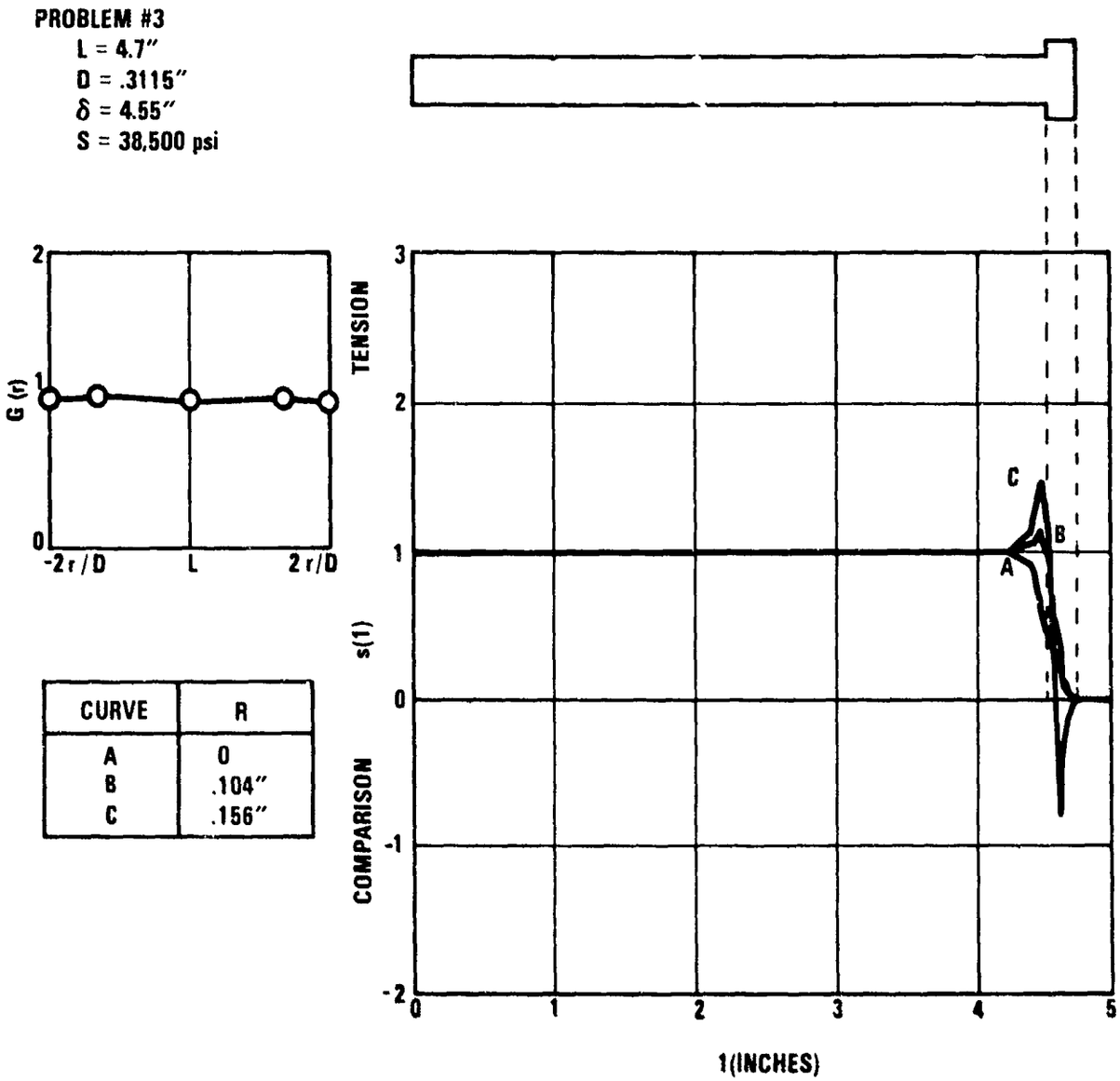

Figure B.5 Coaxial Tensions in a Titanium Fastener Showing Values of the Integral G(r)

PROBLEM #4

L = 3.85″

D = .750″

δ = 2.1″

S = 66,667 psi

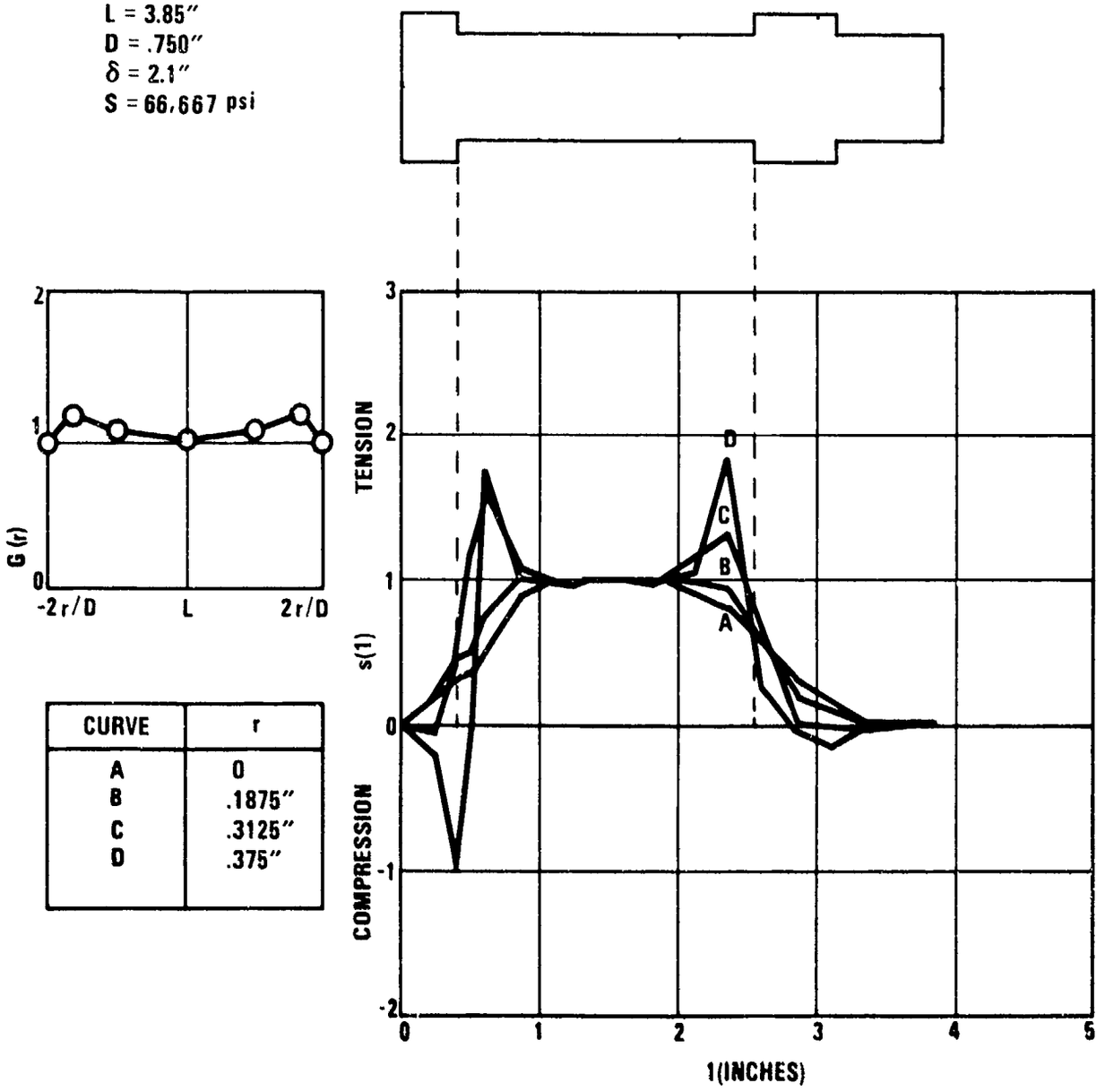

CURVE	r
A	0
B	.1875″
C	.3125″
D	.375″

Figure B.6 Coaxial Tensions in a Titanium Fastener

PROBLEM #5

L = 3.85″

D = .750″

δ = 2.85″

S = 66,667 psi

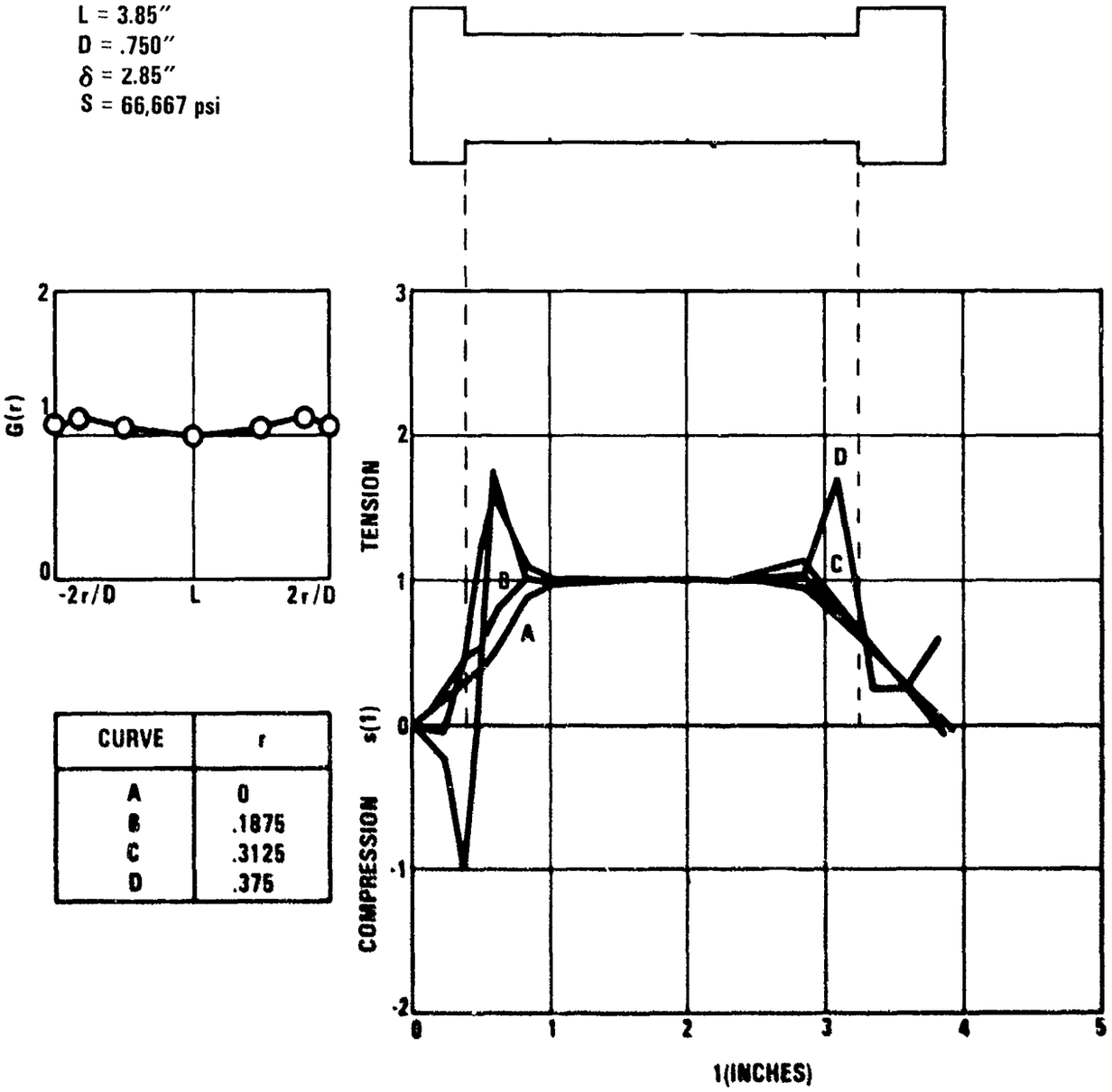

CURVE	r
A	0
B	.1875
C	.3125
D	.375

Figure 8.7 Coaxial Tensions in a Steel Fastener Showing Values of the Integral G(r)

PROBLEM #6

L = 2.85"
D = 1"
δ = .975"
S = 50,000 psi

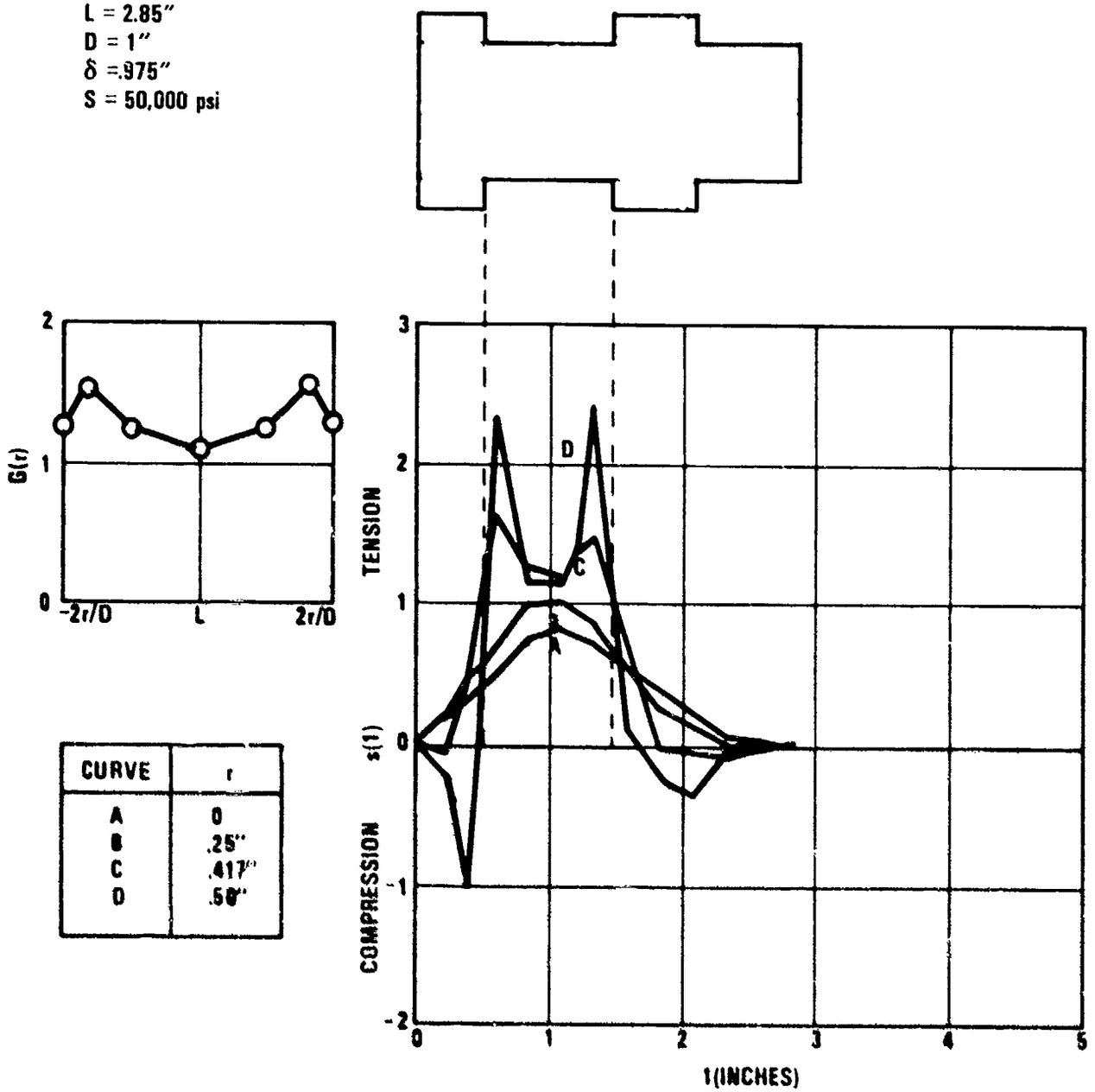

CURVE	r
A	0
B	.25"
C	.417"
D	.50"

Figure B.8 Coaxial Tensions in a Steel Fastener Showing Values of the Integral G(r)

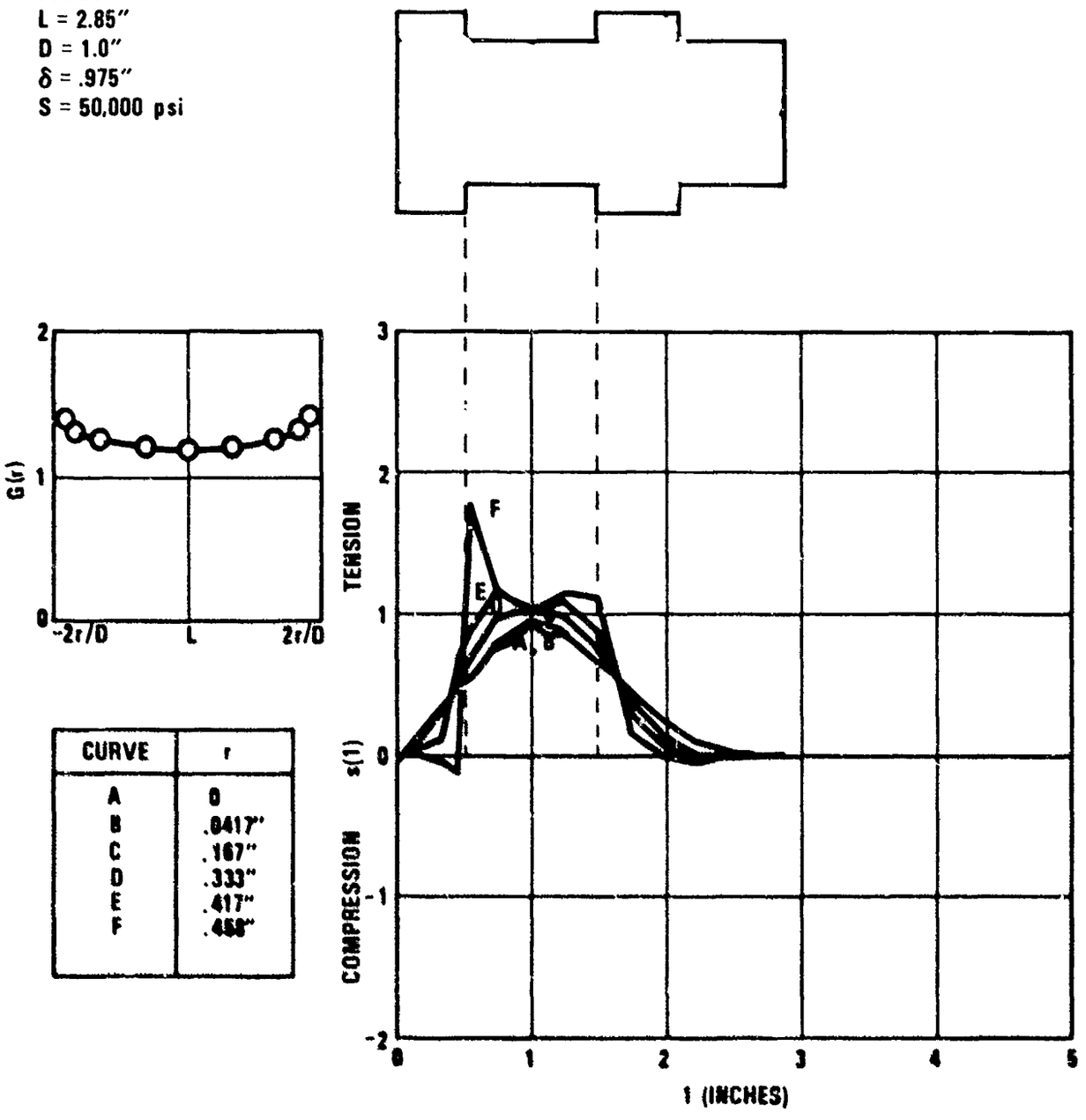

Figure 8.9 Coaxial Tensions in a Steel Fastener Using the 3D Finite Elements Code

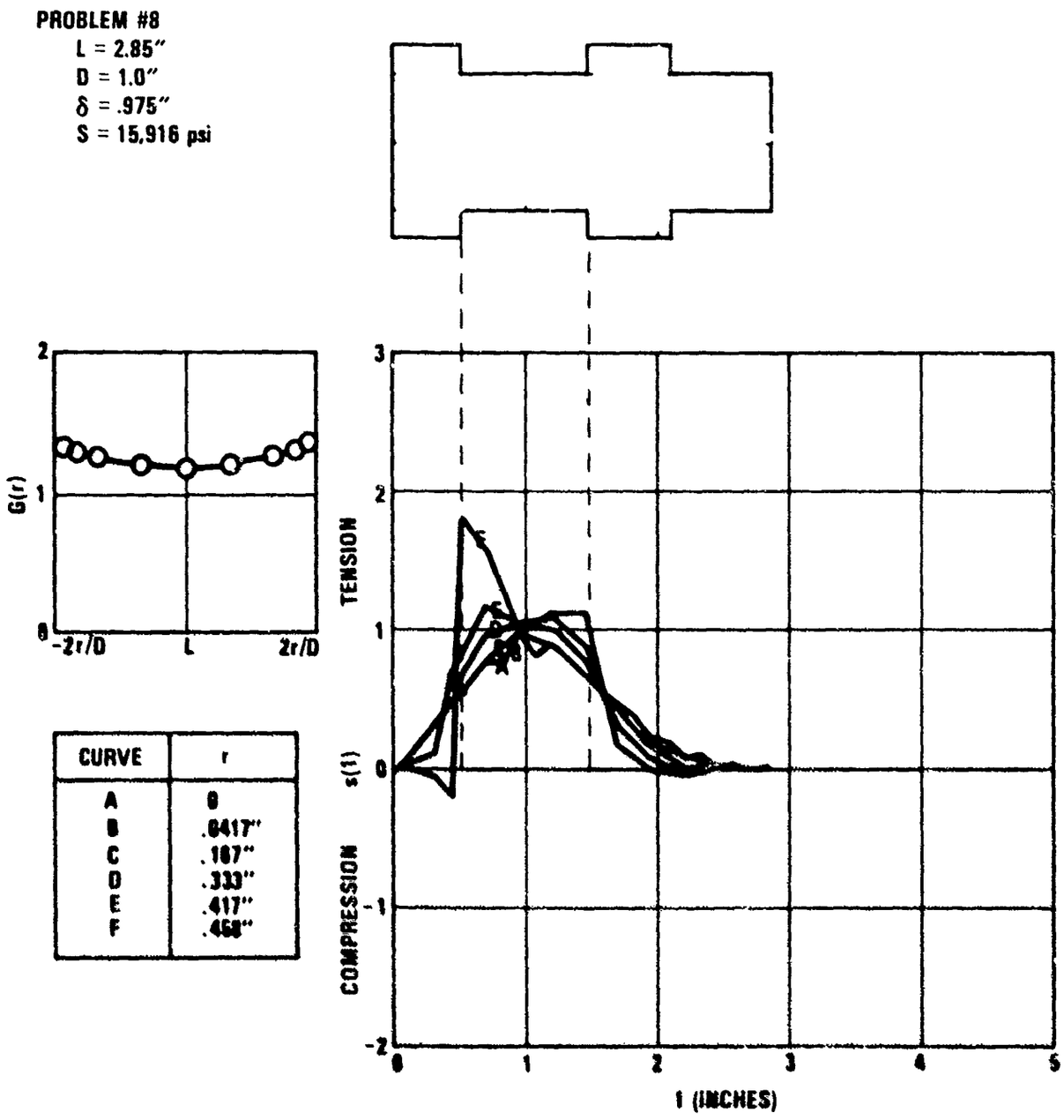

Figure B.18 Coaxial Tensions in a Titanium Fastener Using the 3D Finite Elements Code

PROBLEM #9
L = 2.85"
D = 1.0"
δ = 1.35"
S = 50,000 psi

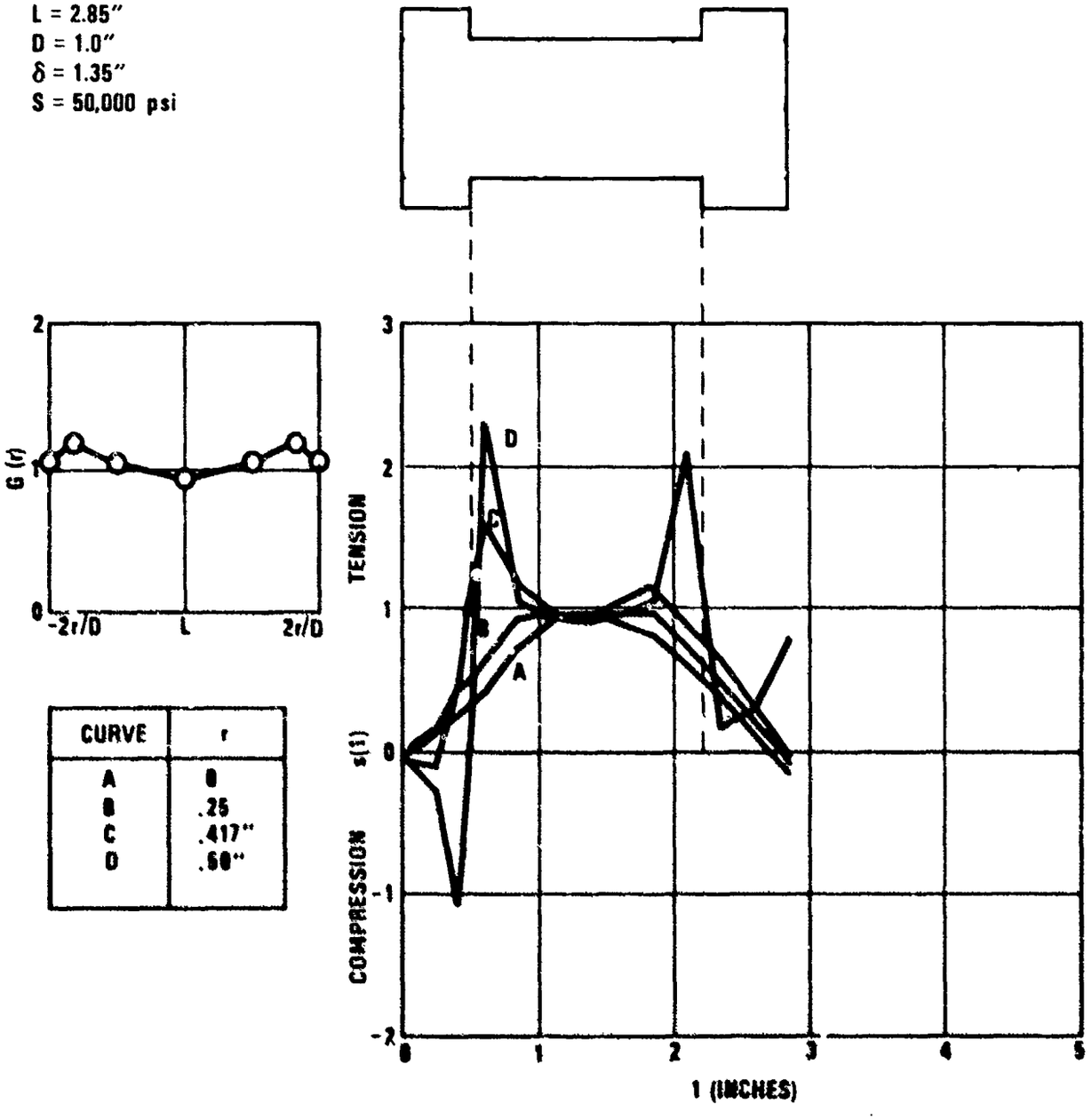

CURVE	r
A	0
B	.25
C	.417"
D	.60"

Figure 8.11 Coaxial Tensions in a Steel Fastener Showing G(r)

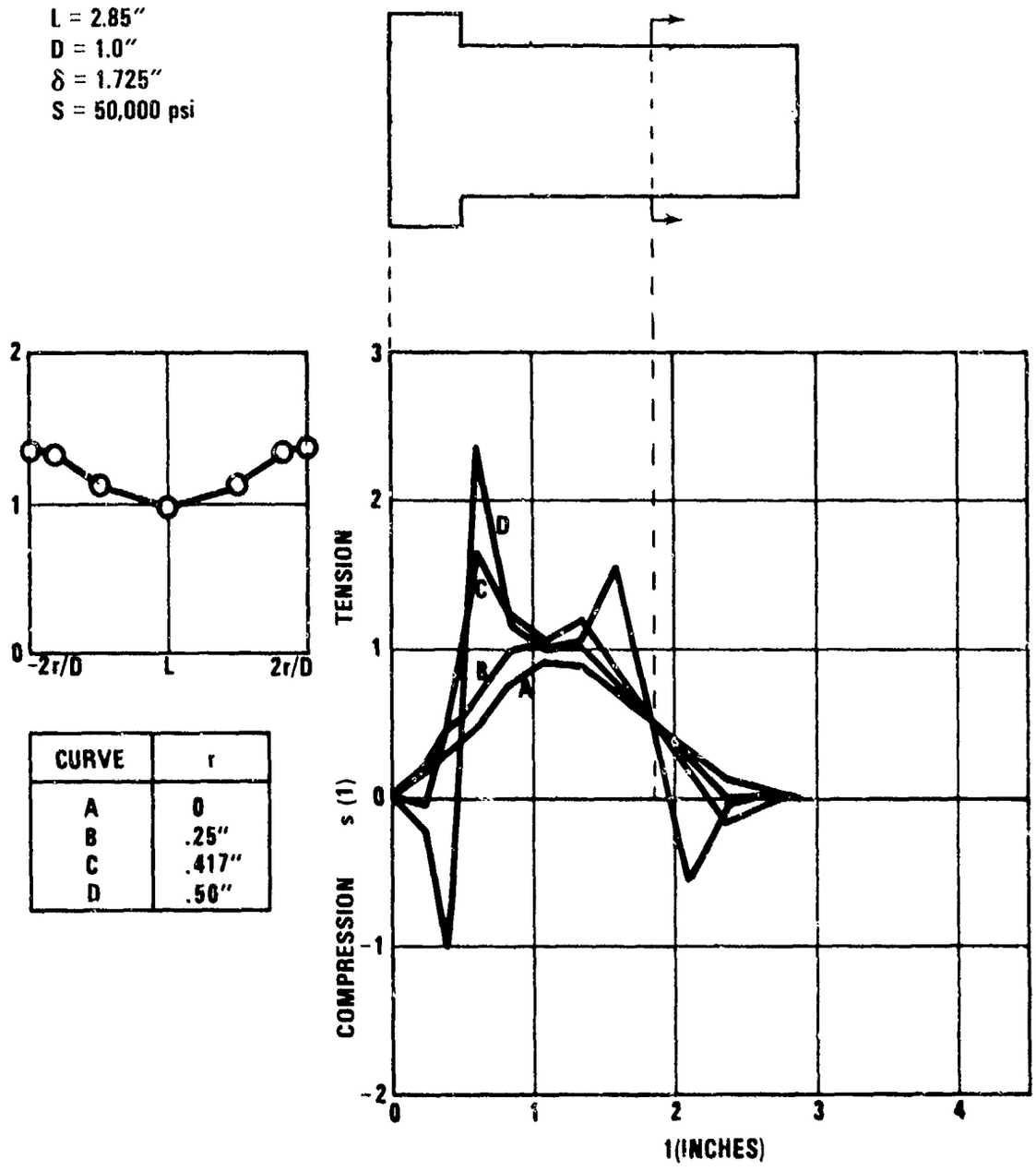

Figure B.12 Coaxial Tensions in a Steel Fastener

Eight of the finite elements calculations were made for a one-mil-thick-slice cross section taken through a fastener. The forces that were applied to the threads by the nut were applied as recommended by Ref. 10). The accuracy of the two dimensional code (ref. 11) was considered good because non-linear elements were modeled. Two of the problems were re-run using a three dimensional finite elements code (ref. 12) in order to verify the validity of trends indicated by the two dimensional calculations. The three-dimensional finite-element code-treated linear elements were therefore considered less accurate than the two-dimensional code was. Findings, however, were consistent with each other.

All calculations showed that there was a uniform tension about one fastener diameter away from where the loads were applied. The tensions were smallest along the centerline of the fastener and tended to drop off rapidly as the fastener head and nut ends were approached. Away from the centerline, peak tensions occurred slightly ahead of the loaded portions of the nut and in some cases these peak tensions were nearly double the average tension values. If smaller finite elements had been used in the calculations, the peak tensions would very likely have been greater. The high-tension regions rapidly go into compression under the nut or head of a fastener and provide the forces necessary for a continuation of the centerline tension clear to the ends of the fasteners.

Figures B.3 through B.12 are a graphical representation of the finite-element calculations. They show the actual size and goemetry of each fastener with the coaxial tensions plotted directly below. The coaxial stresses represent the functions s(1) given in equation B.5. The integral of s(1) (Equation B.9) is also plotted in each figure.

These ten problems have provided insight into the non-uniform stress problem. It may be observed from the graphical plots of G(r) that the coaxial path requiring the least ultrasonic travel time is down the center line of the fasteners. The radial variation is quite small for long fasteners (Figures B.3, B.4, and B.5) but becomes quite significant as δ/D approaches unity, as in Figure B.8. The travel time may vary by as much as 50 percent across the diameter of a fastener. This radial variation would severely effect the Q of a fastener if it were used as a resonant element. These findings place severe demands on the size of the transducer to be used and the precision with which it must be centered on the end of the fastener in order to measure fastener preload by the time of travel technique.

Contrary to what was expected, it is observed that $G(\delta/D)$ plotted in Figure B.13 did not decrease below $\delta/D = 4$ as was experimentally observed during the calibration task (refer back to Figure B.2). This theoretical finding shows that the assumption of an average tension over δ that was made (Appendix A) was not sufficiently accurate. Instead, another basic model had to be found that did not show m decreasing as δ/D drops below 3 or 4 and allows for the average tensions to persist beyond the grip length under the head and nut ends of a fastener.

If equation B.9 is modified to read

$$G = \frac{1}{(\delta + \alpha D)} \int_0^L s(1)\, dl \qquad (B.10)$$

and α is varied until the spread in the finite elements determinations of G are a minimized, we find that only a small increase in δ would be required. The results plotted in Figure B.14 show the mean value of G and the value of $\frac{100\ \sigma(G)}{G}$, which reaches a minimum when $\alpha = .125$ and $G = .97$. A similar study was performed with the calibration data on fasteners.

All of the steel fastener data were combined and α was varied while

$$m = \frac{\delta + \alpha D}{\delta} M \qquad (B.11)$$

was calculated along with

$$\frac{100\ \sigma(m)}{\bar{m}}$$

These results, plotted in Figure B.15, show that there is less variation in M with a value close to .6 for α. Further, if m is plotted as a function of δ/D it can be shown (Figure B.16) to be independent of δ/D with variations around m being random and attributable to other calibration variables.

Choosing $\alpha = .6$ and computing $\bar{m}$ for titanium fasteners it is found that m is rather well distributed around $\bar{m}$ with two or three exceptions. The three fasteners in question, NAS 677 V18, NAS 6?06 L12, and NAS 675 V16, should be recalibrated. Table B.2 is a new listing of calibration data listing values of m for $\alpha = .6$.

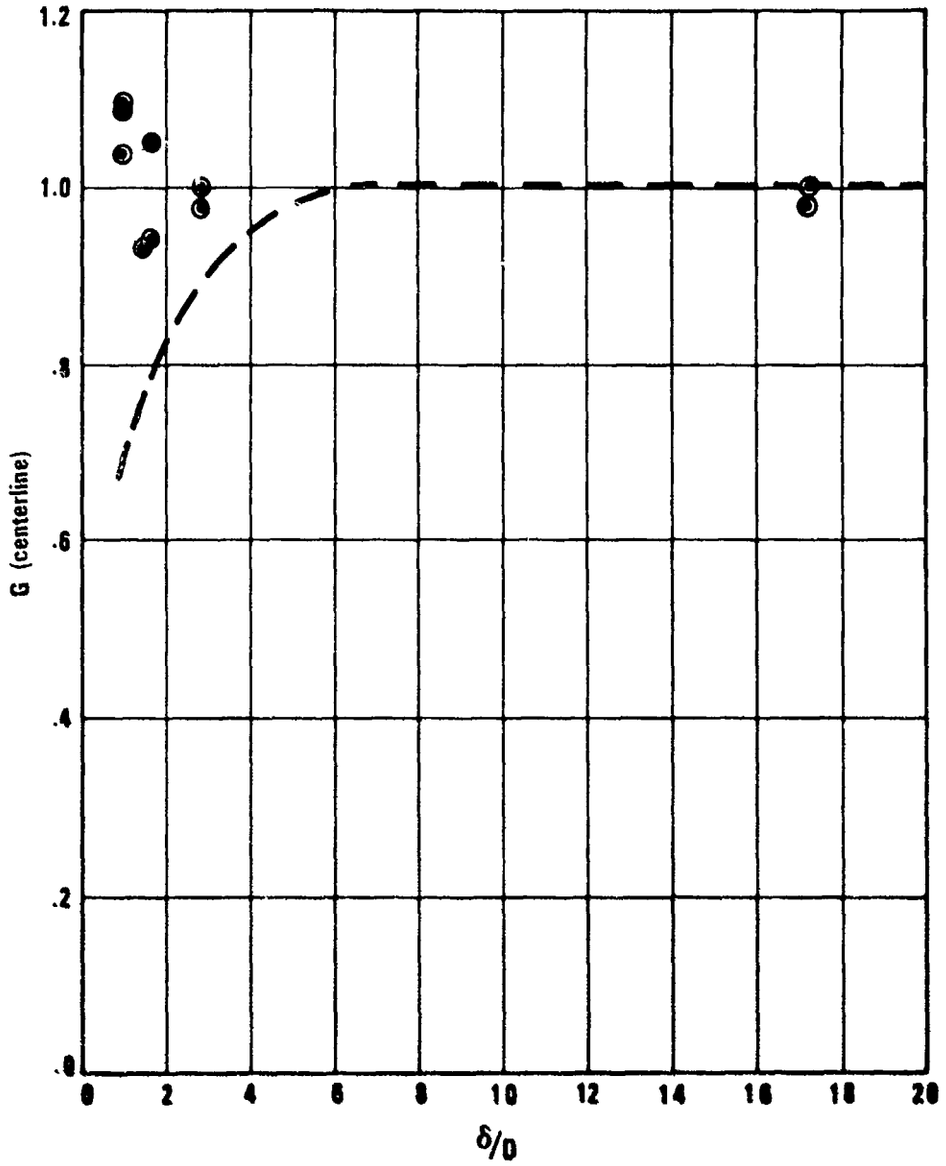

Figure B.13 Non Uniform Distribution Factors Computed From the Finite Elements Code Results With Broken Line Representing the Data Plotted in Figure B.2 (above)

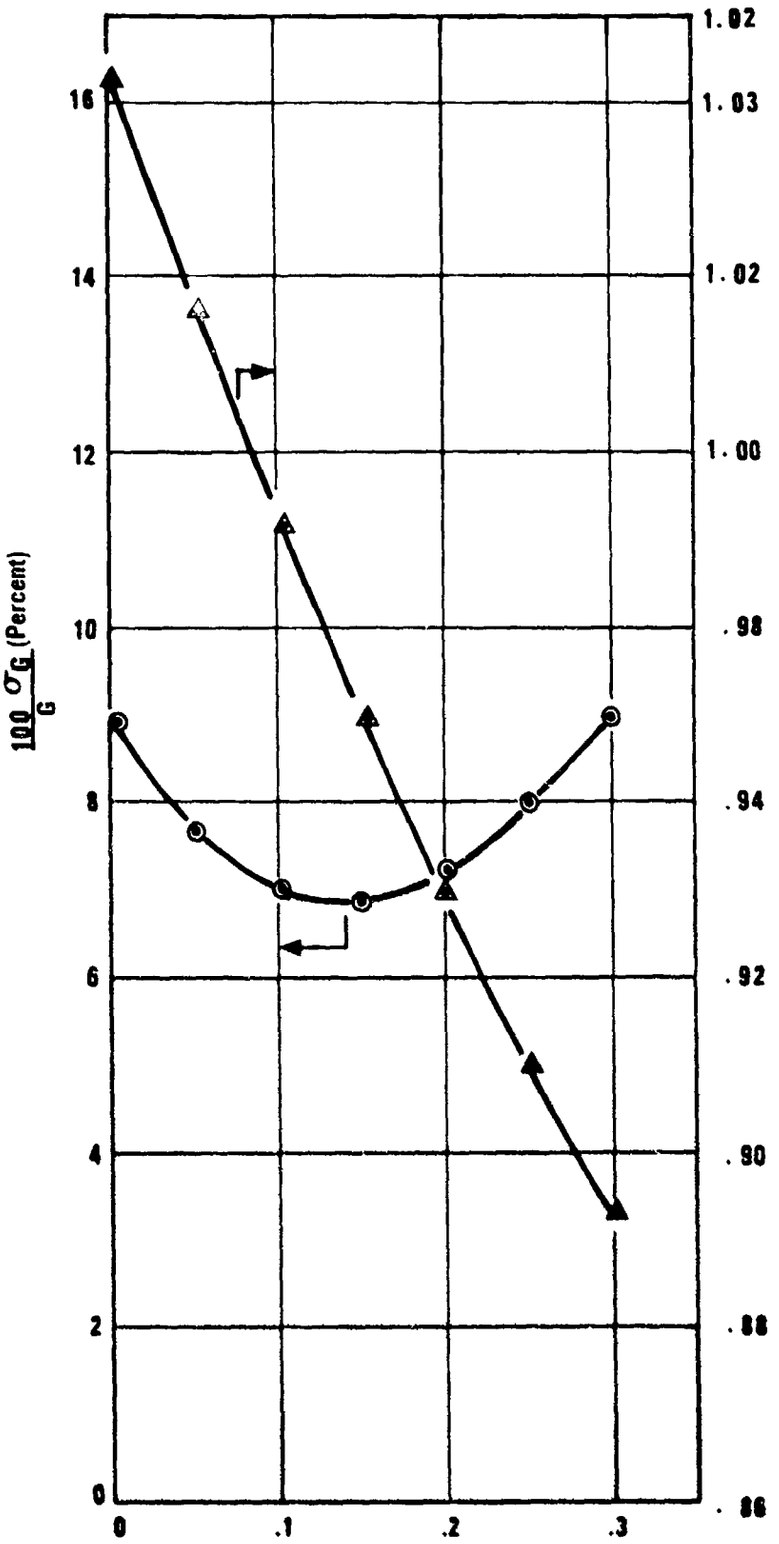

Figure B.14 Redefining G (Equation B.10) and Showing that the Spread in G Values Determined from Finite Elements Calculations is Minimized at $\alpha = .125$.

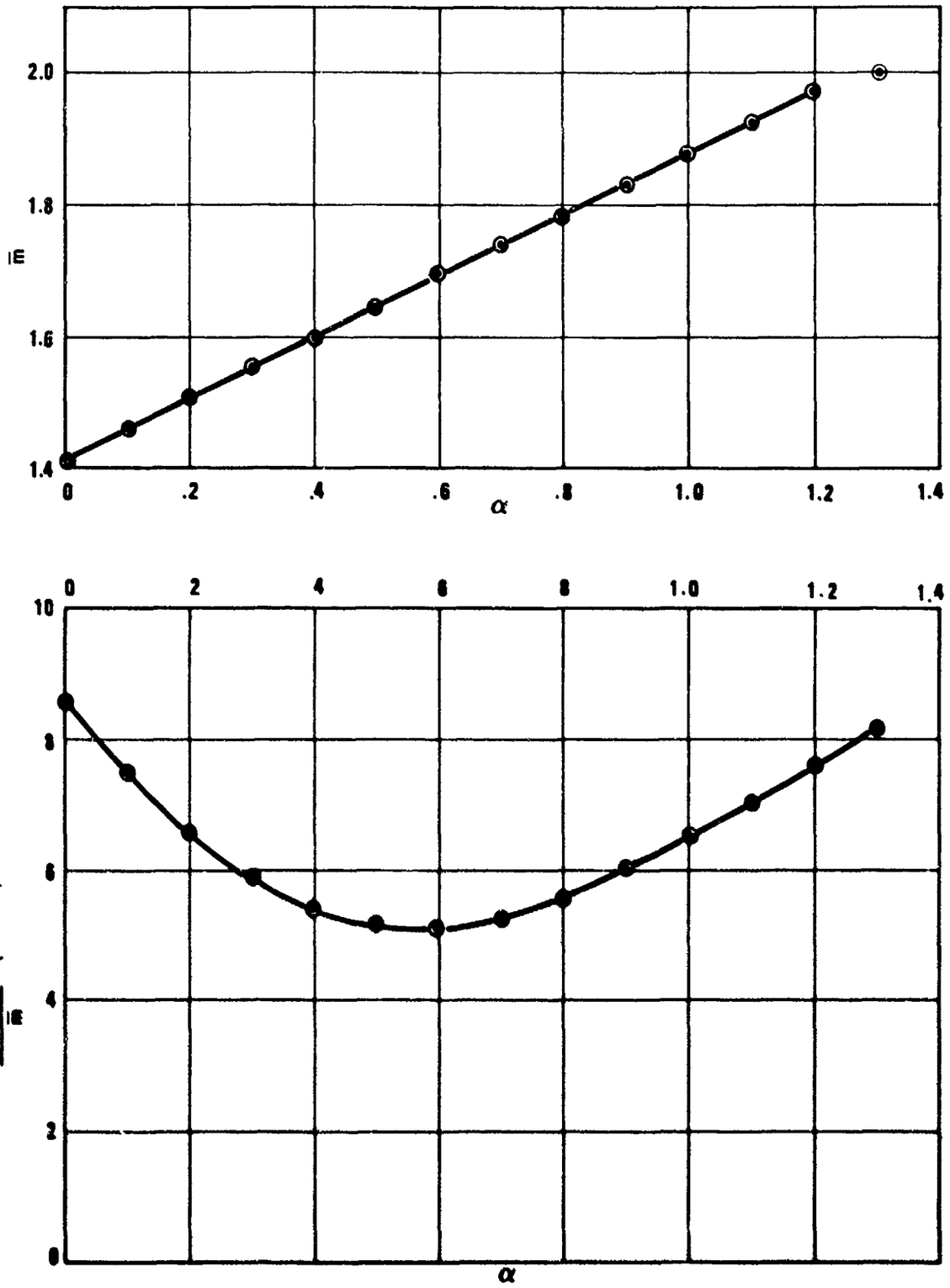

Figure B.15 Spread in $\bar{m}$ is a Minimum when Equation B.11 is Used to Compute m for $\alpha = .6$.

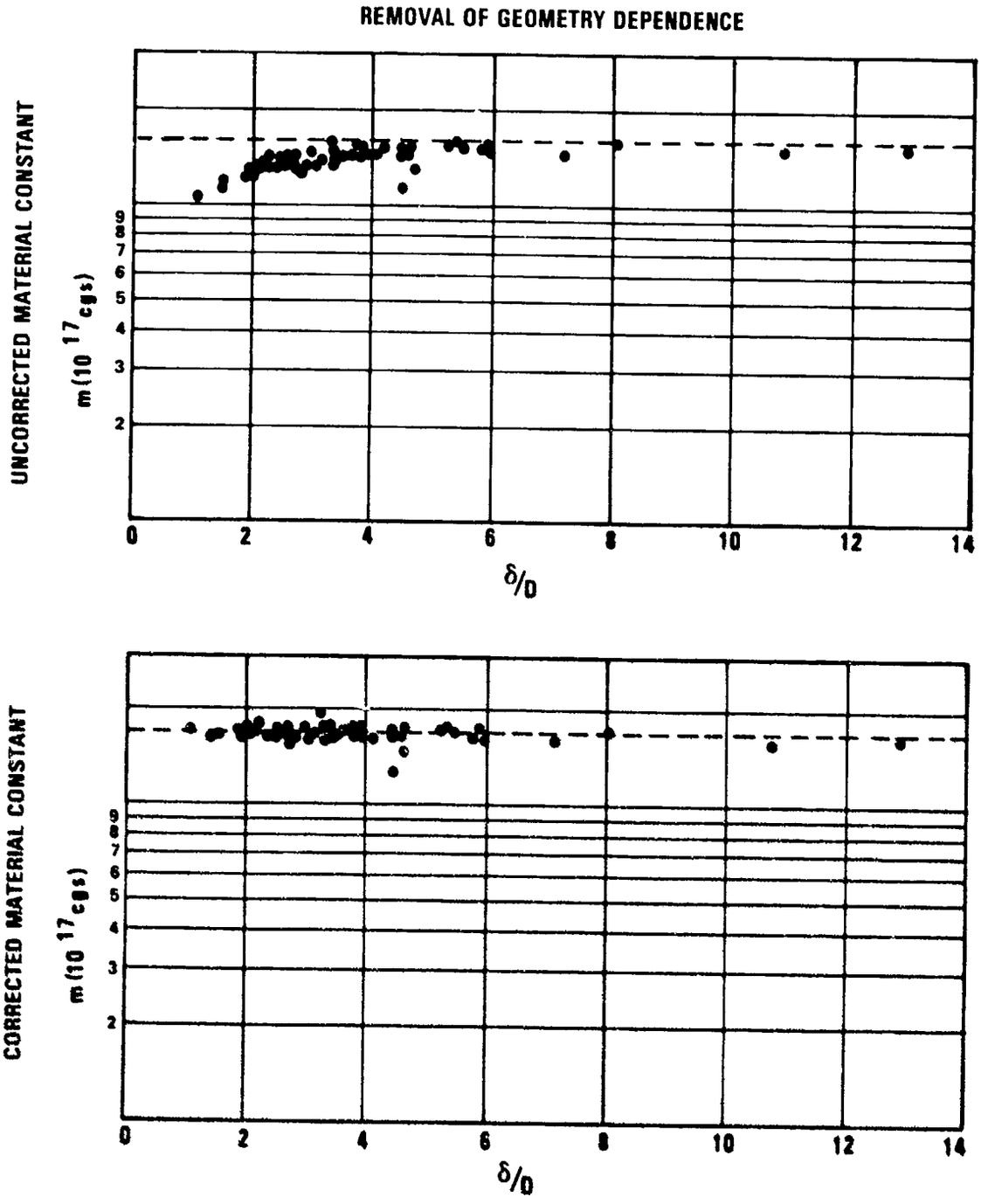

Figure B.16 Comparison of M (Equation B.7) with m (Equation B.11) Showing that the Geometry Related Dip Below $\delta/D = 4$ is Eliminated by Setting $\alpha = .6$ in Equation B.11.

Table B.2 Calibration Results

160 KSI/Steel	L	D	δ	δ/D	M*	m
NAS 1106 16	1.502	.374	1.062	2.840	1.353	1.64
NAS 1112 44	3.521	.747	2.830	3.788	1.554	1.80
NAS 1112 52	4.060	.752	3.321	4.42	1.469	1.67
NAS 1112 96	6.768	.749	6.019	8.04	1.606	1.73
NAS 1312 39	3.710	.747	2.362	3.16	1.407	1.67
NAS 1310 24	2.604	.623	1.564	2.51	1.405	1.74
NAS 1310 29	2.918	.623	1.865	2.99	1.487	1.79
NAS 1306 34	2.806	.374	2.176	5.82	1.554	1.71
NAS 1308 21	2.224	.497	1.345	2.71	1.384	1.69
NAS 1306 34	2.632	.373	2.171	5.82	1.591	1.76
NAS 1316 24	3.140	.998	1.549	1.552	1.203	1.67
NAS 1106 34	2.631	.374	2.163	5.783	1.504	1.66
NAS 1316 32	3.660	.997	2.074	2.08	1.342	1.73
NAS 1312 24	2.786	.747	1.573	2.11	1.378	1.77
NAS 1316 29	3.466	.997	2.026	2.03	1.357	1.76
NAS 1316 72	6.109	.997	4.568	4.582	1.475	1.67
NAS 1316 32	3.633	.997	2.074	2.08	1.300	1.67
NAS 1316 24	3.118	.997	1.532	1.54	1.204	1.67
LSC	2.881	.997	1.039	1.04	1.090	1.71
NAS 1309 28	2.776	.560	1.804	3.221	1.381	1.64
NAS 6206 13	1.384	.374	.844	2.25	1.436	1.81
NAS 6206 10	1.189	.374	.731	1.95	1.315	1.72
220 KSI/Steel	**L**	**D**	**δ**	**δ/D**	**M**	**m**
C081 12A 43	3.942	.747	2.691	3.60	1.468	1.71
C081 8 12	1.550	.497	.932	1.88	1.294	1.71
C7521 80 23	2.435	.497	1.685	3.39	1.490	1.75
C083 5A 72	4.516	.310	3.998	12.90	1.566	1.64
C081 6A 27	2.268	.375	1.765	4.65	1.579	1.78
C081 14A 25	3.040	.872	1.678	1.92	1.243	1.63
C081 14A 48	4.467	.873	3.019	3.46	1.434	1.68
C081 12A 35	3.439	.746	2.200	2.95	1.442	1.74
C081 12A 28	3.014	.747	1.998	2.67	1.383	1.69
C081 12A 14	2.136	.747	1.092	1.46	1.147	1.62
C083 9A 52	4.373	.560	3.320	5.93	1.474	1.62
C081 7A 35	2.903	.435	2.287	5.234	1.577	1.76
C081 7A 36	2.982	.435	2.386	5.485	1.547	1.72
C083 10 32	3.209	.623	2.094	3.36	1.531	1.80
C083 12 34	3.516	.747	2.212	2.96	1.489	1.79
C083 16 64	5.942	.497	4.093	4.11	1.523	1.63
C081 16A 32	3.688	.998	2.026	2.030	1.317	1.71
C083 16 32	3.736	.998	1.963	1.97	1.242	1.62

* X (-10^{17})cgs

Table B.2 (Continued)

260 KSI Steel	L	D	δ	δ/D	M	m
MS 21296 05019	2.035	.310	1.393	4.494	1.143	1.30
MS 21296	3.061	.558	1.868	3.348	1.358	1.60
MS 21297 14056	5.276	.871	3.534	4.057	1.464	1.68
MS 21297 14054	5.196	.872	3.450	3.96	1.465	1.69
MS 21296 09 28	3.128	.562	1.851	3.29	1.362	1.61
MS 21297 A 12044	4.415	.747	2.833	3.79	1.474	1.71
MS 21297 12034	3.774	.747	2.206	2.95	1.414	1.70
MS 21296 10018	2.609	.623	1.404	2.254	1.371	1.74
MS 21296 7 17	2.173	.436	1.172	2.688	1.341	1.64
MS 21296 09026	2.947	.560	1.835	3.277	1.416	1.68
MS 21296 09027	3.046	.560	1.715	3.063	1.343	1.61
MS 21296 05 19	2.031	.311	1.443	4.640	1.327	1.50
MS 21296 06 16	1.959	.372	1.045	2.809	1.292	1.57
MS 21296 07048	4.059	.436	3.114	7.142	1.481	1.61
MS 21296 06016	1.935	.374	1.027	2.746	1.379	1.68
MS 21297 06026	2.536	.373	1.653	4.442	1.543	1.75
MS 21297 08013	2.456	.497	1.339	2.690	1.446	1.77
MS 21297 16072	6.687	1.002	4.538	4.53	1.500	1.70
Mixed Steel	**L**	**D**	**δ**	**δ/D**	**M**	**m**
EWSB 930 5	3.924	.310	3.357	10.82	1.554	1.64
NAS 1005 12	1.581	.311	1.017	3.270	1.649	1.95
EWSB 930 7	3.010	.436	2.354	5.399	1.581	1.76
	1.916	.497	.934	1.879	1.295	1.71
EWSB 930-6	1.507	.372	.930	2.50	1.331	1.65
GD Alloy		.862	3.288	3.81	1.538	1.78
4450-8	1.968	.497	1.184	2.38	1.347	1.69
6Al-4V-Ti	**L**	**D**	**δ**	**δ/D**	**M**	**m**
NAS 675 V16	1.639	.310	1.133	3.645	.979	1.14
NAS 676 V21	2.087	.374	1.422	3.802	1.239	1.44
NAS 675 V17	1.698	.310	1.125	3.629	1.096	1.27
NAS 674 V29	2.375	.249	1.868	7.502	1.430	1.54
NAS 674 V38	2.940	.249	2.461	9.883	1.307	1.39
NAS 674 V36	2.806	.249	2.312	9.285	1.351	1.44
NAS 677 V18	1.946	.437	1.380	3.160	.795	.946
NAS 674 V24	2.054	.246	1.566	6.366	1.365	1.49
NAS 674 V32	THREADS STRIPPED AT 3100#					
NAS 6407 21	2.002	.436	1.439	3.300	1.238	1.46
NAS 674 V28	2.307	.249	1.796	7.213	1.302	1.41
NAS 655 V20	1.784	.311	1.321	4.248	1.066	1.22
NAS 675 V23	2.069	.310	1.504	4.852	1.261	1.42
NAS 676 V20	2.028	.373	1.296	3.475	1.215	1.42
NAS 6406 L 12	1.326	.374	.805	2.152	1.407	1.80
NAS 675 V 32	BOLT BROKE AT 2500#					
NAS 677 V18	1.950	.435	1.192	2.74	1.266	1.54
NAS 674 V48	2.692	.246	2.193	8.915	1.310	1.39
B30 MR 12	3.765	.747	2.444	3.27	1.211	1.35

B.3 Stress Relaxation Phenomena

Because the stress distribution in fasteners has stress concentrations near the head and nut as high as four times the average stress, one can expect to exceed the elastic limit in fasteners and therefore find inelastic strain. This effect manifests itself as a sort of relaxation phenomena and has been observed during the calibration phase of this contract as well as reported by others.

Whenever loads are applied to fasteners, the amplitude of the first and second back surface reflections are reduced and the travel time through the fastener is also reduced. After several minutes, the signal amplitude returns to near the zero load amplitude and the travel time increases to a near constant value. Figure B.17 is a composite set of graphs and photographs which portray this effect.

Since fasteners torqued by the acousto-elastic method can be torqued within a few seconds, stress relaxation does not limit accuracy. It is observed, however, that the change in travel time is reduced while the applied load remains constant. Perhaps the non-uniform distribution parameters α will be found later to depend upon the load-carrying history of a fastener. Such a study would be a logical follow-on to this program. Perhaps one would find that α would approach .125 (See Figure B when fasteners become work hardened.

RELAXATION PHENOMENA

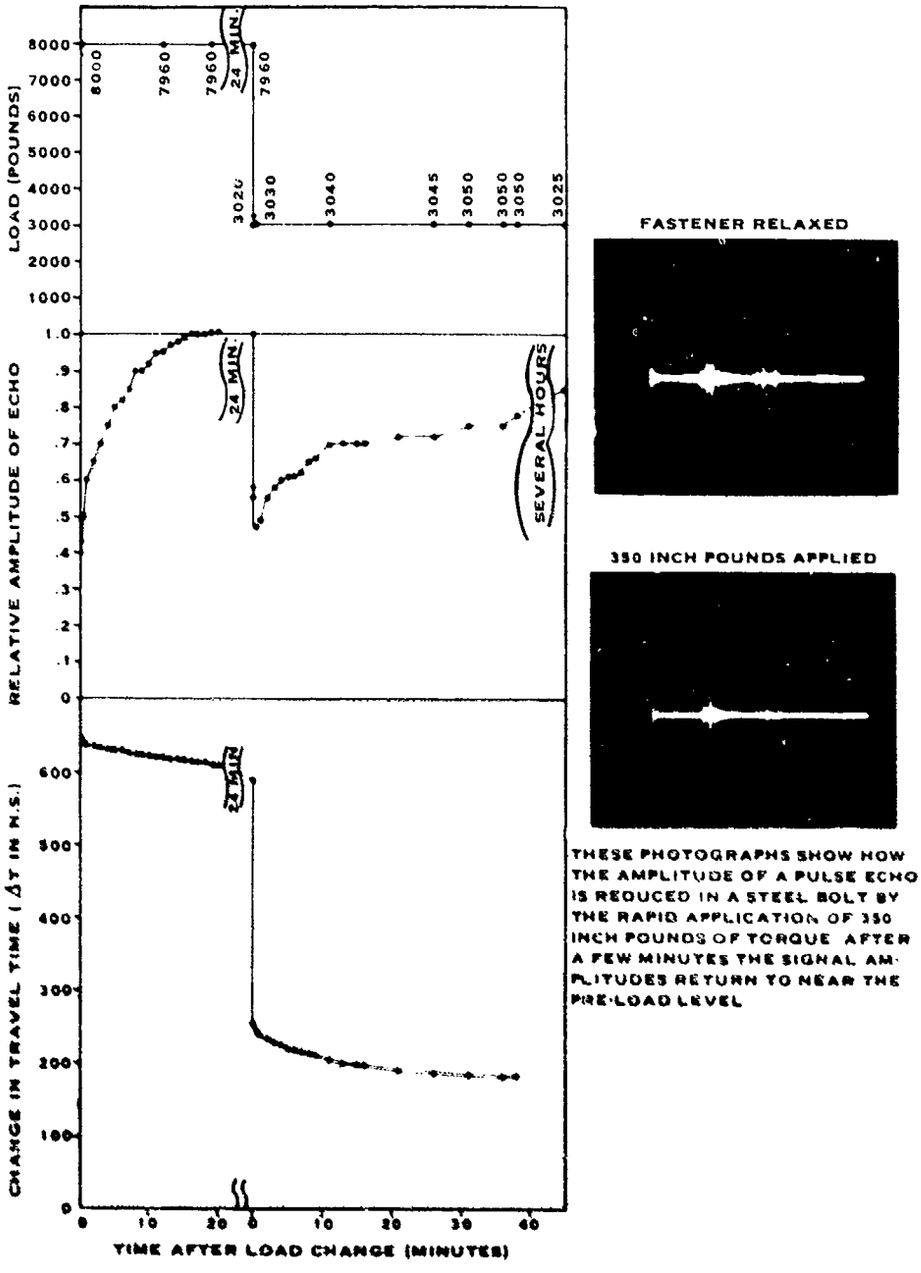

Figure B.17 Time Dependency of Tensions and Ultrasonic Travel Times in Fasteners After Quick Load Changes.

APPENDIX C

PROPERTIES OF FASTENERS CALIBRATED

C.1 Threaded Rod Stock

Six-inch-long threaded-rod stock specimens made of aluminum, steel, and titanium were prepared for use in parametric calibration measurements. Rod stock diameters of 1/4, 1/2, 3/8, 5/8, and 1 inch were included. The .17" diameter specimens were destructively tested to examine their physical (Table C-1) and their metallurgical properties (Figure C-1).

C.2 Fasteners

Seventy-four steel and twenty-two titanium fasteners were selected from the F-16 and F-111 stores. Their dimensions are plotted in Figure C-2. It was found that no aluminum fasteners were available and that no small diameter fasteners were available that were five or six inches long nor were there any short fasteners having large diameters. The larger fasteners were generally one of the heat treatments of steel and the smaller fasteners were most frequently titanium. Table C-2 is a summary of the recorded properties of the various fasteners calibrated (listed in Appendix A).

C.3 Fastener Densities

The normal distributions showing the variation in density (gm/cm^3) of the fasteners that were tested (Figure C-3) shows that densities varied by less than one percent.

C.4 Sound Velocities in Fasteners

Since sound velocity "c" in a metal depends upon density "ρ", Poisson's ratio "ν", and Young's modulus "Y" according to:

$$C = \sqrt{\frac{(1-\nu)}{(1+\nu)(1-2\nu)} \cdot \frac{Y}{\rho}}$$

the variability of C should be indicative of the variability of elasticity of the fasteners. Normal distribution plots of the measured velocities of sound in all fasteners in the unloaded condition are plotted in Figure C-4. These data show that the variation in C is of the order of one percent.

Table C.1 Material Data Report of the Physical Properties of the Rod Stock Tested

	Bolt Diameter	Area	Yield Point		Ultimate		% Elongation
			Pounds	Ksi	Pounds	Ksi	
6061-T6 Aluminum	.174"	.0238 $in.^2$	1020	42.9	1100	46.2	21.3
4130 Steel	.175"	.0241 $in.^2$	2210	91.7	2440	101.2	17.2
6-Al-4V Titanium	.171"	.023 $in.^2$	3480	151.3	3577.5	154.7	10.2

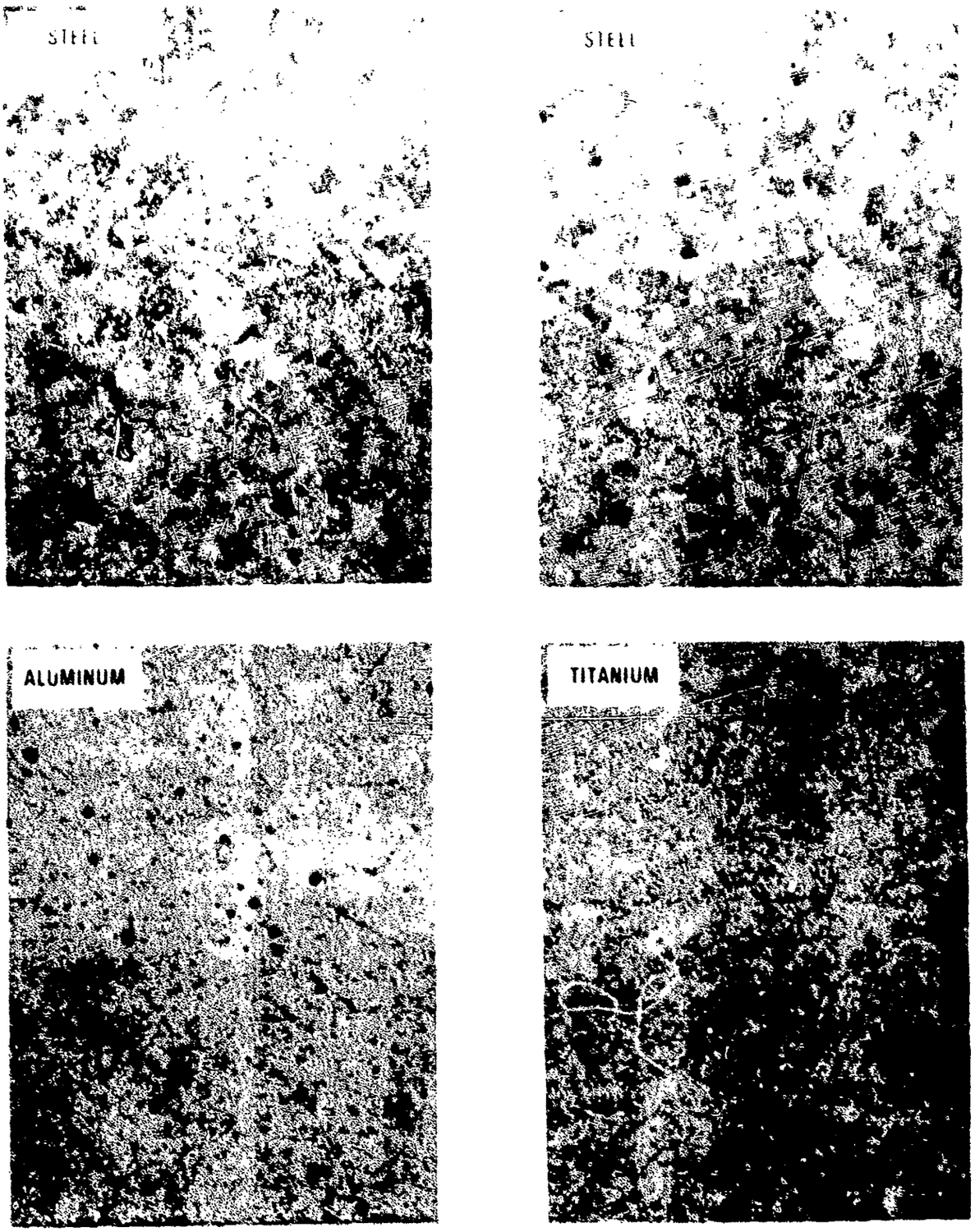

Figure C.1 Metallographic Micrographs (250X) of the Grain Structure of Threaded Rod Specimens Tested

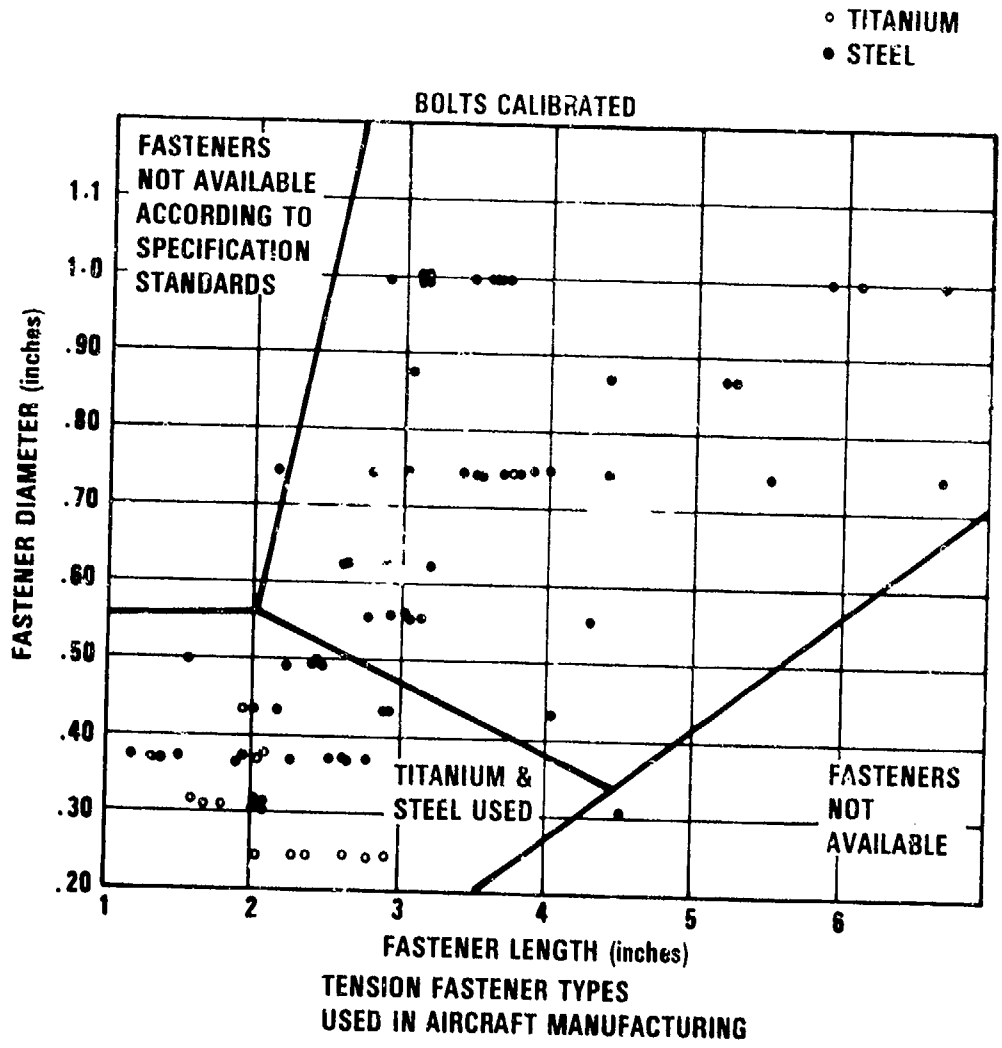

Figure C.2 Graphical Representation of Steel and Titanium Fasteners Calibrated in this Program

Table C.2 Properties of
Bolts Selected for Prototype Calibration

Fastener Designation: MS 21297

Type: Bolt, Tension, Steel 220 KSI Ftu 450°F
External Wrenching; Spline Drive, Flanged Head.

Material: Alloy Steel per AMS 6487

Heat Treatment: 220 ksi UTS

Hardness: Rc 46-50.

Fastener Designation: NAS 1580

Type: Bolt 100°Flush Head

Material: Alloy Steel Or A286
6 Al - 4V Titanium

Heat Treatment: 160,000 - 180,000 PSI UTS min. - Alloy Steel
160,000 - 180,000 PSI UTS min. A286
160,000 - 180,000 PSI UTS min. 6A1-4V. Ti

Fastener Designation: NAS 1151 Thru 1158

Type: Screw, Machine-Flat 100 Deg Head
Close Tol, Short Thd, Torq-Set

Material: Alloy Steel 4140 per Mil-S-5626
Alloy Steel 4340 per Mil-S-5626
Alloy Steel 8740 per MIL-S-6049
Titanium: 6 Al-4V designated by V code

Heat Treatment: 160,000-180,000 PSI UTS per MIL-H-6875
For Alloy Steel
160,000 PSI UTS Min. for 6 Al -4V.

Table C.2 (Continued)

Fastener Designation: MS 21296

Type: Bolt, Tension Steel 260 Ksi Ftu 450°F

External Wrenching, Spline Drive, Flanged Head

Material: Alloy Steel per AMS 6487

Heat Treatment: 260 KSI UTS

Hardness: Rc 51-54.

Fastener Designation: NAS 6403-6420

Type: Bolt, Hex Head, Close Tolerance

Materials: 6A1 -4V Titanium Alloy per AMS 4928
4967

Heat Treatment: 160-180 ksi ultimate tensile
95 ksi ultimate shear

Fastener Designation: NAS 4450

Type: Pin, Crimp, Protruding Shear Head

Materials: (1) A1S1 8740 or 4340 Alloy Steel
and
108 ksi minimum shear
Heat Treat

(2) H-11 Alloy Steel
156 ksi minimum shear

(3) 6A1-4V Titanium
95 ksi minimum shear

Table C.2 (Continued)

Fastener Designation: NAS 1578

Type: Bolt, Flat Pan Head

Materials: Alloy Steel and A-286 Cres.

6 Al-4V Titanium

Heat Treatment: Alloy Steel 160,000 - 180,000 PSI UTS min.

A 286 Cres 160,000 - 180,000 PSI UTS min.

6 Al - 4V Ti 160,000 - 180,000 PSI UTS min.

Fastener Designation: NAS 673 Thru 678

Type: Bolt, Close Tolerance - Hexagon

Head, Titanium, .190 to .500

Material: 6Al - 4V Titanium

Heat Treatment: Not specified (But probably in the 160,000 -

180,000 PSI UTS Range)

Fastener Designation: NAS 6303-6320

Type: Bolt, Hex Head, Close Tolerance

Material: A-286 per AMS 5731

Heat Treat: 160 KSI ultimate tensile

95 KSI ultimate shear

Fastener Designation: NAS 1303-1320

Type: Bolt, Shear-Hexagon Head

Material: Alloy Steel per procurement spec.

Heat Treat: 160-180 KSI, ultimate tensile per MIL-H-6875

Rc. 36-40

Table C.2 (Continued)

Fastener Designation: NAS 6203-6220

Type: Bolt, Hex Head, Close Tolerance, Alloy. Steel

Materials: Alloy Steel per Procurement Spec

Heat Treat: 160-180 KSI ultimate strength
95 KSI ultimate shear

Fastener Designation: NAS 1103 - 1120

Type: Bolt, shear - Hexagon head modified

Material: Alloy steel per Procurement Spec.

Heat Treat: 160-180 KSI UTS per MIL-H-6875

Fastener Designation: NAS 4452

Type: Pin, Crimp, 100° Flush Shear Head

Materials And Heat Treat:
1) AISI 8740 or 4340 Alloy Steel
108 KSI minimum shear
2) H-11 Alloy Steel
156 KSI minimum shear
3) 6 Al-4V Titanium
95 KSI minimum shear

Table C.2 (Continued)

Fastener Designation: C7549

Type: Bolt, Double Hex Head, 132 KSI shear, 450°F

Material: 5% chrome die steel alloy per AMS 6485

Heat Treat: 220 KSI ultimate tensile, 132 ultimate shear
Rc 46-50.

Fastener Designation: NAS 1151-1158

Type: Screw, machine-flat 100 deg. head
close tol.

Material: Alloy steel per MIL-H-6875

and Heat 160-180 KSI ultimate tensile

Treat: 6Al-4V Titanium
160 KSI ultimate tensile
Corrosion resistant steel
160 KSI ultimate at room temp.

Fastener Designation: C7984

Type: Bolt 100° Flush head, torq-set recess

Material: H-11 alloy steel per AMS-6487

Heat Treat: 220 KSI min. tensile
132 KSI min. shear

VARIATION OF MATERIAL PROPERTIES (BOLT DENSITY)

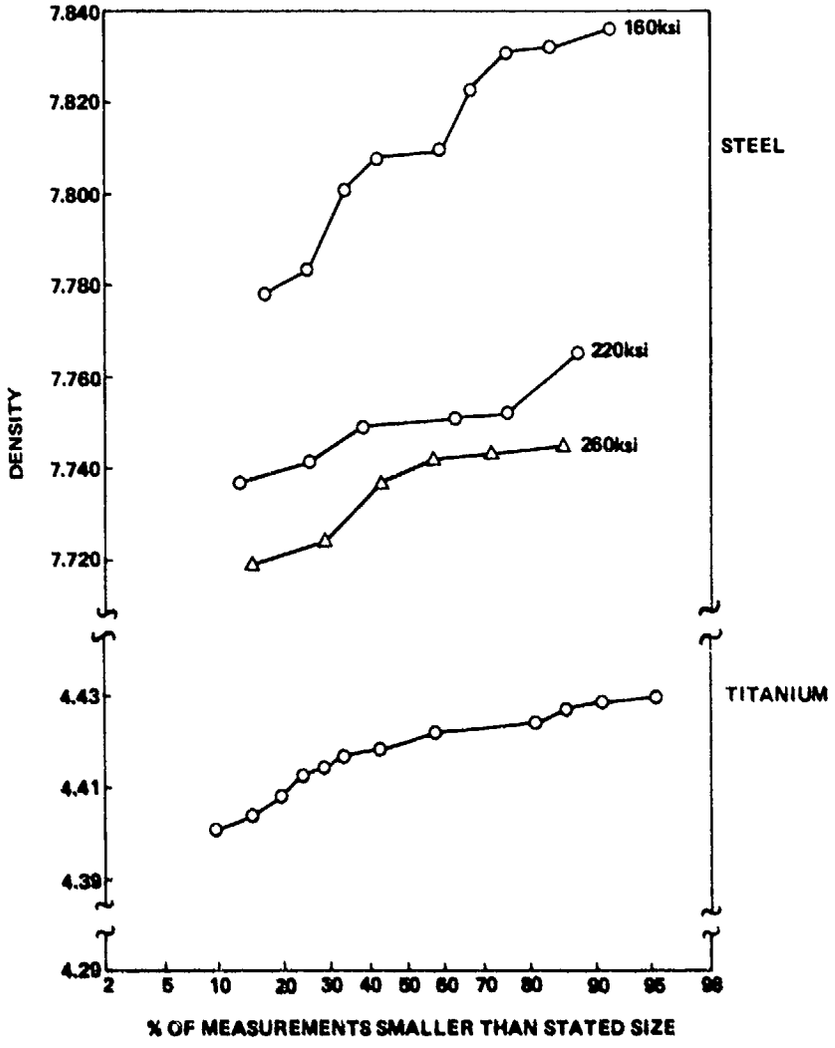

Figure C.3 Normal Distribution Plots of the Densities of Fasteners Selected for Calibration

VARIATION OF MATERIAL PROPERTIES (VELOCITY OF SOUND)

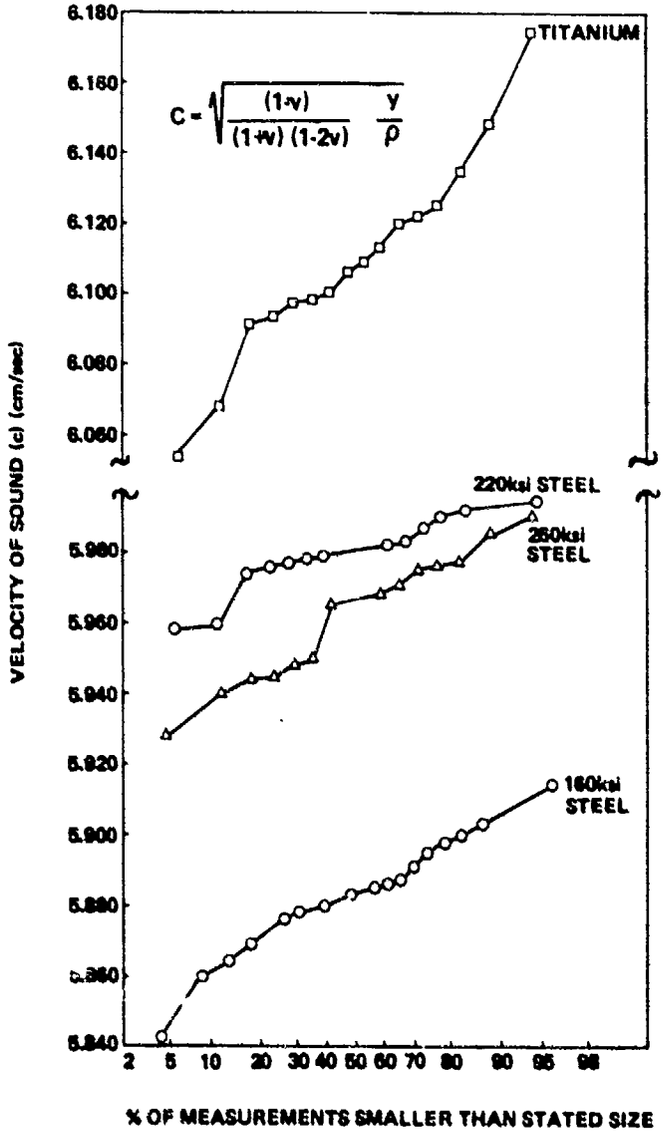

Figure C.4 Normal Distribution Plots of the Velocities of Sound Measured in Unloaded Fasteners Selected for Calibration.

APPENDIX D

TEMPERATURE EFFECTS

Studies have shown that ΔT is very sensitive to temperature. An experiment was performed in which fasteners were placed in an oven and the travel time was measured as the temperature was raised above room temperature. It was observed (Figure D.1) that large changes in ΔT followed changes in temperature. It was determined that the ΔT due to the thermal expansion of fasteners was only .293 times the total ΔT measured. The remaining .707 ΔT was due to the effects of the higher-order elastic constants. This 1/3 due to expansion and 2/3 due to elastic constants has already been observed by others (ref. 4).

There is a possibility, of course, that some relationship exists between temperature effects and relaxation phenomena. When fasteners are torqued very quickly there is no evidence that the accuracy in measuring fastener preload is effected by either temperature or relaxation. Special studies were performed to detect temperature effects without success.

In fact, it may be shown later that tension in fasteners does vary with temperature and that what is being measured by the acousto-elastic effect are the true tension changes that we are interested in monitoring; temperature corrections will then be needed to obtain directly related strain determinations.

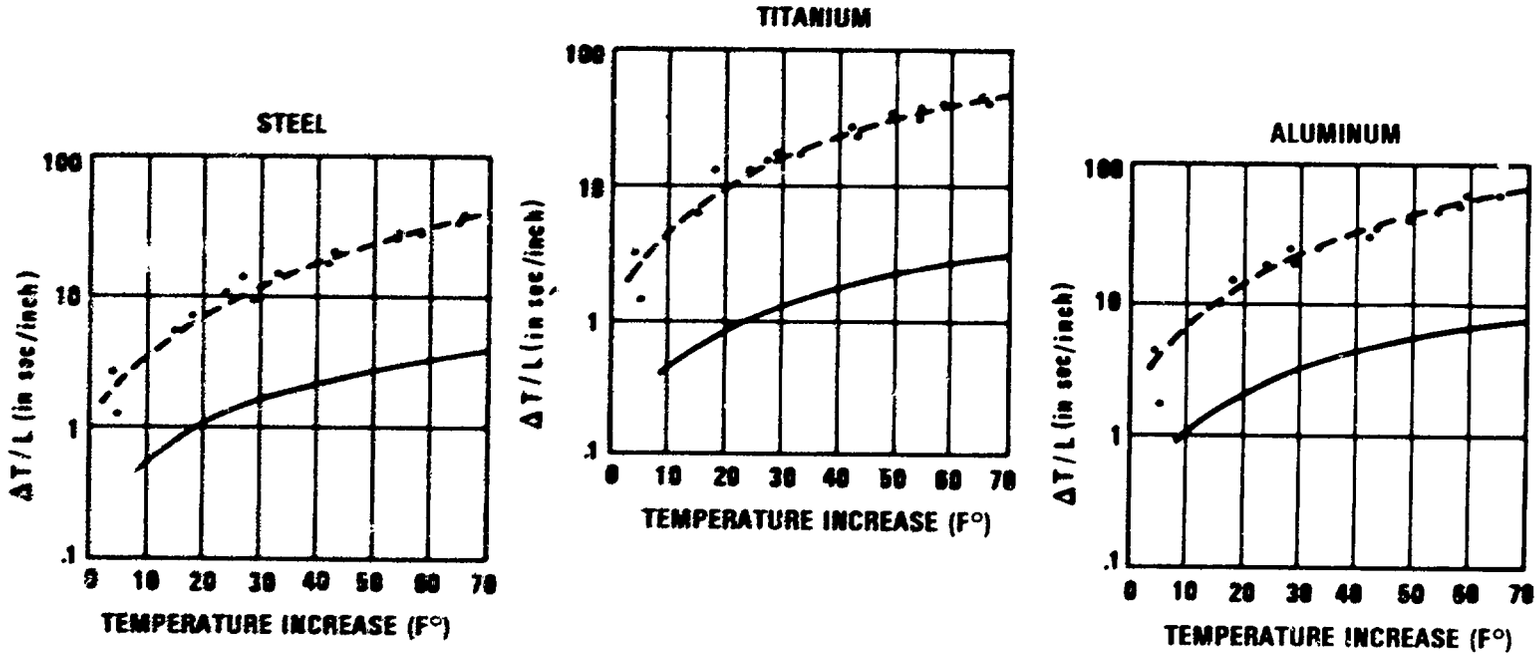

Figure B.1 Experimentally Measured Changes in Ultrasonic Travel Time per Unit Length of Fastener Material as Temperature was Increased Above Room Temperature

APPENDIX E

FACTORS EFFECTING FREQUENCY SPECTRA OF ECHOED ULTRASOUND

E.1 Surface Roughness Factors

A 15-MHz broadband transducer was used in a study of the effects of surface upon the shape (especially of the leading edge) of an ultrasonic pulse echoing normally from the surface. This is an important study since the timing reference point should be a common reference position on the incident (as portrayed by the echo from a smooth surface) and other beams echoing from rough surfaces (See Figure E.1). System accuracy will be severely degraded when fasteners have rough heads or ends.

E.2 Stress Distribution Factors

It was observed that even when fastener ends are relatively flat and smooth the shape of the leading edge of the full wave rectified R.F. changes (Figures E.2 and E.3). This can cause errors in ΔT of the order of half wave length in fasteners unless (1) high-frequency ultrasound is used ($>$ 100 MHz) (2) the pulses are phase shifted by 90^{o} then re-added to remove the leading-edge dips.

Since a phase-shift adjustment would require a different delay line for each transducer frequency the less attractive approach of using real-time pulse integration was used in the fastener preload indicator prototype (See Process Specifications Report).

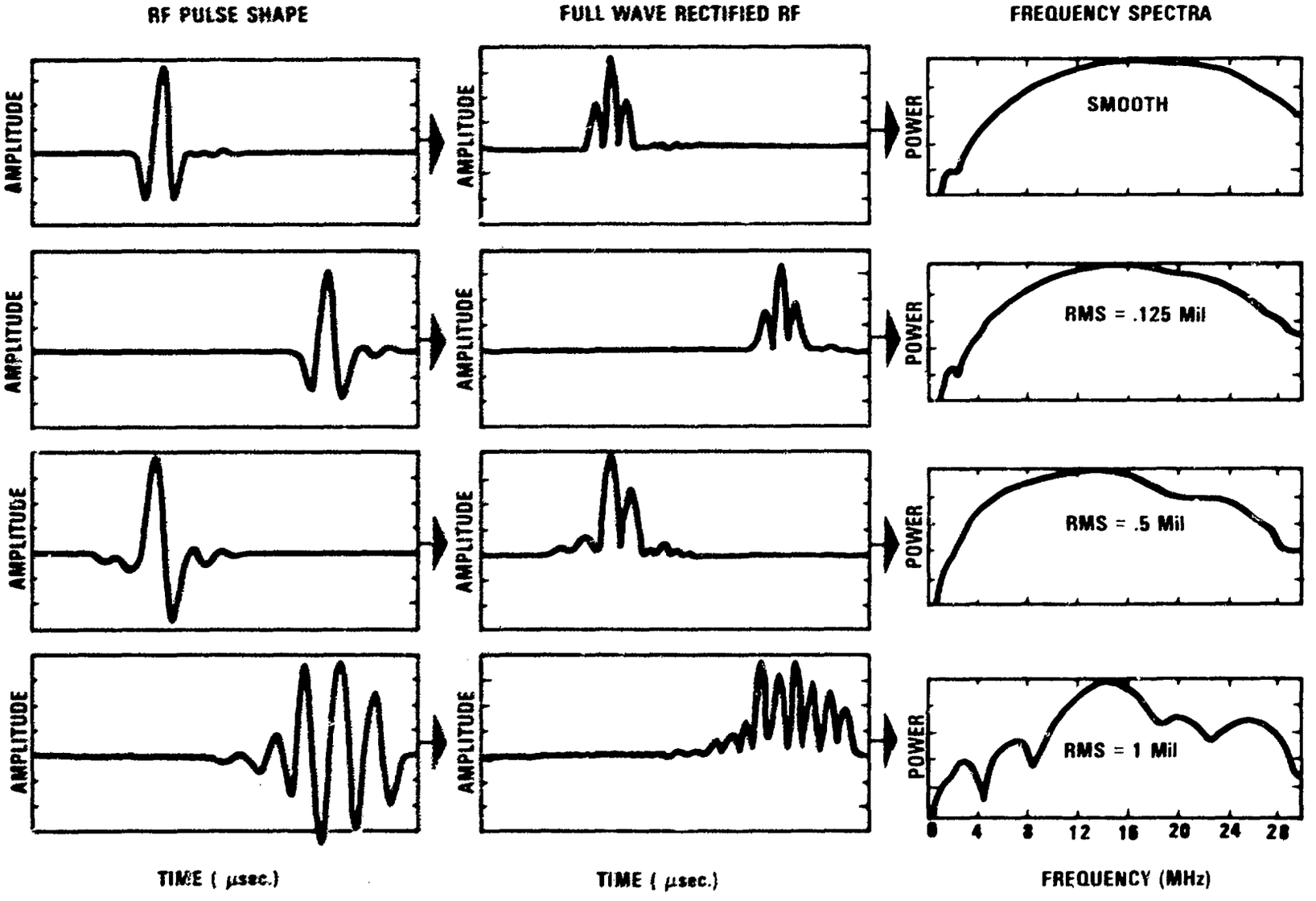

Figure E.1 Effects of Surface Roughness on the Shape and Frequency Spectra of a 15 MHz Broad Band Ultrasonic Pulse

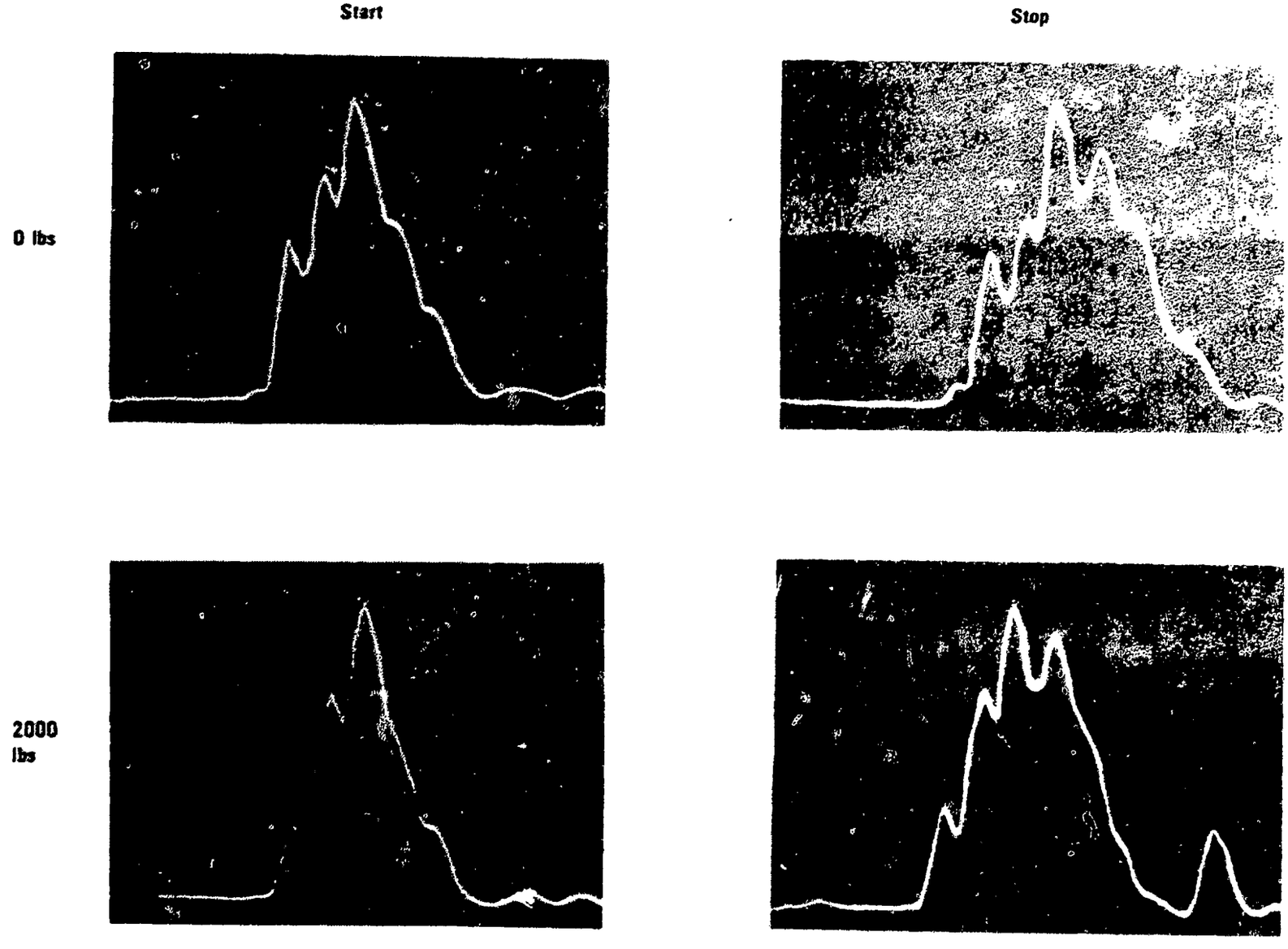

Figure E.2 Full-Wave-Rectified Start and Stop Pulses for Threaded Titanium Unloaded and Loaded to 2000 lbs.

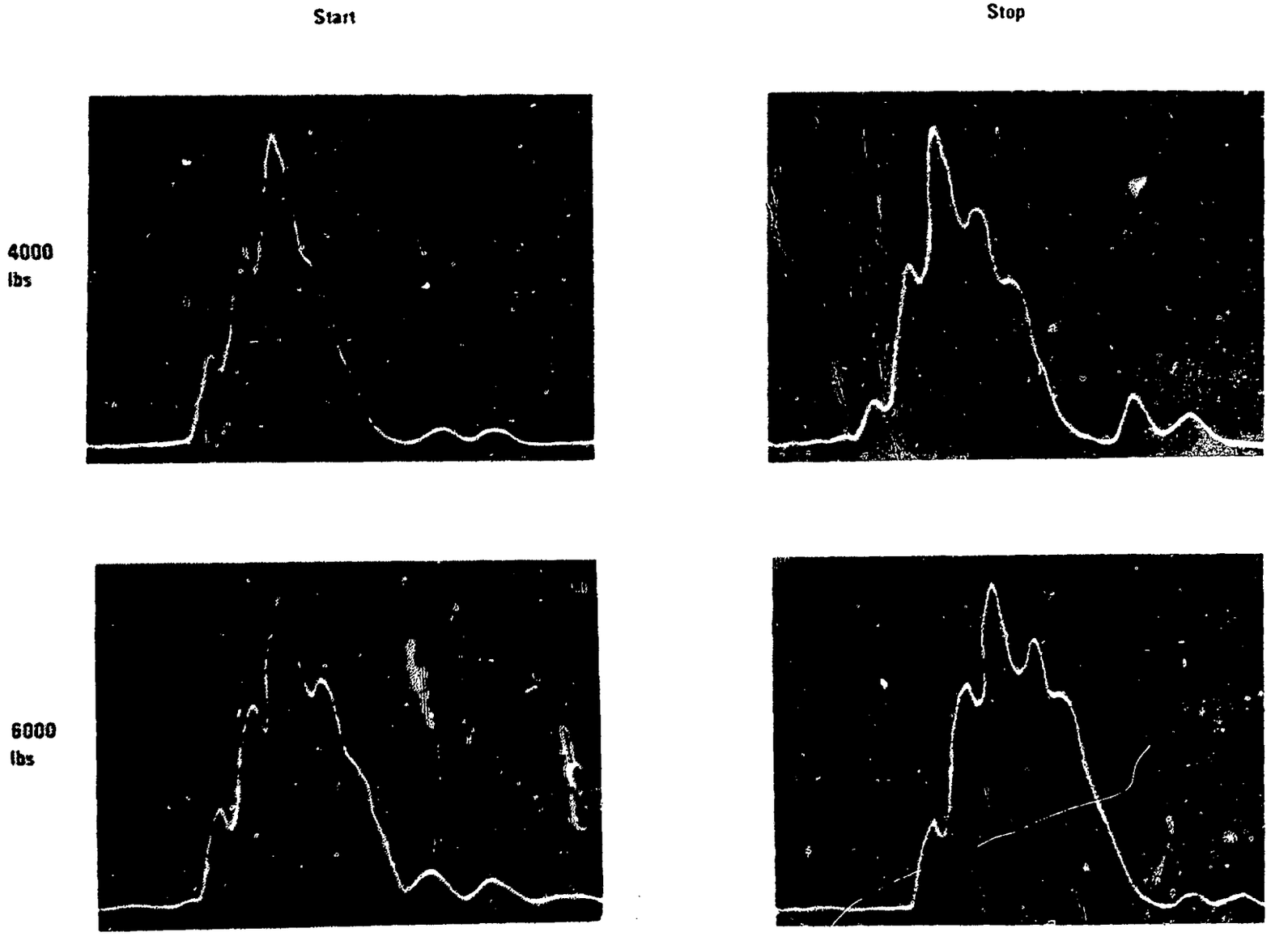

Figure E.3 Full-Wave-Rectified Start and Stop Pulses for Threaded Titanium Loaded to 4000 and 6000 lbs

Bibliography of Thickness
and Stress Gages

1. Rollins, F. R., Jr., Fastener Load Analyses Method - Final Report to NASA NAS-8-25362, April 1971.

2. Branson 101 Digital Caliper

3. SPS Preload Monitor, S.P.S. Laboratories Standard Pressed Steel Co., Jenkinton, PA.

4. Ultrasonic Time Intervalometer, Panametrics, 221 Crescent St., Waltham, MA 02154.

5. Ultrasonic Thickness Gage - Model 5221, Panametrics, 221 Crescent St., Waltham, MA 02154.

6. Digital Thickness Gage, Automation Industries, Inc., Sperry Division, Shelter Rock Road, Danbury, CT 06810.

7. Ultrasonic Digital Thickness Meter, Mitsubishi Electric Corporation, Box 406, Rt. 33N, Lancaster, OH 43130.

8. Neva 201 Digital Ultrasonic Thickness Gage, NDT Instruments, Inc. 15622 Graham St., Huntington Beach, CA 92649.

9. Closed Loop Ultrasonic Thickness Measuring System, C. L. Holland, General Dynamics Report CASD-ERR-76-003-804, 1976.

10. CL 204 Ultrasonic Thickness Gage, Krautkramer-Branson, Inc., 250 Long Beach Blvd., Stratford, CT 06497.

11. 733 (Series) Ultrasonic Extensiometer, Erdman Instruments, Inc., 1179 Romney Drive, Pasadena, CA 91105.

12. Erdman Extensiometer Mated to Torque Wrench, Power-Dyne Torque Products Division, Raymond Engineering, Inc., 217 Smith Street, Middletown, CT 06457.

13. Mark III Ultrasonic Thickness Tester, Sonic Instrument, Inc., 1018 Whitehead Road Ext., Trenton, NJ 08638.

14. Ultrasonic Stress Gage, Thermo Electron

15. Heyman, J. S., "Ultrasonic Bolt Stress Monitor" Industrial Research, October 1976.

16. ROUS Bolt Tensioning Monitor, NASA Tech. Briefs, Langley Research Center, Summer 1976.

REFERENCES

1. AFML RFP F33615-76-R-5251 Fastener Preload Indication.

2. Dunn, R. T. (Editor) "How Much Preload in Fasteners?" Machine Design, Aug. 21, 1975 p. 66-69.

3. Editorial Note in Ultrasonics, July 1968, pages 4 and 5.

4. Moropis, N. and Meyer, F. R., Ultrasonic Wrench for Flared Tubing Connections, NAS-8-11965 by Technidyne, Inc., Sept. 1967.

5. "Process Specification for Prototype Fastener Preload Indicator" #_____, June 1978.

6. Couchman, J. C. "Fastener Preload Indicator", Interim Progress Report No. IR 818-6(II), January 1977.

7. Coper, E. G. and Filon, L. N. G., Cambridge University Press, 2nd Edition, 1957 pg. 685.

8. Couchman, J. C. "Fastener Preload Indicator", Interim Progress Report No. IR 818-6 (III), April 1977.

9. Couchman, J. C., "Fastener Preload Indicator," Interim Progress Report No. IR 816-6 (IV), July 1977.

10. Iverson, T. A., "Some Aspects of the Finite Elements Method in Two Dimensional Problems", Book, Finite Elements Methods in Stress Analysis, Topics (Technical University of Norway), Trondheim 1969 (Chapt. 3).

11. Lynch, R. W., "BOBTRAN - Computer Program for Stress Analysis in Membrane Type Structures", General Dynamics Report MRS-71-001 (1971:.

12. NASTRAN Users Manual, NASA Publication, SP-222 (03), July 1976.

*U.S.Government Printing Office: 1979 — 657-002/618

THIS REPORT HAS BEEN DELIMITED AND CLEARED FOR PUBLIC RELEASE UNDER DOD DIRECTIVE 5200.20 AND NO RESTRICTIONS ARE IMPOSED UPON ITS USE AND DISCLOSURE.

DISTRIBUTION STATEMENT A

APPROVED FOR PUBLIC RELEASE; DISTRIBUTION UNLIMITED.